

7-1-2016

Evaluation of the Epidermal Growth Factor Receptor Signaling Pathway as a Therapeutic Target in Human Papillomavirus-Associated Disease

Anastacia Griego

Follow this and additional works at: https://digitalrepository.unm.edu/biom_etds



Part of the [Medicine and Health Sciences Commons](#)

Recommended Citation

Griego, Anastacia. "Evaluation of the Epidermal Growth Factor Receptor Signaling Pathway as a Therapeutic Target in Human Papillomavirus-Associated Disease." (2016). https://digitalrepository.unm.edu/biom_etds/155

This Dissertation is brought to you for free and open access by the Electronic Theses and Dissertations at UNM Digital Repository. It has been accepted for inclusion in Biomedical Sciences ETDs by an authorized administrator of UNM Digital Repository. For more information, please contact disc@unm.edu.

Anastacia M. Griego

Candidate

Molecular Genetics and Microbiology

Department

This dissertation is approved, and it is acceptable in quality and form for publication:

Approved by the Dissertation Committee:

Dr. Michelle A. Ozbun, Chairperson

Dr. Laurie Hudson

Dr. Bryce Chackerian

Dr. Helen Hathaway

Dr. Bridget Wilson

**Evaluation of the Epidermal Growth Factor Receptor
Signaling Pathway as a Therapeutic Target in
Human Papillomavirus-Associated Disease**

by

ANASTACIA MARIA GRIEGO

B.S., Biology, University of New Mexico, 2007

DISSERTATION

Submitted in Partial Fulfillment of the
Requirements for the Degree of

Doctor of Philosophy

Biomedical Sciences

The University of New Mexico
Albuquerque, New Mexico

July 2016

Copyright © Anastacia M. Griego 2016

DEDICATION

This work is dedicated to all of the people who continued to believe in me when I no longer believed in myself. Most especially, to my parents, Orlando and Lori Griego – your love and prayers have carried me through. Words cannot express how much I love you both.

ACKNOWLEDGMENTS

I would first like to acknowledge my Ph.D. advisor, Dr. Michelle Ozbun. Thank you for the opportunity to work in your lab. I am so thankful for the amazing opportunities that allowed me to grow as a scientist and as a person. Thank you for giving me the freedom to make mistakes and the push I needed get up and try again every time I fell flat on my face. You took a timid and naïve biology student and helped her become a scientist. For that, I will be forever grateful.

I owe a huge debt of gratitude to my Committee on Studies, Dr.'s Laurie Hudson, Bryce Chackerian, Helen Hathaway, and Bridget Wilson. You have all been influential in this journey. Thank you for your guidance and support, which have helped me grow as a scientist. A very special thank you to Dr. Hudson, your constant encouragement has meant more to me than you will ever know.

To the current and former members of the Ozbun lab: Each of you was instrumental in helping me get this far. I could not have done this without your help and support. A very special thank you to the former trainees in the lab, especially Pamela Barraza, Sonya Flores, Mickey Kivitz, Dr. Kelly Higgins, and Dr. Agnieszka Dziduszko – I learned so much from each one of you. Your presence made the lab a great place and I miss you all. Thank you to Dr. Lanlan Wei for believing in me and for all of your encouragement over the years. I am sincerely grateful to the current members of the lab, Dr. Zurab Surviladze, Nicole Patterson, Alex Fowler, and Adrian Luna, for their help and support. And lastly, thank you, Rosa Sterk, for all of your help over the last few years. Words cannot express how thankful I am to know you. Without your encouragement and amazing immunoblot skills I could not have completed this project.

This project would not have been possible without the help of numerous individuals on the UNM HSC campus. Dr. Jamie Hu and Laura Laidler of the UNM Animal Core – thank you both for your exceptional skill and patience as well as entertaining conversations. Tamara Howard, your assistance and willingness to answer all of my questions was much appreciated – the world needs more individuals like you. The administration and staff of the UNM HTR, especially Dr. Kelly Higgins and Cathy Martinez, thank you so much for answering my seeming unending questions and always being willing to let me send samples at the last minute. Dr. Donna Kusewitt, thank you for lending your expertise to this project, I've learned so much in the short time we worked together. I am so thankful for the support of the UNM BSGP staff: Mary Fenton, Alec Reber, and Ignacio Ortiz.

To my science family, Dr.'s Dominique Price, Jenna Lilyquist, and Christopher Lino: You all mean the world to me and I literally would not have made it without you. If all that came out of this experience was having you as friends, it would have been totally worth it. Thank you for coffee breaks, movies, girls' nights, boxes of kleenex, and talking me out of quitting every Tuesday afternoon. Most of all, thank you for bringing joy and fun to this journey.

I would not be where I am today without my amazing family. To all the Griego's and Luna's – thank you for your love and support, especially over the last six years. Mom and Dad, thank you for setting an amazing example of what it is to live with integrity. You taught me that, in Christ, I could accomplish anything and continued to believe in me when I doubted myself. To my siblings, Jessica, Jacob, and Vanessa – thank you for your unending support. I am honored to be your sister. Nate and Britney, your presence in our family has made it more complete and I am grateful that you chose to join our craziness. For my nieces and nephew, Chloe Bethany, Cali Joy, and Jacobito – thank you for bringing so much joy to my world with your smiles and laughter. I love you to pieces.

Lastly, and most importantly, all glory to God for giving me the strength to complete this journey (Philippians 4:13).

EVALUATION OF THE EPIDERMAL GROWTH FACTOR RECEPTOR
SIGNALING PATHWAY AS A THERAPEUTIC TARGET IN
HUMAN PAPILLOMAVIRUS-ASSOCIATED DISEASE

by

Anastacia Maria Griego

B.S., Biology, University of New Mexico, 2007
Ph.D., Biomedical Sciences, University of New Mexico, 2016

ABSTRACT

Human papillomaviruses (HPVs) are the most common sexually transmitted infectious agents. They are responsible for >99% of all cervical cancers as well as subsets of other anogenital cancers. HPVs are also the causative agents of a growing number of head and neck cancers. As such, they present a significant health problem both in the U.S. and developing countries. Much is still unknown regarding the factors underlying progression from HPV infection to cancer or maintenance of viral oncoprotein expression following oncogenic transformation.

Previous studies reported significant interplay between the epidermal growth factor (EGFR) pathway and HPV oncoproteins. HPV oncoproteins E5, E6, and E7 have been implicated in upregulation of EGFR signaling and expression. Additionally, downstream effectors of EGFR signaling were shown to upregulate HPV early gene expression. These reports led us to hypothesize that, in infected cells, HPV establishes a positive feedback loop with the EGFR pathway, wherein viral proteins upregulate EGFR signaling, which then leads to enhanced viral oncogene expression. We further postulated that interruption of this feedback loop, via inhibitors of the EGFR signaling

pathway, would result in decreased viral oncoprotein levels and increased sensitivity to apoptotic stimuli.

In a model of early, persistent infection, we found that EGFR signaling modulated HPV early gene expression, including upregulation of viral oncogene expression upon EGFR stimulation. We discovered that EGFR inhibition by cetuximab, a monoclonal antibody targeting EGFR, had antiviral effects including downregulation of HPV oncogene expression levels in this model. Furthermore, in cells harboring episomal viral genomes, inhibition of this pathway led to reduced viral genome burden and sensitization to apoptotic stimuli.

Our study further reveals that EGFR/MEK inhibition can lead to downregulation of HPV oncogene expression in vivo, in subsets of HPV-positive xenografts, concomitant with delayed tumor growth. These results suggest a possible role for antiviral effects in the therapeutic outcomes observed following EGFR-inhibitor treatment of HPV-associated diseases in the clinic. Together, these data indicate that use of EGFR/MEK inhibitors may be beneficial in the treatment of HPV-associated diseases. Furthermore, the results of this study set the frame work to better understand the role of growth factor signaling in the HPV lifecycle.

TABLE OF CONTENTS

DEDICATION.....	iii
ACKNOWLEDGMENTS	iv
ABSTRACT.....	vi
TABLE OF CONTENTS.....	viii
LIST OF FIGURES	x
LIST OF TABLES.....	xii
CHAPTER 1 - Introduction	1
1.1 History of Viruses and Cancer.....	1
1.2 HPV Types and Infection.....	2
1.3 HPV Lifecycle and Replication	3
1.4 HPV Gene Expression	5
1.5 HPV Oncoproteins.....	7
1.6 HPV-Associated Diseases.....	10
1.7 HPV Vaccines and Screening.....	14
1.8 The EGFR Pathway	15
1.9 Importance of EGFR Signaling in HPV-Associated Cancers.....	18
1.10 Rationale, Hypothesis, and Goals of This Study	19
CHAPTER 2 - Materials and Methods.....	22
2.1 Cell Culture.....	22
2.2 Flow Cytometry	23
2.3 Nucleic Acid Extraction.....	24
2.4 RNA Extraction from Xenografts.....	24
2.5 DNase Treatment of RNA	25
2.6 RT-qPCR	25
2.7 Immunoblotting.....	26
2.8 Xenograft Preparation.....	27
2.9 Immunohistochemistry	28
2.10 Histological Evaluation.....	29
2.11 RNAscope® - RNA ISH.....	30
2.12 Statistical Analysis.....	31
CHAPTER 3 - Inhibitors of the EGFR and MEK signaling pathways have antiviral activities in HPV16-infected keratinocytes	32
Abstract.....	32
3.1 Introduction.....	34
3.2 Methods.....	38
3.2.1 Cell Culture	38
3.2.2 Cell Viability Assays.....	39
3.2.3 Treatment With Targeted Inhibitors.....	39
3.2.4 Cisplatin Treatment	39
3.2.5 Protein Isolation and Immunoblot.....	39
3.2.6 Nucleic Acid Collection and Analysis	40
3.2.7 Measurement of Cell Surface EGFR.....	41
3.3 Results.....	43

3.3.1 EGF Stimulation Results in Increased Viral Transcription in HPV16-Positive Human Keratinocytes	43
3.3.2 HPV16 Infection Does Not Significantly Alter EGFR Expression or Signaling in Proliferating Cells	44
3.3.3 HPV16-Positive Cells Are Sensitive to EGFR and MEK Inhibitors	46
3.3.4 EGFR Signaling Dependency in HPV16-Positive Cells	47
3.3.5 EGFR/MEK Inhibition Has Antiviral Effects	48
3.3.6 HPV-Infection Does Not Significantly Alter p53 Levels in NIKS-SG3.....	50
3.3.7 EGFR Inhibition Sensitizes HPV-Positive Cells to Apoptotic Stimuli.....	53
3.4 Discussion	55
3.5 Limitations of this study	61
CHAPTER 4 - Evaluation of Anti-Viral Effects of the EGFR-Inhibitor Cetuximab in HPV-Positive Xenografts.....	63
Abstract	63
4.1 Introduction	64
4.2 Methods	68
4.2.1 Cell Culture	68
4.2.2 Xenograft Preparation	69
4.2.3 RNA Extraction	70
4.2.4 RT-qPCR	70
4.2.5 Immunohistochemistry	71
4.2.6 Histological Evaluation	72
4.2.7 RNAscope® - RNA in situ hybridization	73
4.2.8 Statistical Analysis	73
4.3 Results	75
4.3.1A Effect of Cetuximab Treatment on Viral Oncogene Expression in UM-SCC47 Tumor Xenografts.....	75
4.3.1B UM-SCC47 Biomarker Detection by Histology and IHC	78
4.3.1C Effect of Trametinib Treatment on Viral Oncogene Expression in UM-SCC47 Tumor Xenografts.....	87
4.3.2A Effect of Cetuximab Treatment on Viral Oncogene Expression in UM-SCC104 Tumor Xenografts.....	89
4.3.2B UM-SCC104 Biomarker Detection by Histology and IHC	92
4.4 Discussion	100
4.5 Limitations of This Study	111
Chapter 5 - Discussion and Future Directions	113
LIST OF APPENDICES.....	123
Appendix A – Abbreviations	124
Appendix B – Supplemental Xenograft Data	126
Appendix C - References	137

LIST OF FIGURES

Figure 1.1 TEM image of HPV particles	3
Figure 1.2 The lifecycle of papillomaviruses.	4
Figure 1.3 HPV16 genome organization.	6
Figure 1.4 HPV oncoproteins E6 and E7 target p53 and pRb for degradation.....	7
Figure 1.5 Burden of HPV-positive cancers.	13
Figure 1.6 The EGFR signaling pathway.	17
Figure 3. 1 Hypothesized feedback loop between HPV and EGFR.	37
Figure 3.2 EGF stimulation results in increased viral transcription in HPV16-positive NIKS-SG3 cells.	44
Figure 3.3 Cells maintaining HPV16 genomes do not exhibit significantly heightened EGFR signaling, and remain sensitive to EGFR pathway inhibition.	45
Figure 3.4 Dependence of HPV-positive and HPV-negative NIKS on EGFR and MEK 1/2 signaling for cell survival.	47
Figure 3.5 Inhibition of EGFR signaling decreases viral early transcript levels in NIKS cells maintaining episomal HPV16 genomes.	49
Figure 3.6 Inhibition of EGFR and MEK signaling decreases viral genome copy numbers in NIKS cells maintaining episomal HPV16 genomes.	50
Figure 3.7 HPV-infection does not significantly alter p53 levels in NIKS-SG3 cells but increases levels of p16.	52
Figure 3.8 EGFR inhibitors sensitize HPV16-positive cells to apoptotic stimuli.	54
Figure 4.1 Low-dose cetuximab does not affect tumor growth or viral oncogene levels in SCC47 xenografts.	75
Figure 4.2 Cetuximab delays tumor growth independent of normalized viral oncogene expression levels in SCC47.	77
Figure 4.3 Cetuximab treatment induces differentiation and morphologic changes in SCC47 xenografts.	80
Figure 4.4 Cetuximab decreases levels of active EGFR and ERK1/2 in SCC47 xenografts.....	83
Figure 4.5 E6/E7 expression and p53 levels change concomitant with cellular differentiation in SCC47.	85
Figure 4.6 Trametinib produces antitumor effects concomitant with downregulation of viral oncogene expression in SCC47 xenografts.	88
Figure 4.7 Cetuximab downregulates tumor growth rate while producing increased E6 and E7 transcript levels in SCC104 xenografts.	91
Figure 4.8 Cetuximab treatment induces morphologic changes in SCC104 xenografts. .	94
Figure 4.9 Cetuximab decreases levels of active EGFR and ERK1/2 in SCC104 xenografts.....	96
Figure 4.10 Cetuximab decreases p16 but not p53 or Ki-67 levels in SCC104 xenografts.	99
Supplemental Figure 1 Determination of epithelial area in SCC47 xenograft sections.	126
Supplemental Figure 2 Determination of epithelial area in SCC104 xenograft sections.	127

Supplemental Figure 3 Cetuximab treatment leads to lower levels of smooth muscle actin (SMA) in tumor infiltrating fibroblasts.....	128
Supplemental Figure 4 Cetuximab delays tumor growth and decreases viral oncogene expression along with c-Fos and JunB expression levels in SiHa xenografts.	132
Supplemental Figure 5 Cetuximab produces antitumor effects independent of viral oncogene expression in CaSki xenografts.	135

LIST OF TABLES

Table 2.1 Short Tandem Repeat Profiles of Cell Lines	23
Table 2.2 Primer Sequences and qPCR Cycle Conditions	26
Table 2.3 Antibodies and Conditions Used for Immunoblotting.....	27
Table 2.4 Antibodies and Conditions Used for Immunohistochemistry.....	29
Table 4.1 List of HPV-Positive Cancer Cell Lines Used.....	69
Table 4.2 IHC Scores for UM-SCC47 5mg/kg Cetuximab Cohort	81
Table 4.3 IHC Scores for UM-SCC104 5mg/kg Cetuximab Cohort	95
Supplemental Table 1 Summary of SCC47 xenograft data	129
Supplemental Table 2 Summary of SCC104 xenograft data	130

CHAPTER 1 - Introduction

1.1 History of Viruses and Cancer

The discovery of a transferable oncogenic agent in cell-free tumor lysates by Ellerman and Bang in 1908 ushered in a new era in cancer research [1]. The causative infectious agent was later identified as the oncogenic retrovirus, avian sarcoma leukosis virus (ASLV). Subsequent to this initial discovery, multiple DNA and retroviruses have been found to be associated with carcinogenesis, both in animals and humans. The discovery of another transmissible filterable agent, Rous Sarcoma Virus (RSV), in 1911 by Peyton Rous, eventually led to the identification of the viral oncogene *src* by other groups [2, 3]. Rous received a Nobel Prize in Physiology or Medicine for his work. This paved the way to the discovery of the first cellular proto-oncogene, *c-src*, for which Bishop and Varmus shared the Nobel Prize in Physiology or Medicine in 1989 [4]. In the following years, additional viruses including retroviruses (MMTV, HTLV-1) herpesviruses (KSV, EBV), polyomaviruses (SV40, MCV), hepadnaviruses (HBV, HCV), adenoviruses (Ad2, Ad5), and papillomaviruses (e.g. HPV16, -18, -31) have been associated with cancer or shown to have transforming abilities *in vitro*.

The strongest link between viruses and human cancer is the relationship between infection with certain types of HPV and cervical cancer as shown by H. zur Hausen in the late 1970's. HPV is the causative agent of nearly 100% of cervical cancers as well as a number of other anogenital and head and neck cancers [5-7]. For his work identifying HPV as a causative agent of cervical cancers, zur Hausen was awarded a Nobel Prize in 2008.

While oncovirus research has provided a wealth of information about carcinogenesis, targeting the causative infectious agents to reduce cancer burden has proven difficult. In the case of HPV, there are currently three highly effective vaccines available. However, vaccine coverage remains low and the current vaccines offer no therapeutic protection for individuals already infected with the most common oncogenic HPV types. Additionally, many of the individuals at the greatest risk of developing HPV-associated cancers do not have access to the vaccine [8].

1.2 HPV Types and Infection

Papillomaviruses (PVs) are small, non-enveloped, icosahedral viruses encapsidating a circular double-stranded DNA genome of approximately 8 kilobases (Fig 1.1). The Family *Papillomaviridae* is comprised of hundreds of species, divided into 39 genera based on species and tissue specificity; PVs that infect humans (HPVs) are found in five of these genera. Over 150 genotypes of HPV have been sequenced (see [9, 10] and Papillomavirus Episteme (PaVE); <http://pave.niaid.nih.gov/#home>). HPVs exhibit specific tropism for either cutaneous or mucosal squamous epithelium, with members of the Beta PV genus primarily infecting the former and Alpha PVs responsible for infections of the mucosa [10]. Tropism is thought to be controlled at the level of gene expression through regulatory elements in the viral long control region (LCR) [11]. All PVs cause either benign or malignant hyperplasia and are thus divided into low- and high-risk types depending on the probability of infection progressing to malignancy [10].

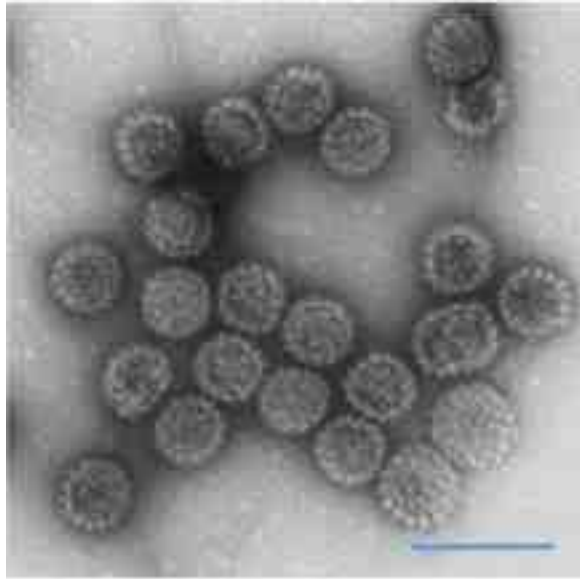


Figure 1.1 TEM image of HPV particles

A transmission electron micrograph (TEM) of negatively stained pseudovirus particles composed of HPV16 L1 and L2 proteins showing the icosahedral form of the viral capsid. Capsomeres, each composed of five L1 proteins, can be seen. Blue bar represents 100nm. Image was generated by A. Griego using the UNM Electron Microscopy Shared Facility supported by the University of New Mexico Health Sciences Center.

1.3 HPV Lifecycle and Replication

HPVs establish infections in the basal cells of stratified squamous epithelium, to which they gain access through a wound or break in the overlying epidermal layers (Fig 1.2) [12, 13]. Following entry of the virus into a host cell, viral genomes are amplified and infection is established. HPVs exhibit a differentiation dependent lifecycle wherein temporal expression of viral genes is regulated by the host cell differentiation process, therefore, a productive infection can only occur in stratified epithelium [11, 14-16].

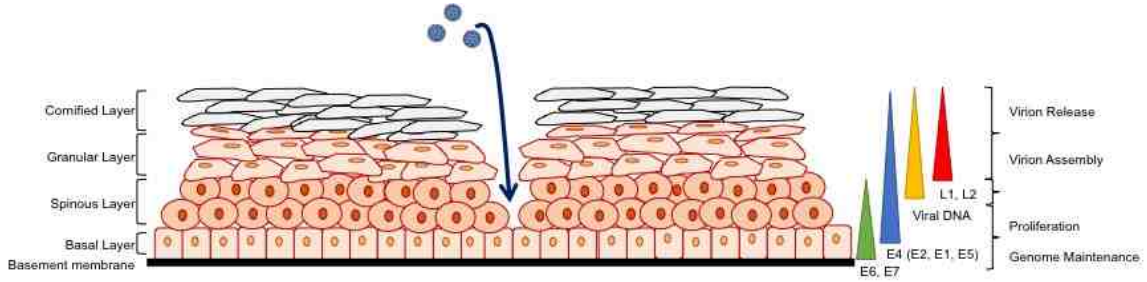


Figure 1.2 The lifecycle of papillomaviruses.

Papillomaviruses infect the basal layer of the epidermis through a break, or wound, in the upper layers. Upon infection, viral genomes are replicated and maintained at low levels; early viral gene expression is kept tightly regulated. As basal cells divide, viral genomes are distributed to each daughter cell. As infected daughter cells differentiate and enter the spinous layer, expression of viral early genes is increased to enable enhanced proliferation of the cell and facilitate amplification of viral genomes. Downregulation of viral early gene expression and expression of late viral proteins, which compose the viral capsid, occurs in the granular layer, wherein virion assembly occurs. Release of viral particles occurs upon sloughing off of the cornified layer of the epidermis. Adapted from [17].

Viral proteins E1 and E2 are essential for replication of the viral genome and maintenance of infection. E1 is the only enzyme produced by HPVs and serves as the essential DNA helicase for viral DNA replication [18]. E2 has multiple binding sites in the LCR and recruits E1 to initiate viral genome replication [19, 20]. In addition to its role in recruiting E1 to the origin of replication, E2 also facilitates maintenance of infection. During cellular division, viral protein E2, in association with cellular protein bromodomain-4 (BRD4), attaches viral genomes to host mitotic chromosomes allowing distribution of viral genomes between daughter cells, further propagating infection [21-23]. Other E2 binding partners are also considered to have a role in division of viral genomes [24, 25].

As the infected epithelial cells undergo early differentiation events, viral proteins E6 and E7 are expressed and enable the cells to undergo increased proliferation by dysregulation of cell cycle checkpoints. In the upper layers of the epithelium, viral

genomes are amplified. Downregulation of E6 and E7 expression, reinitiation of cellular differentiation, and expression of L1 and L2, the major and minor viral capsid proteins, follow genome amplification respectively. L1 and L2 encapsidate newly synthesized viral genomes, forming new infectious particles or virions. Expression of E4 is also amplified during late infection. The E4 protein is thought to facilitate virion release by interacting with cytokeratins and disrupting the cytoskeletal network of intermediate filaments; this function is most apparent in cutaneous HPV genotypes [26]. Progeny virions are spread by the sloughing off of the cornified layer of infected epithelial cells (reviewed in [27]).

1.4 HPV Gene Expression

The circular double-stranded DNA genomes of PVs are maintained extrachromosomally during a productive infection. HPV encodes four major early proteins (E1, E2, E6/E6*, E7) and four to five late proteins (E4, E5a/b, L1, L2, and sometimes E8) (Fig. 3). HPV genes are transcribed and undergo splicing to produce polycistronic RNAs [17, 20].

Control of viral gene expression is mediated by an ~800 bp stretch of DNA between the late and early coding regions of the genome, known as the long control region (LCR) or upstream regulatory region (URR). As previously mentioned, the LCR contains multiple binding sites for viral proteins E1 and E2 as well as cellular factors. HPV early gene expression is initiated from one or more promoters located in the LCR [28-30]. In HPV16, gene expression is controlled from two main promoters, p97 (the early proximal promoter) and p670 (the major late promoter) [31, 32]. Viral genes are

expressed temporally and control of their expression appears to be mediated by differentiation-associated changes in cellular transcription factors (reviewed in [20]).

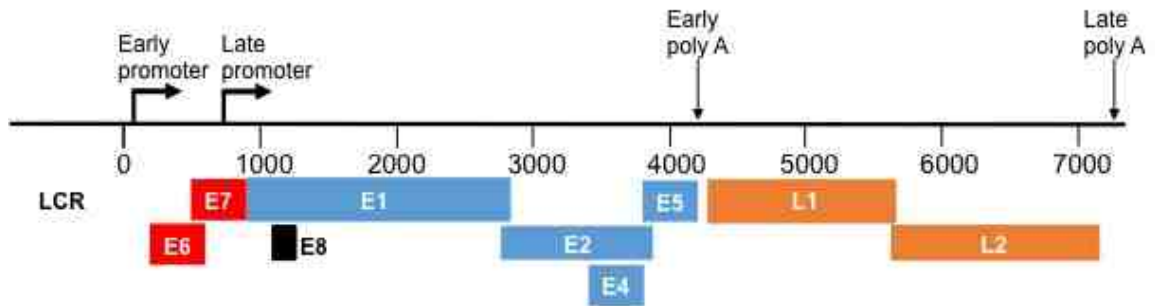


Figure 1.3 HPV16 genome organization.

Linearized representation of the alpha-papillomavirus genome organization. The LCR contains at least two promoters, depicted here are the early and late promoters. Colored boxes represent ORFs for each gene. Red boxes indicate the major oncogenes E6 and E7. The remaining early genes E1 and E2 as well as intermediate-late genes E4 and E5 are depicted in blue. E8 is an intermediate-late protein that is expressed in only a few papillomavirus genotypes. Orange boxes denote genes for major and minor capsid proteins L1 and L2, respectively.

The early proteins, particularly E6 and E7, are important in the regulation of cellular proliferation and differentiation. In addition to facilitating genome replication and maintenance of infection, E2 regulates expression of viral oncogenes E6 and E7. As E6 and E7 enhance proliferation and inhibit differentiation to ensure viral genome amplification in intermediate epithelial layers, strict control of their expression is necessary for reinitiation of cellular differentiation and completion of the viral life cycle. Binding of E2 to the LCR near the early promoter inhibits E6 and E7 expression [33, 34]. This is thought to occur by steric hindrance of TFIID binding or recruitment of transcriptional repressors, including Sp1 [20]. Loss of E2 expression or ability to bind to the LCR, for example through integration into the host DNA or via DNA methylation events, is thought to be important in the progression of lesions to cancer [35-38].

1.5 HPV Oncoproteins

High-risk HPVs encode three oncoproteins: E5, E6 and E7. These proteins are produced early in the viral lifecycle and expression is kept under strict viral control. E6 and E7 are the best studied of these proteins and are expressed at high levels in HPV-associated cancers. E6 and E7 are each capable of causing immortalization when ectopically overexpressed *in vitro* [39-42].

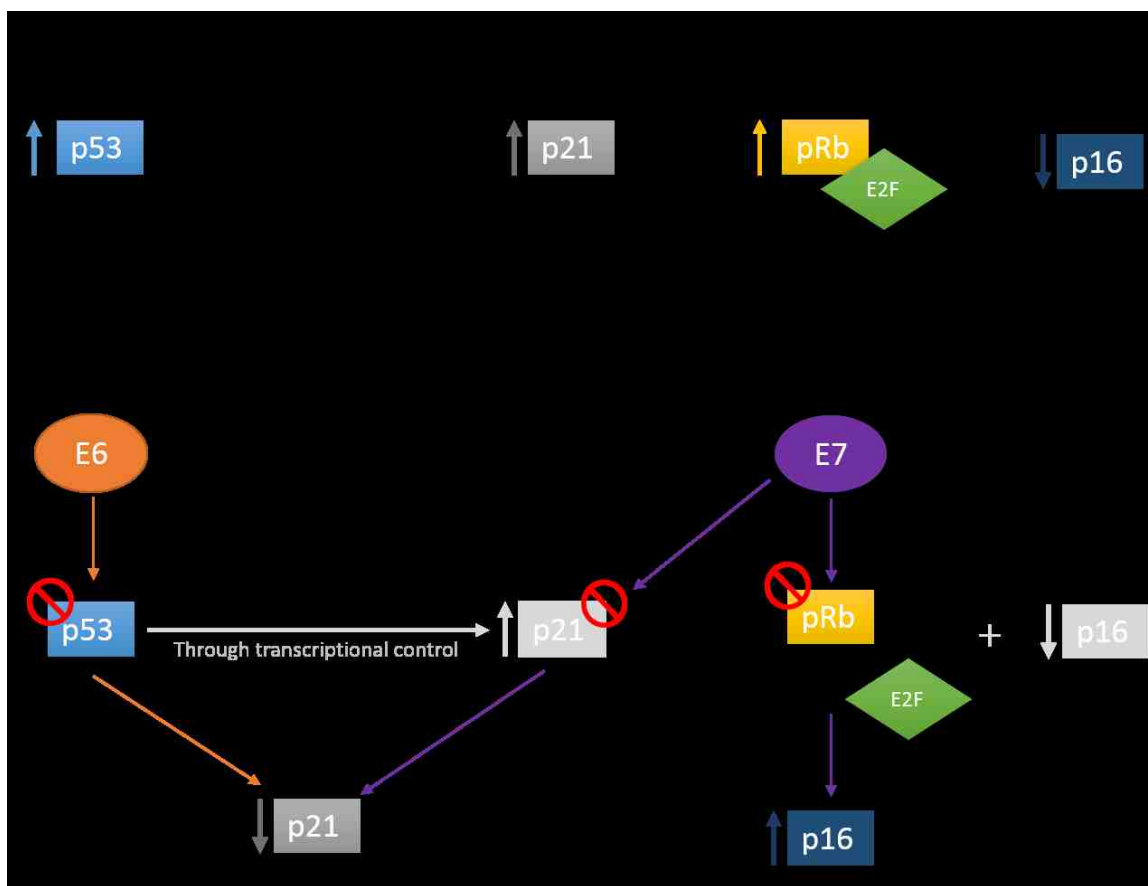


Figure 1.4 HPV oncoproteins E6 and E7 target p53 and pRb for degradation.

HPV infection results in loss of normal cell cycle control and increased cellular proliferation. E6 degrades p53 resulting in loss of p21 upregulation. Additionally, E7 can degrade remaining p21, resulting in downregulation of p21 protein levels. Levels of p16 are elevated in HPV-positive cancers due to degradation of pRb.

The most well-known function of E6 is degradation of the tumor suppressor protein, p53 (Fig 1.4) [43, 44]. E6 interacts with the cellular protein E6-associated protein (E6AP, also known as UBE3A), an ubiquitin protein-ligase. The E6-E6AP complex then binds cellular p53 [45]. p53 is subsequently ubiquitinated and degraded through the proteasomal pathway. Loss of p53 in cells results in dysregulation of cell cycle checkpoints and allows infected cells to reenter the cell cycle in the intermediate layers of the epidermis. The resulting hyperproliferation enables expansion of the number of infected cells. S-phase reentry is also necessary for amplification of the viral genome in the upper epithelial layers. E6 also interacts with numerous cellular proteins (reviewed in [46]). For example, E6 can bind PDZ domain-containing cellular proteins including, MAGI1 and MUPP1, resulting in loss of cell polarity [47-51]. Additionally, E6-E6AP complex can facilitate cellular immortalization by activating telomerase expression through upregulation of c-Myc expression [52-56].

The other viral protein responsible for driving cellular proliferation and enabling S-phase reentry is E7 (Fig 1.4). E7 from high-risk HPVs functions to downregulate pRb levels in infected cells by binding the active form of the protein and inhibiting its interaction with the transcription factor E2F [57, 58]. E7 then directs pRb for degradation resulting in cellular progression to S-phase [59]. The resulting increase in free E2F transcription factor levels also augments E6-mediated telomerase expression [55, 60, 61]. As with E6, HPV E7 interacts with numerous other cellular proteins. These interactions are reviewed in detail by Roman and Munger [62].

E5 is the least well understood of the HPV oncoproteins. E5 from HPV16 upregulates epidermal growth factor receptor (EGFR) expression and signaling [63-68].

The specific mechanism by which this is done is currently unknown. Studies of BPV E5 show that the viral protein directly binds the growth factor receptor, PDGF β R, and cross-links homodimers to initiate activation of the receptor [69-71]. However, direct binding between HPV E5 and EGFR has not been demonstrated. E5 is the only membrane associated protein produced by HPV and Wetherill, *et al.* recently showed that E5 from HPV16 is capable of forming viroporin-like structures [72]. The viroporin inhibitor rimantidine, as well as a novel, empirically designed, E5 specific inhibitor, was reported to decrease endosome acidification in HPV16 E5 expressing HaCaT cells and reduce E5-associated ERK activation following EGF stimulation of cells. These data indicate that HPV E5 may undertake EGFR upregulation through inhibition of early endosome acidification resulting in recycling of the EGFR back to the cell membrane.

Although cell cycle dysregulation and heightened proliferation are necessary for large-scale replication of the viral genome, expression of E6 and E7 must be tightly controlled in order to reinitiate cellular differentiation and complete the viral lifecycle. Uncontrolled E6 and E7 expression is understood to underlie oncogenic transformation of HPV infected cells. As discussed previously, E2 inhibits expression of E6 and E7 and loss of E2 expression or ability to bind inhibitory sites in the LCR is considered to precede cancer development. In cancers, viral genomes can be found either episomally, integrated into the host genome, or as a mixed population. HPV cancers typically contain low levels of the tumor suppressor proteins p53 and pRb due to high E6 and E7 expression. Conversely, levels of the cellular protein p16 are increased as a result of pRb loss. In fact, high p16 expression is commonly used as a biomarker for HPV-associated cancers in the absence of genomic testing [73-76].

As E6 and E7 drive HPV-associated cancers, reducing levels of these proteins should have therapeutic effects. In fact, knockdown of E6 and E7 levels in cancer cell lines by siRNA results in increased p53 levels and apoptosis *in vitro* [77, 78]. Additionally, siRNA knockdown of E6 and E7 in SiHa and HeLa xenograft tumors *in vivo* effected inhibition of tumor growth and increased p53 and radiosensitization [79, 80]. These reports demonstrate that reducing E6 and E7 levels in HPV-positive cancers reduces tumor burden and may sensitize the cells to chemotherapy and radiation *via* reinstatement of p53 levels.

1.6 HPV-Associated Diseases

HPVs infect cutaneous and mucosal epithelium and are associated with numerous diseases. HPVs are responsible for over 71% of all sexually transmitted infections and as such are the single most prevalent sexually transmitted infectious agents [81]. Transmission of HPV happens readily and 8 out of 10 sexually active women will become infected in their lifetime. Prior to HPV vaccine program initiation in the U.S., there were 79 million Americans infected at any one time, with 6 million new infections annually [81]. Since introduction of the vaccine in the U.S., rates of new infections have decreased by half in the target group of adolescent girls. However, uptake of the vaccine in the U.S. is still low; with only 40% of girls and <30% of boys in the target age range receiving the recommended 3-doses of the vaccine [8].

Low-risk HPV types 6 and 11 are associated with 90% of genital and anal warts. From 2-10% of adults in the U.S. and Europe report being diagnosed with genital warts at sometime during their life [82]. The transmission rate of the virus types associated with

genital warts is reported to be ~60% and transmission can occur even if visible lesions are not present [83]. Infection with these HPV types is typically not associated with cancer progression. Clinical intervention for these lesions includes topical treatments, ablation, or surgical removal [84].

Recurrent respiratory papillomatosis (RRP) results from infection of the respiratory tract with HPV, and types 6 and 11 are most commonly associated with this disease [85]. Incidence of this condition is rare with only 4/100,000 children and half as many adults diagnosed each year [84]. Occurrence in children can be associated with vertical transmission of the virus from mother to child in utero or during birth. Incidence in adults is commonly linked to sexual transmission. Papillomas frequently recur and can cause blockage of the airways requiring medical intervention especially in young children. Treatment for RRP includes repeated surgical removal of papillomas, resulting in high morbidity, especially in young children. Case studies have reported beneficial outcomes of chemotherapeutics including inhibitors of EGFR and vascular endothelial growth factor (VEGF) inhibitors in a small number of patients [85]. A large-scale clinical trial investigating the efficacy of cyclooxygenase-2 (COX-2) inhibitors in controlling the disease has also been undertaken [85].

High-risk HPVs are responsible for nearly 5% of all cancers worldwide [6]. Although high-risk HPVs are commonly associated with cancer of the uterine cervix, they also cause subset of vulvar, vaginal, penile, anal, and head and neck squamous cell carcinomas (HSNCC) (summarized in Fig 5) [6, 82]. While the majority of infections with high-risk HPVs are naturally cleared within 12-18 months due to effective immune intervention, 10-20% of cases are thought to persist and develop into recurrent or

possibly latent infections [86]. A portion of these persistent infections may progress to cancer.

High-risk HPVs are responsible for nearly 100% of cervical cancers, with HPV types 16 and 18 alone responsible for 70% of these cancers [5]. Cervical cancer is currently the 3rd most common cancer in women worldwide. Although the incident number of cases of cervical cancer has decreased by 1/3 in the U.S. since 1975 due to an effective screening program, cervical cancer remains a substantial health burden in developing countries [6]. Even with the decline in new cervical cancer cases in that time period, there has not been a significant decrease in the number of cervical cancer-associated deaths. In fact, the 5-year progression-free survival has remained fairly constant at ~70% (NCI SEER 9 Incidence & U.S. Mortality 1975-2012, All Races, Females. Rates are Age-Adjusted).

HPVs are associated with ~60% of oropharyngeal squamous cell carcinomas (OPSCC) and the number of new cases is predicted to rise [5]. HPV16 is the type most commonly found in OPSCC and it is responsible for 90% of these cancers [87]. The increasing rates of HPV-positive OPSCC are most dramatic in developed countries including the U.S. and incidence is higher in men (Fig 1.5) [82, 88]. As with genital HPV infections, viral transmission to oral tissues is associated with sexual behaviors [88, 89].

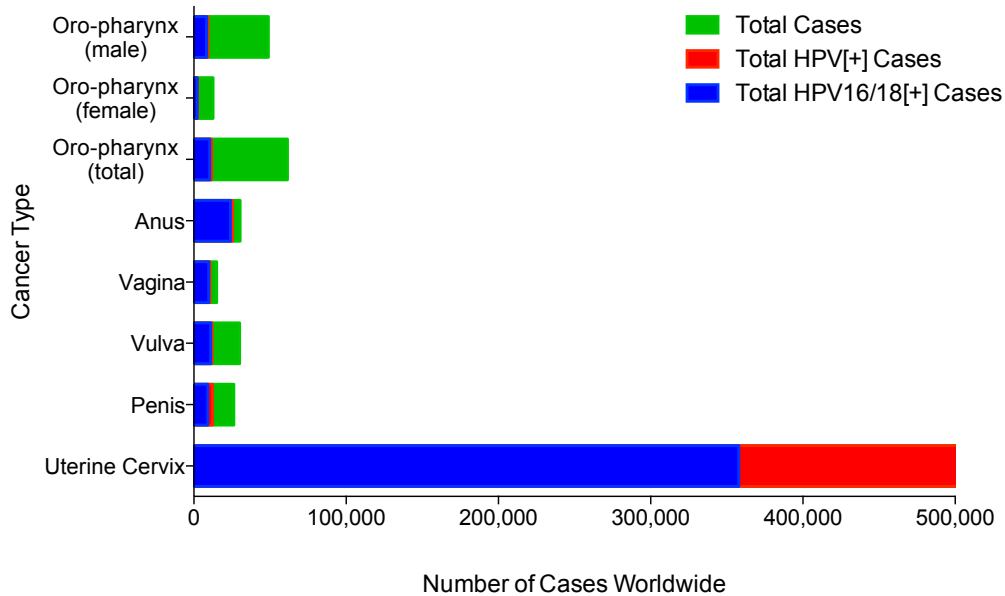


Figure 1.5 Burden of HPV-positive cancers.

Data highlighting the burden of HPV-associated cancers throughout the world. Cancer type is listed on the left. Total number of cases for each cancer type is shown in green while those cases attributed to HPV are shown in red. The number of cancer cases associated with HPV types 16 or 18 are depicted in blue. Data represent the total number of reported cases worldwide as collected by the EUROGIN 2011 Roadmap [82].

Current treatment of HPV-associated cancers includes surgical intervention as well as treatment with chemotherapy and radiation. Multiple targeted therapies, including EGFR inhibitors, have been attempted for cervical cancer but have shown no benefit over current standard of care treatments. The EGFR inhibitor, cetuximab, is FDA approved in conjunction with chemoradiotherapy for the treatment of HNSCC and large scale clinical trials have reported mixed outcomes in patients with HPV-positive HNSCC [90]. However, a recent retrospective analysis was conducted of patients with locoregionally advanced HNSCC receiving radiotherapy with or without cetuximab. In contrast to previous reports, p16 status and HPV-positivity were correlated with increased overall survival, progression-free survival and locoregional control [91]. This report

indicates that further investigation is needed in determining the efficacy of cetuximab and other EGFR inhibitors in the treatment of HPV-associated cancers.

1.7 HPV Vaccines and Screening

There are currently three FDA approved vaccines against HPV. All three of the vaccines, Cervarix (GSK), Gardasil-4 and Gardasil-9 (both Merck), offer protection against the most common high-risk HPV types 16 and 18, which are responsible for 70% of all cervical malignancies and >90% of HPV-associated HNSCC. Gardasil-4 also includes HPV types 6 and 11, which cause genital warts. In order to expand the number of covered HPV types, in 2014, the FDA also approved the first nonavalent vaccine against HPV. Gardasil-9 provides the same protection as the original quadrivalent Gardasil vaccine as well as an additional five oncogenic types (types 31, 33, 45, 52, 58).

Although the vaccines are highly effective at preventing HPV infection, there are still concerns. The largest concern is in regard to vaccine uptake. A complete series of the vaccine requires 3 doses over a period of one year. The vaccine also requires cold chain storage, limiting its feasibility in developing countries, which carry the highest burden of cervical cancer. The cost is also prohibitive with each dose costing ~\$130 USD, although the price has been reduced to \$5/dose in some developing countries (American Cancer Society). In order to be effective, the vaccine must be administered prior to sexual debut causing some concern among parents of adolescents. There are also limited studies on long-term efficacy of the vaccine [92, 93]. To address some of these issues, studies are being conducting to determine the efficacy of a partial vaccine series in inducing a protective immune response. Several recent reports indicate sufficient

protection following only one or two doses of the quadrivalent vaccine [94-96]. However, further study is needed to confirm these results. Additionally, to date, none of the vaccines have shown therapeutic effects in patients already infected with the target virus types. Therefore, there exists a large patient population who are not able to benefit from these vaccines. In light of these limitations to the vaccines, development of more effective treatment options remains critical.

In developed countries, cervical cancer surveillance through Papanicolaou testing (also known as a Pap smear) has decreased the number of cases of cervical cancer [82]. Routine HPV testing has also been included in the screening protocol. However, in developing countries, which lack the resources to undertake a screening program of this nature, cervical cancer remains a significant health burden, where it responsible for 13% of all cancers in women [82]. Additionally, there are no clinically validated tests to screen for early detection of HPV-associated HNSCC. Therefore, the need for development of more cost effective screening and treatment strategies is apparent.

1.8 The EGFR Pathway

The EGFR pathway appears to be important in multiple stages of HPV infection and disease progression. Previous studies have shown that EGFR plays an important role in HPV entry into keratinocytes [97, 98]. Additionally, as outlined earlier, HPV oncoproteins can upregulate EGFR expression and signaling, indicating this signaling pathway is significant in the viral lifecycle. Finally, high EGFR has been seen inconsistently in cervical cancer [99].

The epidermal growth factor receptor (EGFR, ErbB1/HER1) is a member of the ErbB family of transmembrane protein tyrosine kinases. The ErbB protein family is composed of four members, ErbB1-4, which interact with each other to form homo- or heterodimers [100, 101]. EGFR contains 3 domains; an extracellular domain that binds ligand, a hydrophobic transmembrane domain, and an intracellular tyrosine kinase domain [102]. EGFR is ubiquitously expressed in epithelial cells and performs important roles in tissue development, growth, and wound healing [103, 104]. Overexpression or mutation of EGFR is associated with multiple cancer types, including subsets of HPV-associated cancer [99, 105].

Traditional activation of EGFR is initiated by ligand binding to the extracellular domain [106]. However, ligand-independent activation can also occur *via* receptor dimerization in the absence of ligand [107]. Multiple proteins are capable of functioning as activating ligands for EGFR including its cognate ligand, EGF, as well as TGF- α or amphiregulin (reviewed in [101, 108]). Binding of a ligand to the extracellular portion of the receptor induces receptor dimerization facilitating transphosphorylation of the C-terminal tail of the receptors [106]. Specific phosphorylation patterns on the intracellular domain of EGFR are triggered in response to the activating ligand, ligand strength, and environmental milieu (reviewed in [101]). It is these phosphorylation patterns that are responsible for directing the intracellular pathway that is to be activated. Following activation, EGFR is downregulated by endosomal internalization; receptors are then degraded or recycled back to the plasma membrane [109, 110].

Cellular effects of receptor activation are mediated through downstream signaling pathways including: PI3K/Akt, Ras/MEK/ERK, JAK/STAT, and phospholipase C [105,

111]. Activation of PI3K/Akt and JAK/STAT pathways facilitate cell survival, whereas the Ras/MEK/ERK and phospholipase C signaling pathways mediate cell proliferation and survival [112] (Fig 6). Activation of the Ras/MEK/ERK pathway is mediated through recruitment of Grb2/Sos by activated EGFR. Which in turn signals downstream effector proteins in the Ras/MAPK pathway [113].

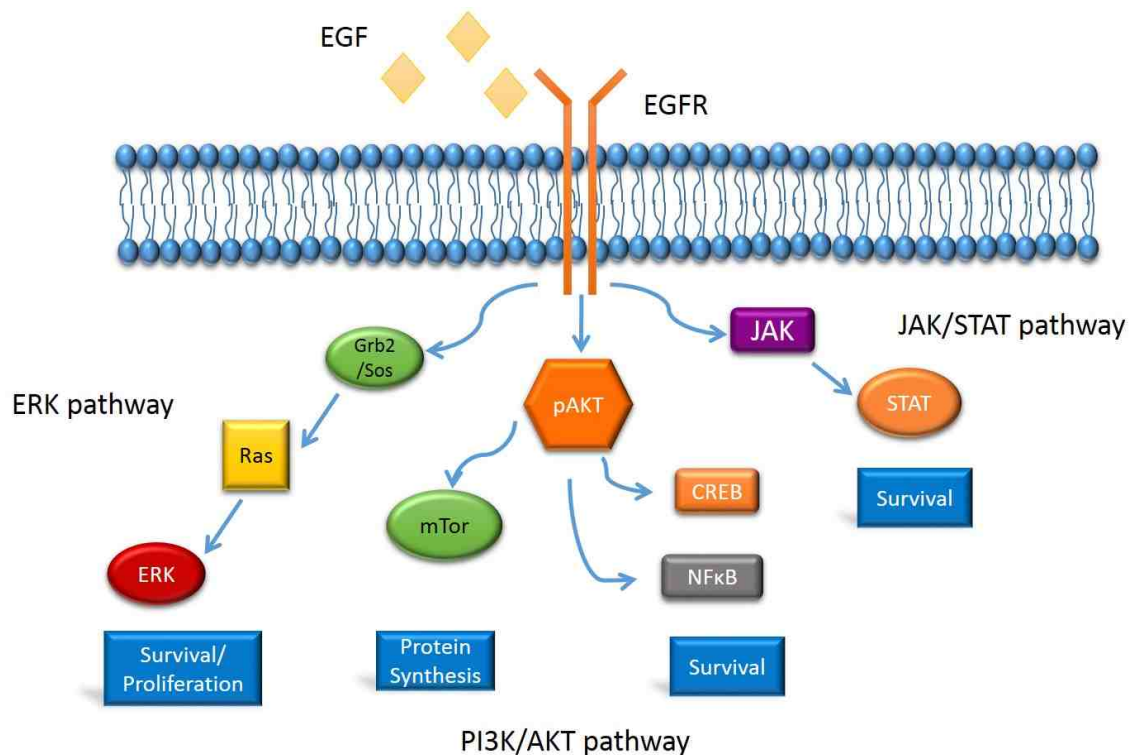


Figure 1.6 The EGFR signaling pathway.

Upon ligand binding, EGFR dimerizes and transphosphorylation of the C-terminal tail of the receptor occurs. Signal transduction can proceed through multiple pathways depending on the initiating ligand as well as environmental factors. Activation of the MEK/ERK signaling pathway occurs through phosphorylation of Grb2/Sos, which activates Ras. Activation of this pathway results in cell survival and proliferation. Activation of Akt results in enhanced protein synthesis (activation of mTor) or cell survival (CREB, NFκB). Signaling through the JAK/STAT pathway also results in cell survival.

The importance of EGFR in cancer development and progression has made it an attractive target for therapy [114]. To date, multiple small molecule tyrosine kinase inhibitors and monoclonal antibodies directed at the extracellular domain of EGF have

been tested in clinical trials and a small number have been FDA approved as targeted chemotherapeutics [115, 116]. Cetuximab, a humanized monoclonal antibody against EGFR, was first FDA approved for the treatment of metastatic colorectal cancer with wild-type *KRAS* in 2009 and approval has since been granted for metastatic non-small cell lung cancer and head and neck cancer [117]. Cetuximab works by binding the extracellular portion of EGFR and inhibiting ligand binding and receptor dimerization [118]. Binding of cetuximab to EGFR also triggers receptor internalization, effectively downregulating membrane-associated EGFR levels [119]. There is also thought to be an immune component in cetuximab's mechanism of action including activation of complement and induction of antibody-dependent cellular cytotoxicity (ADCC) [120].

1.9 Importance of EGFR Signaling in HPV-Associated Cancers

HPV oncoproteins are involved in upregulation of EGFR expression and pathway activation at multiple nodes. HPV16 immortalization of human keratinocytes was reported to increase EGFR levels and activation leading to growth factor independence [121]. EGFR gene expression was also enhanced by E6 and E7 expression in human keratinocytes retrovirally transduced with the HPV16 genome [122]. Conversely, inhibition of E6 and E7 in tumor cells reduces EGFR levels as well as cell proliferation [123]. Additionally, HPV16 E6 activates mTORC1 and MAPK pathways by upregulation of RTK signaling, including EGFR [124]. As described previously, E5 increases EGFR activation and signaling potential by enhancing receptor recycling back to the cell membrane after internalization [63-66, 72].

The EGFR pathway influences expression of the AP-1 family of transcription factors, which are involved in the regulation of HPV early gene transcription [20, 125, 126]. The AP-1 transcription factor, cFos, which is upregulated upon EGFR activation, is important in transcription of HPV16 early genes, further indicating that this pathway plays an important role in the viral lifecycle [127-131]. Also, cells expressing HPV16 E5 have higher levels of c-fos and c-jun transcription factors as well as higher levels of viral transcription [132].

In cervical cancers, high EGFR expression has been shown in multiple studies. However, in HNSCCs, high p16 levels, commonly used as a biomarker for HPV, are inversely correlated with EGFR overexpression [99, 133]. The disparate expression profiles of EGFR in HPV-associated HNSCC *versus* cervical cancer are confusing in light of the aforementioned studies implicating HPV oncoproteins in EGFR upregulation. However, the majority of the studies investigating the interplay between HPV oncoproteins and EGFR were performed in overexpression systems utilizing expression of a single HPV protein and not in the context of viral regulation of gene expression [63-67, 72, 122, 123]. Therefore, the extent to which these functions occur in a natural infection is not known.

1.10 Rationale, Hypothesis, and Goals of This Study

Several reports of the effect of EGFR activation on HPV early transcription have been published. While it is clear that EGFR activation can modulate HPV transcription, the studies have not agreed on whether EGFR signaling enhances or inhibits viral gene expression. Yasumoto, *et al.* claimed that EGFR activation resulted in downregulation of

HPV oncogene transcripts E6 and E7, while at the same time enhanced cell proliferation and c-myc expression [134]. Another group asserted that EGFR activation in SiHa, an HPV-positive cervical carcinoma cell line, resulted in enhanced E6 and E7 transcript levels [130]. However, no studies have described the role of EGFR in persistent HPV infection. In this study, we sought to define the role of EGFR as a mediator of HPV oncogene transcription in a model of early/persistent infection as well as in a preclinical model of cancer.

Previous studies implicated HPV oncoproteins in upregulation of EGFR pathway signaling and highlighted the importance of downstream mediators of EGFR activation, namely the AP-1 family of transcription factors, in expression of viral oncogenes. Based on these studies, we hypothesized that upon infection HPV establishes a positive feedback loop with the EGFR pathway whereupon HPV oncoproteins upregulate EGFR pathway activity thereby enhancing expression of viral early genes. We furthermore hypothesized that creating a break in this feedback loop, by inhibition of EGFR or downstream signaling molecules, would lead to decreased viral activities and restored levels of p53 tumor suppressor protein.

The goals of the research presented in this dissertation are to (a) determine the role of EGFR in controlling HPV oncogene transcription in a model of preneoplasia; (b) define the effect of HPV infection on EGFR signaling in early infection/preneoplasia; and (c) determine the ability of EGFR inhibitors to inhibit HPV activities *in vivo*.

The research for this project has been organized into two chapters. In chapter 3, I address the first two goals in a model of preneoplasia using a cell line maintaining episomal HPV16 genomes, NIKS-SG3, and its isogenically matched HPV-negative

parental cell line, NIKS [135]. Chapter 4 reports the data from my *in vivo* work, addressing the third goal of this study, using a cohort of four HPV-positive cancer cell lines propagated to form subcutaneous tumors in the NOD/SCID-gamma xenograft system.

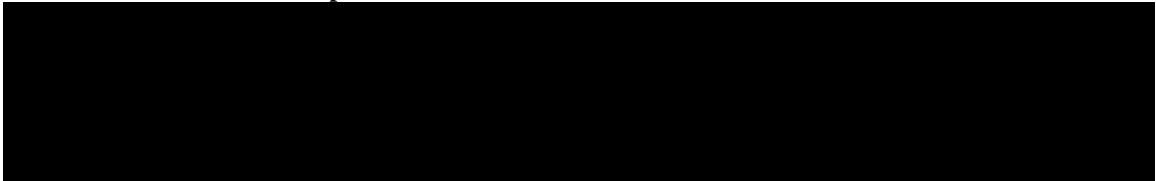
CHAPTER 2 - Materials and Methods

2.1 Cell Culture

The NIKS cell line was derived from Normal Immortalized human foreskin Keratinocytes [136]. The NIKS-SG3 cell line was created by stable transduction of episomal wild-type HPV16 genomes into NIKS cells, and was a gift from Professor Paul Lambert (Univ. Wisconsin-Madison) [135]. NIKS and NIKS-SG3 cell lines were co-cultured with mitomycin C-treated NIH 3T3 J2 fibroblast feeder cells in E media containing 10% fetal calf serum (FCS) (Sigma; Atlas Biologicals), with or without 10ng/mL murine EGF (mEGF) (BD Bioscience) as described previously [137]. J2 fibroblasts were cultured in high-glucose DMEM (Irvine Scientific) containing 10% newborn calf serum, 2mM glutamine (Gibco), 100U penicillin, 1 µg/mL streptomycin (Sigma), and 5 µg/mL Plasmocin (Invivogen). J2 fibroblasts were treated with 24µM mitomycin-C (Sigma) for 2 hours followed by washing 3x with at least 5 mL of 1x phosphate buffered saline (PBS) each. Fibroblast-conditioned E media was obtained from mitomycin C-treated J2 cells that were incubated 24 h with normal E medium lacking EGF; media were collected, cell debris removed and media stored at 4°C until use. For all experiments, keratinocytes were plated without feeder cells in regular E media or fibroblast-conditioned E media as indicated. SiHa and CaSki HPV16-positive cervical cancer cell lines were obtained from American Type Culture Collection (ATCC) and were cultured in Eagle's Minimum Essential Medium (Corning) or RPMI-1640 (Corning), respectively, supplemented with 10% FCS (Sigma; Atlas Biologicals). UM-SCC-47 and UM-SCC-104 HPV16-positive head and neck squamous cell carcinoma (HNSCC) cell lines were obtained from Prof. Thomas Carey (Univ. of Michigan).

HNSCC cell lines were cultured in E media containing 10% FCS (Sigma; Atlas Biologicals). Cell lines not obtained from ATCC were authenticated by short tandem repeat (STR) analysis (Genetica) and used within 10 passages of verification (Table 2.1).

Table 2.1 Short Tandem Repeat Profiles of Cell Lines



2.2 Flow Cytometry

Keratinocytes were co-cultured with J2-3T3 cells until 1 day prior to assay. J2-3T3 cells were differentially trypsinized with 1X trypsin/EDTA (Sigma) for 5 minutes. Plates were washed with 1X PBS and keratinocytes were dissociated from the plate using 0.25% trypsin/EDTA (Sigma). Cells were plated at subconfluent density and allowed to attach overnight. Subconfluent cells were washed with 1x PBS and incubated with 0.25% trypsin/EDTA (Sigma) for 20 minutes. Trypsin was quenched with an equal volume of media containing 10% FCS. Cells were pelleted at 1K RPM for 5 minutes and resuspended in 1X PBS, 2 µg of Alexa-fluor 647 labeled anti-EGFR antibody (clone R-1, Santa Cruz) was added and cells incubated at 4°C for 30 minutes to allow antibody binding. Labeling of microspheres was carried out alongside cells for each experiment. Cells and microspheres were held on ice following labeling. Cells and microspheres were pelleted and washed with cold 1x PBS. Following washes, cells and microspheres were resuspended in cold 1x PBS and held on ice. Cells and microspheres were analyzed on LSRFortessa flow cytometer (Becton Dickinson). Microspheres were gated on most populated area, cells were gated on live singlets. Unlabeled cells and microspheres were

run as controls on every run. Median fluorescence intensity was taken for each sample at using the full width of the peak at mid-height. Regression curves were created using *QuickCal v2.3 Data Analysis Program* (Bangs Laboratories) and antibody binding capacity for cells was determined from that experiment's standard curve. Experiments with a r^2 of <0.95 were not used. Average of r^2 for the experiments was 0.98. Data were reported as the number of antibodies bound per cell. Anti-EGFR clone R-1 is a monoclonal antibody which binds EGFR at a 1:1 ratio, therefore data can be expressed as the number of receptors per cell. Data shown are the result of at least 3 independent experiments.

2.3 Nucleic Acid Extraction

Cells were collected in TriReagent (Sigma) at 500 μL /well of 12-well plate. Plates were incubated at room temperature for 5 minutes and cell lysates transferred to Eppendorf tubes. Samples were stored at -20°C until extraction. RNA and DNA extraction were carried out according to manufacturer's protocol. RNA was DNase treated and yield determined as outlined in section 2.5.

2.4 RNA Extraction from Xenografts

Total RNAs were extracted from frozen tumors using Direct-zol RNA MiniPrep kit (Zymo) according to manufacturer's protocol. Briefly, frozen tissues were weighed, thawed in TriReagent (at least 1ml Trizol per 100mg tissue) (Sigma) and homogenized using a Pro200 rotary homogenizer (Pro Scientific). Lysates were held at 4°C overnight. Non-soluble material was removed by centrifugation ($12\text{K} \times \text{g}$ for 10 minutes) at 4°C and supernatant was transferred to a fresh tube. An equal volume of 100% ethanol was added to supernatant to precipitate nucleic acids. Solution was applied to Zymo column and

washed. Following wash steps, RNA was eluted in RNase-free dH₂O. DNase treatment was carried out as outlined in following section.

2.5 DNase Treatment of RNA

To remove contaminating DNA from RNA, samples were DNase treated using Turbo DNA free kit (Ambion) according to the manufacturer's directions. RNA concentration and purity was determined by spectrometry (Nanodrop, ThermoScientific). Quality and concentration of RNA was determined by spectrometry (Nanodrop, BioRad) and agarose gel electrophoresis as described in [138].

2.6 RT-qPCR

Reverse transcription of total RNAs was carried out at 42°C for 60 minutes using M-MLV reverse transcriptase and random primers (Applied Biosystems). 25ng of template (10ng for UM-SCC47, 5mg/kg cetuximab cohort) was used for each qPCR reaction. Sequences of primer/probes and cycling conditions are provided in Table 2.2. iQ Master mix (BioRad) was used for hydrolysis probes, JunB primers were obtained from Applied Biosystems and used with TaqMan Advances Master mix (Applied Biosystems), all other reactions used SsoFast Evagreen Master mix (BioRad) All qPCR reactions were run on CFX96 thermocycler (BioRad) and data analyzed using BioRad CFX Manager (version 3.1.1517.0823). C_q values for targets were normalized to human B-actin expression levels using the ΔC_q method.

Table 2.2 Primer Sequences and qPCR Cycle Conditions

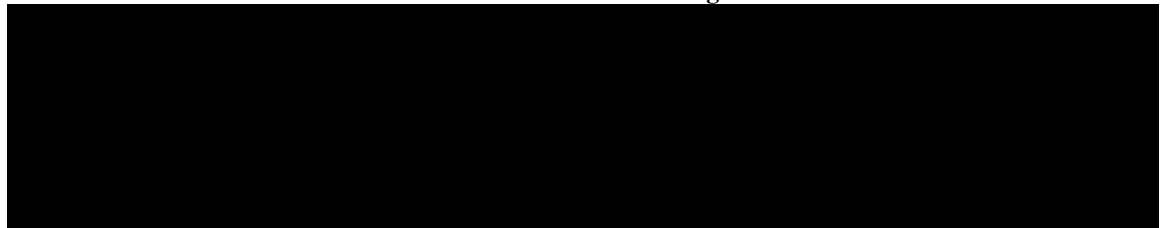
Primer/Probe	Sequence (5' to 3') [Dye/Quencher]	Strand	Product length (bp)	Cycle conditions	Amplification Efficiency (%)
16QE6.A	GAACAGCAATACAACAACCG	Sense	132	Hot start: 95°C, 5 min; 39 cycles at: 95°C, 10 sec; 60°C 20 sec, 72°C, 20 sec	97%
16QE6.B	CCACCGACCCCTTATATTATG	Antisense			
16QE7A	CAGCTCAGAGGAGGAGGATG	Sense	114	Hot start: 95°C, 5 min; 39 cycles at: 95°C, 10 sec; 60°C 20 sec, 72°C, 20 sec	100%
16QE7B	CACAACCGAAGCGTAGAGTC	Antisense			
16QE1E4A	CCATCTGTTCTCAGAAACCAT	Sense	90	Hot start: 95°C, 5 min; 39 cycles at: 95°C, 30 sec; 60°C 30 sec	98%
16QE1E4B	GGCCAAGTCTGCCTAAT	Antisense			
E1*E4 PROBE	[DFAM]ATACTTCGTTGCTGCTGCAGGATCAGCCAT[DTAM]	Probe			
BACTIN QA	AGCCTCGCCTTTGCCGA	Sense	174	Hot start: 95°C, 5 min; 49 cycles at: 95°C, 15 sec; 67°C 30 sec	102%
BACTIN QB	CTGGTGCCTGGGGCG	Antisense			
BACTIN PROBE	[HEX]CCGCCGCCCGTCCACACCCGCC[BHQ1]	Probe			
16QLCRA	TTCCTGACCTGCACTGCTTG	Sense	129	Hot start: 95°C, 5 min; 39 cycles at: 95°C, 30 sec; 60°C 30 sec	97%
16QLCRB	CAGCGGTATGTAAGGCGTTG	Antisense			
cFosA	AAAAGGAGAATCCGAAGGGAAA	Sense	81	Hot start: 95°C, 5 min; 39 cycles at: 95°C, 10 sec; 60°C,20 sec; 72°C, 20 sec	97%
cFosB	GTCTGTCTCCGCTTGAGTGAT	Antisense			
JunB	TaqMan primer/probe mix Catalog# Hs00357891_s1 (Applied Biosystems)		89	50°C, 3 min, 95°C, 30 sec; 39 cycles at: 95°C, 3 sec; 60°C,30 sec	95-100%

2.7 Immunoblotting

Cells were washed in cold 1X PBS and lysed on ice for 5 minutes with cold 1X radioimmunoprecipitation assay (RIPA) buffer (50 mM Tris pH 8.0, 150 mM NaCl, 1% Triton-X 100, 0.1% sodium dodecyl sulfate, 5mM EDTA, 1% deoxycholic acid) supplemented with 1X HALT protease inhibitors (Thermo Scientific) and 0.2 mM activated sodium orthovanadate. Lysates were transferred to an Eppendorf tube and centrifuged at 12K x g for 15 minutes at 4°C. Supernatant containing soluble protein was transferred to a fresh tube and protein concentration determined by Bradford Assay (BioRad). 6X Sample Loading Buffer (0.35 M Tris-Cl pH 6.8, 0.347 M SDS, 0.602 M dithiothreitol, 40% glycerol, 0.5% bromophenol blue) was added to a final concentration of 1X, samples were boiled for 10 minutes and stored at -20°C.

Proteins were separated on SDS-PAGE gel (TGX, BioRad) and transferred to PVDF or nitrocellulose membranes. See Table 2.3 for antibody specific blocking and incubation information. Following transfer, membranes were incubated in blocking buffer at room temperature for 1 hour. Primary antibody diluted in blocking buffer was added and incubated overnight. Secondary HRP-conjugated anti-mouse or anti-rabbit antibody (GE) diluted 1:10K in blocking buffer was added and membrane incubated at room temperature for 1 hour. When required, membranes were stripped (Western stripping buffer, pH 2.5 - 0.05% Tween-20, 0.2M glycine in 1X PBS) and reblocked prior to reprobing. Membranes or exposed films were scanned using a ChemiDoc (BioRad) and densitometry performed using Bio-Rad Image Lab software (version 2.0).

Table 2.3 Antibodies and Conditions Used for Immunoblotting



2.8 Xenograft Preparation

To establish xenografts, cells ($1-2 \times 10^6$ mixed 1:1 with Matrigel (BD Biosciences) were injected subcutaneously into flanks of 8-10 week old, female NOD/SCID-gamma (NSG) mice. Once tumors were palpable, they were measured by caliper, stratified by size, and animals randomized into treatment and control groups. Cetuximab (0.5, 1, or 5 mg/kg) or 0.9% saline control was administered 3x/week by i.p. injection. Trametinib (1 mg/kg) or vehicle control (10% Cremophor EL, 10% PEG 400) was administered daily by oral gavage. Tumors were measured by caliper 3x/week and volumes calculated using the

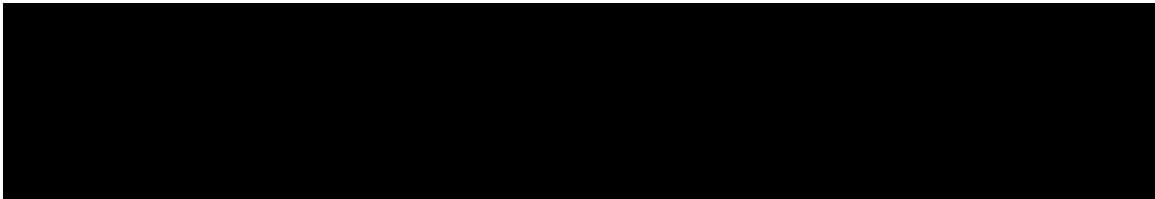
formula: length x width x width/2. Xenografts were harvested when the control group reached 1 cm in size. Tumors were surgically removed, divided for histology, RNA, and protein extraction. Tumor sections were snap frozen in liquid nitrogen, histology portions were embedded in OCT and snap frozen except UM-SCC47/cetuximab 5mg/ml and UM-SCC104 which were fixed in 10% formalin overnight then transferred to 100% ethanol until processed. Frozen tumor sections were stored at -80°C until use. The Institutional Animal Care and Use Committee of the University of New Mexico Health Sciences Center (Albuquerque, NM) approved all animal procedures (UNM HSC Protocol # 100924).

2.9 Immunohistochemistry

Formalin-fixed paraffin embedded (FFPE) blocks were sectioned at 5 µm thickness and transferred to charged slides (Fisher Scientific). Sections were deparaffinized in Citrisolv (Fisher Scientific) and rehydrated through 70% ethanol followed by 10 minutes in dH₂O (for H&E) or 1X PBS (for IHC). For manually stained IHC slides, antigen retrieval was performed by boiling slides in appropriate buffer for indicated times (see Table 2). Blocking was performed in 5% normal horse serum (Vector Labs), 1 hour at room temperature. The following antibodies were used for IHC: total-EGFR (Cell Signaling), phospho-EGFR(Y1173) (Cell Signaling), phospho-p44/42 (Cell Signaling), Ki-67 (BD Biosciences/Thermo Scientific), p16^{INK4a} (Roche/Ventana, performed by UNM Human Tissue Repository), p53-D07 (Novocastra, performed by MD Anderson Research Park Histology Core), human mitochondria marker (Chemicon, done by MD Anderson Research Park Histology Core). Manually stained sections were incubated with primary antibody in blocking solution overnight at 4°C in a humidified chamber (see Table 2 for

antibody concentrations). Slides were washed in TBS-T, and incubated with biotinylated anti-mouse/rabbit secondary antibody (VECTASTAIN Elite Universal ABC Kit, Vector Labs) for 30 minutes followed by 30 minutes incubation with ABC reagent. Sections were incubated with DAB (Vector Labs) for 15 minutes. Slides were counter stained with hematoxylin, dehydrated and cleared in Citrisolv. Coverslips were mounted with Permount mounting media.

Table 2.4 Antibodies and Conditions Used for Immunohistochemistry



2.10 Histological Evaluation

Blinded tumor sections were evaluated and all HALO analysis was performed by a certified pathologist (Dr. Donna Kusewitt of the UNM Comprehensive Cancer Center). IHC stained tissues were assigned a score between 0-3 based on epithelial staining intensity with 0 representing the lowest intensity and 3 representing the strongest. For evaluation of tissue morphology, Aperio-scanned H&E-stained slides and the HALO (Indica Labs) morphometry system were used. The entire tumor mass was outlined to obtain the total tumor area. HALO was then trained to recognize viable tumor epithelium, keratin, stroma, large blood vessels, and background (no tissue) within the tumor. Necrotic areas within the tumor epithelium were outlined by hand for exclusion in calculations. HALO was reprogramed for each cell line because of vastly different

morphologies. HALO determined the area of these components and percentage of the entire tumor occupied by these areas was calculated by the pathologist. Areas of tumor epithelium were confirmed by IHC for human mitochondrial marker. Ki67 IHC slides were also scanned into Aperio and analyzed using HALO. HALO was trained to recognize epithelium and then to identify Ki67-positive nuclei in that epithelium. Positive nuclei were classified as strongly (+3), moderately (+2), or weakly (+1) positive (considered background). The number of strongly and moderately positive nuclei (+2, +3) were normalized to the area of the epithelium.

2.11 RNAscope® - RNA ISH

FFPE sections were stained according to manufacturer's protocol (2.5 HD Detection Kit – Brown) using a probe to high-risk HPV E6/E7 (hrHPV 7, Advanced Cell Diagnostics). Briefly, fresh cut sections were deparaffinized in xylenes (2 x 5 minutes each) and washed in 100% ethanol (2 x 1 minutes each). Exogenous peroxidase was quenched by incubation with 3% H₂O₂ (Advanced Cell Diagnostics) for 15 minutes then washed with dH₂O. Slides were submerged in sub-boiling temp Antigen Retrieval Buffer (Advanced Cell Diagnostics) for 15 minutes followed by washing in dH₂O then 100% ethanol. Tissues were encircled with a hydrophobic pen and slides were allowed to dry overnight. Slides were incubated in protease (Advanced Cell Diagnostics) 30 minutes, 40°C then washed in dH₂O. High risk HPV E6/E7 probe was hybridized for 2 hours at 40°C. AMP steps 1- 4 were performed for recommended lengths of time at 40°C, with 2 minute washes in 1x Wash Buffer (Advanced Cell Diagnostics) between each amplification step. The final two AMP steps (5 and 6) were performed at ambient temperature for recommended times, slides were washed with 1x Wash Buffer after each step. Signal

detection was performed with DAB (Advanced Cell Diagnostics) for 10 minutes at ambient temperature. Tissues were counterstained with 50% Gil's hematoxylin solution, coverslipped and allowed to dry overnight. Slides were digitally scanned (Aperio Slide Scanner) and analyzed using HALO software by Dr. Kusewitt.

2.12 Statistical Analysis

All statistics for growth curves and RT-qPCR experiments were performed in GraphPad Prism version 6.0g for Mac. Statistical analysis for in vitro experiments was performed using the Student's *t*-test or 2-way ANOVA. Growth curves for xenografts were compared by multiple *t*-tests (unpaired). RT-qPCR data was compared by *t*-test. Correlation between tumor size and transcript expression levels was determined by Spearman's *r* test. Statistical outliers were determined for each experimental group using Grubb's outlier test. Semi-quantitative histology results were compared using Mann-Whitney. Error bars represent the standard error of the mean (SEM) for each group. *P*-values of less than 0.05 were considered to be significant.

CHAPTER 3 - Inhibitors of the EGFR and MEK signaling pathways have antiviral activities in HPV16-infected keratinocytes

Abstract

Human papillomaviruses (HPVs) are the most common sexually transmitted infectious agents. A subset of HPVs are oncogenic and can initiate cancers of the mucosal epithelium. HPVs are involved in >99% of all cervical cancers, as well as other anogenital cancers. An increasing percentage of oropharyngeal cancers are also associated with HPV16 infection. Previous studies suggest there is interplay between the EGFR pathway and oncogenic HPV activities including the ability of viral oncoproteins to augment EGFR signaling and EGFR effectors to influence HPV gene expression. We therefore hypothesize that, upon infection, the oncogenic HPVs establish a positive feedback loop with the EGFR pathway wherein viral oncoproteins enhance host cell signaling, which in turn results in upregulation of early viral gene transcription. We further postulate that interruption of this loop would lead to decreased viral oncoprotein levels and sensitize the cells to apoptotic stimuli. To test these hypotheses we used syngeneic HPV-negative and HPV16-positive cell lines, the latter harboring episomal viral genomes and modeling early HPV infection. We found that EGFR stimulation upregulated viral early transcription whereas treatment with cetuximab, an EGFR inhibitor, resulted in decreased viral transcript levels, as hypothesized. Furthermore, in the cell line harboring episomal HPV16 genomes, sustained EGFR inhibition led to reduced viral genome levels. Our results demonstrate that EGFR inhibitors display antiviral activity including reduction of viral oncogene expression and diminished episomal viral genome burden. These data suggest that EGFR inhibitors should be

investigated clinically for their anti-HPV effects, which may reduce tumor growth and/or be useful as neoadjuvants to sensitize HPV-induced tumors to effective doses of DNA damaging agents.

3.1 Introduction

Human papillomaviruses (HPVs) are the most prevalent cause of sexually transmitted infections and the majority of sexually active individuals will become HPV infected in their lifetime [81]. There are over 100 genotypes of HPVs that are grouped into high- and low-risk types based on their ability to cause lesions with a high-risk of progressing to malignancies [10]. The oncogenic HPVs are estimated to be responsible for nearly 5% of all cancers worldwide [5]. The role of oncogenic HPVs, including HPV types 16, 18 and 31, in the development of cervical cancers is well-documented [139]. Additionally, HPVs are implicated as etiological agents of cancers at other anogenital sites, as well as a subset of cancers of the oropharynx [5-7].

The HPV oncogenes E5, E6 and E7 are required for a productive viral infection. These proteins are expressed early in the viral life cycle and enhance cellular proliferation and survival, enabling a productive viral lifecycle ending in production of viral progeny [140]. The best-known functions of E6 and E7 are inactivation of key cell cycle checkpoint and tumor suppressor proteins, p53 and pRb, respectively. E6 degrades p53 *via* the ubiquitin ligase pathway, whereas E7 destabilizes and inactivates pRb [43, 44, 58, 141, 142]. The E5 protein augments epidermal growth factor receptor signaling and enhances transformation by E6 and E7 [143]. However, the functions important in the productive life cycle can become dysregulated and lead to transformation. E6 and E7 can each induce cellular immortalization [39-42]. In a productive infection, the viral E2 protein negatively regulates E6 and E7 expression, thus striking a balance between host cell proliferation and the need for increased epithelial differentiation to complete the later stages of the HPV life cycle [144].

The EGFR signaling pathway appears to be vital in HPV infections both during entry and establishment of infection as well as the maintenance of a persistent infection. EGFR is a crucial regulator of many epithelial processes and mediates responses to various external stimuli [110]. Normally, activation of EGFR occurs by binding of ligand to the extracellular portion of the receptor, followed by receptor dimerization, trans-phosphorylation and activation of downstream signaling molecules. EGFR signal transduction leads to cellular proliferation, migration and/or survival and is important in tissue development, growth and wound-healing responses [108, 110].

We previously showed that EGFR activation plays an essential role in the initial infection of human keratinocytes by oncogenic HPVs, perhaps by regulating virus uptake into cells [98, 145, 146]. EGFR also appears to be important following establishment of infection. Many prior studies reported that HPV proteins, typically when ectopically over-expressed in isolation or in transformed cells, augment EGFR signaling and provide a cellular growth advantage. For instance, E6 and E7 each upregulates EGFR expression at the genome level [122, 123]. E5 increases EGFR recycling to the cell surface after activation-induced internalization, possibly through E5's viroporin-like activities in the early endosome [63-67, 72]. In addition to providing a cellular phenotype that is favorable to the HPV life cycle, EGFR signaling may play a more direct role in the establishment and maintenance of a productive infection. The long control regions (LCR) of oncogenic HPV genomes contain multiple binding sites for many transcription factors including AP-1 transcription factors, which are downstream effectors of EGFR signaling (reviewed in [125]). AP-1 family members have been shown to mediate early transcription of HPV16 [127-131] and HPV18 [147, 148 Zenz, 2005 #3596, 149].

The data showing that HPV16 oncoproteins can increase EGFR signaling and that EGFR's downstream effectors can upregulate HPV early transcription led us to hypothesize that oncogenic HPV infection establishes a positive feedback loop with the EGFR signaling pathway (Fig 3.1A). We posit that HPV mediated upregulation of EGFR signaling in infected cells promotes increased transcription of viral oncogenes and contributes to the maintenance of infection. The corollary to this hypothesis is that creating a break in this pathway, through inhibition of EGFR, would downregulate viral oncogene transcription and allow recovery of functional p53 facilitating sensitization of cells to apoptotic stimuli (Fig 3.1B).

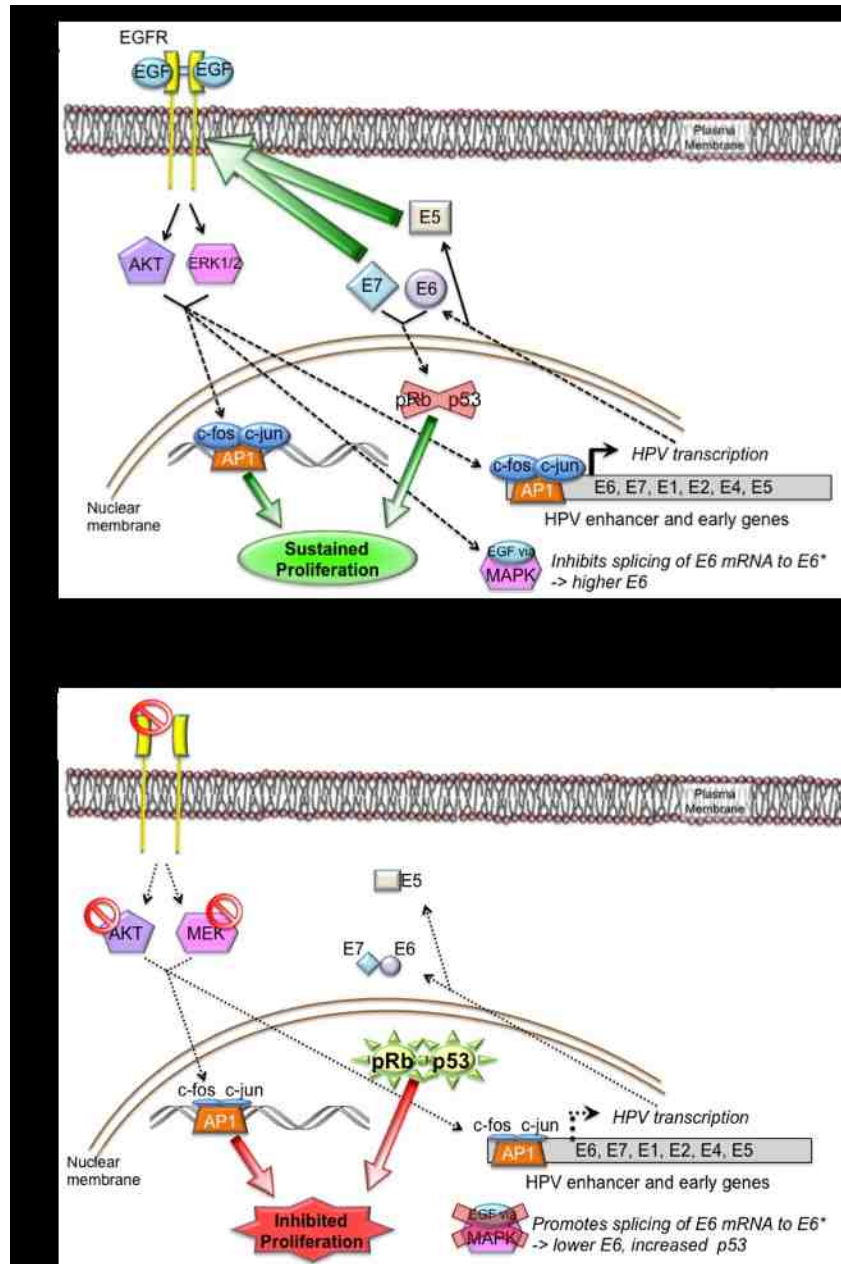


Figure 3.1 Hypothesized feedback loop between HPV and EGFR.

HPV enhances EGFR expression and signaling, resulting in upregulation of viral oncogene expression (A). We hypothesize that creating a break in the feedback loop via use of EGFR pathway inhibitors is hypothesized to downregulate viral oncogene expression and protein levels and allow recovery of functional p53 and pRb (B).

3.2 Methods

3.2.1 Cell Culture

The NIKS cell line was derived from normal immortalized human foreskin keratinocytes [136]. The NIKS-SG3 cell line was created by stable transduction of an episomally replicating, circular wild-type HPV16 genome into NIKS cells and was a gift from Prof. Paul Lambert (Univ. Wisconsin-Madison) [135]. NIKS and NIKS-SG3 cell lines were co-cultured with mitomycin C-treated NIH 3T3 J2 fibroblast feeder cells in E media containing 10% fetal calf serum (FCS) (Sigma; Atlas Biologicals), with or without 10 ng/mL murine EGF (mEGF) (BD Bioscience) as described previously [137]. J2 fibroblasts were propagated in high-glucose DMEM (Irvine Scientific) supplemented with 10% newborn calf serum (Atlas Biologicals), 2mM glutamine, 100U penicillin, 1 ug/mL streptomycin (Sigma), and 5 ug/mL Plasmocin (Invivogen). J2 fibroblasts were treated with mitomycin C (24uM) for 2 hours followed by washing 3x with at least 5 mL of 1X phosphate buffered saline (PBS) each. Cell lines were authenticated by short tandem repeat analysis (Genetica) and used within 10 passages of verification. Fibroblast-conditioned E media was obtained from mitomycin C-treated J2 cells that were incubated 24 h with normal E medium lacking EGF; media were collected, cell debris removed and media stored at 4°C until use. For all experiments, keratinocytes were plated without feeder cells in regular E media or fibroblast-conditioned E media as indicated.

3.2.2 Cell Viability Assays

Cells were treated for 7 days in fibroblast-conditioned E medium lacking exogenous EGF; media were replaced every 48 hours. MTT assays were performed according to the manufacturer's directions (Invivogen).

3.2.3 Treatment With Targeted Inhibitors

Cetuximab (2 mg/mL, Bristol-Myers Squibb) was obtained from the University of New Mexico Hospital Pharmacy. Stock solutions of PD98059 (Sigma), BKM120, and SB202190 (both Selleck Biochemicals) were prepared in DMSO at 50 mM, 1 mM, and 50 mM respectively. Experimental samples were normalized to vehicle-only treated cells containing an equal concentration of 0.9% NaCl (cetuximab and EGF) or DMSO (tyrosine kinase inhibitors).

3.2.4 Cisplatin Treatment

To evaluate changes in levels of p53 induction in EGF and EGFR inhibitor treated cells, DNA damage was initiated by addition of 6.6 μ M (IC₃₀ as determined by MTT assay) cisplatin (Sigma) to cell culture media. Where indicated, cells were treated with cisplatin for 24 hours prior to protein harvest.

3.2.5 Protein Isolation and Immunoblot

Subconfluent plates of cells were lysed on ice in RIPA buffer (50mM Tris, 150mM NaCl, 1% Triton X-100, 0.1% SDS, 5mM EDTA, 1% deoxycholic acid) supplemented with 1X HALT protease/phosphatase inhibitor (Pierce), and 0.2mM sodium orthovanadate. Samples were centrifuged at 12K x g for 15 minutes at 4°C and supernatants transferred to new tubes. Protein concentrations were determined by Bradford assay (BioRad

Protein Reagent). Laemmli sample loading buffer (6X) (62.5 mM Tris-HCl pH 6.8, 2% sodium dodecyl sulfate, 40% glycerol, 0.05% bromophenol blue) with 0.05% β -mercaptoethanol was added to samples to a final concentration of 1%. Total proteins (10-20 μ g) were subjected to 10% sodium dodecyl sulfate-polyacrylamide gel electrophoresis. Proteins were transferred to Immobilon-P PVDF membrane (Millipore) using the TransBlot Turbo semi-dry transfer system (BioRad) or wet transfer using western transfer buffer (0.25 M Tris, 0.192 M glycine, 20% methanol). Membranes were blocked with 1% bovine serum albumin in Tris buffered saline-Tween-20 (20 mM Tris, 137 mM NaCl, 0.1% Tween-20) (TBS-T) and incubated with primary antibodies overnight at 4°C. Antibodies from Cell Signaling: p-EGFR (Tyr1173) (53A5) and p-EGFR (Tyr1068) (D7A5), p-p44/42 MAPK (20G11), total EGFR (D83B1) (each 1:1000 overnight at 4°C). Antibodies from Calbiochem: p53 (DO-1) (1:1000), p16 (NA29) (1:200). HRP-conjugated anti-mouse and anti-rabbit secondary antibodies (Abcam and Millipore) were used at a 1:10,000 dilution. Separate blots were prepared for phospho and total proteins. Membranes were stripped using mild PVDF stripping buffer (399.6 μ M glycine, 3.5 μ M SDS, 1% Tween 20, pH 2.2) for 10 min at room temperature followed by extensive washing in TBST. Stripped blots were re-blocked as described above then re-probed for β -actin as a loading control. Blots were visualized on a Bio-Rad ChemiDoc station and analyzed by densitometry using Bio-Rad Image Lab software (version 2.0).

3.2.6 Nucleic Acid Collection and Analysis

Cells were lysed in TriReagent (Sigma) and RNA and DNA extracted per the manufacturer's directions. RNA was DNase treated using the TURBO DNA-free kit

(Ambion). Reverse transcription of total RNAs (0.5-1 ug each) was performed at 42°C for 60 minutes. Quantitative polymerase chain reaction (qPCR) was used to quantify HPV16 transcript (cDNA) levels as previously reported [137]. The HPV16 transcripts targeted included E6 and E7 (Bio-Rad SsoFast EvaGreen Supermix) and E1^{E4/E5} (Bio-Rad iQ Supermix); viral cDNA levels were normalized to cellular β-actin cDNA levels (Bio-Rad iQ Supermix). Total DNA (0.5ug) was used for qPCR analysis of viral genome copy numbers using primers targeted to the HPV16 long control region (LCR) (Bio-Rad SsoFast EvaGreen Supermix). qPCR reactions were performed on a Bio-Rad CFX96 and analyzed using Bio-Rad CFX Manager (version1.6.541.1068). All qPCR data were normalized to reference levels using the ΔC_q method [$\text{Ratio (reference/target)} = 2^{C_q(\text{reference}) - C_q(\text{target})}$] and expressed as percent or fold change relative to mock or untreated sample. Statistical analysis was performed using the Student's *t*-test or 2-way ANOVA in GraphPad Prism statistical software (Version 6).

3.2.7 Measurement of Cell Surface EGFR

Keratinocytes were seeded at 1×10^6 cells/well of a 6-well plate without fibroblast feeder cells in complete E media lacking EGF and allowed to attach overnight. Cells were dissociated using 0.25% trypsin-EDTA (Sigma) for 20 minutes. Trypsin was quenched with complete E medium and cells pelleted at 1K RPM for 5 minutes followed by washing with 2 mL cold 1X PBS. Cells were resuspended in 100 μ L of cold 1X PBS and incubated with 2 μ g AlexaFluor-647 labeled anti-EGFR antibody R-1 (Santa Cruz Biotechnology) for 30 minutes at 4°C with mixing. Antibody-binding beads from Quantum Simply Cellular anti-Mouse Kit (Bangs Laboratories) were labeled concurrently for each experiment. Cells and beads were each washed and resuspended

according to manufacturer's directions. Fluorescence signal was detected by flow cytometry using BD LSR Fortessa (Flow Cytometry Shared Resource Center supported by the University of New Mexico Health Sciences Center and the University of New Mexico Comprehensive Cancer Center) and data were analyzed using FACS DIVA software. Regression curves were created using median fluorescence from each bead population with the *QuickCal v2.3 Data Analysis Program* (Bangs Laboratories).

3.3 Results

3.3.1 EGF Stimulation Results in Increased Viral Transcription in HPV16-Positive Human Keratinocytes

Previous studies indicated that EGFR signaling can modulate HPV early transcription. For example, EGF stimulation of SiHa cells, a cervical cancer cell line harboring integrated HPV16 genomes, resulted in increased E6 and E7 gene expression [130]. However, EGFR activation in other keratinocyte cell lines immortalized with HPV16 and harboring integrated viral genomes inhibited HPV early transcription [134]. NIKS-SG3 is an HPV16-positive cell line developed from the near diploid NIKS human keratinocyte cell line, and maintains \approx 1-10 copies per cell of extrachromosomal HPV16 genomes. These cells initiate late virus life cycle stages when cultured as differentiating organotypic tissues [135], thus representing a persistently HPV16-infected, pre-neoplastic state. To determine how EGF stimulation affects viral transcription in the proliferative context of episomally replicating HPV16 genomes, NIKS-SG3 cells were cultured in the presence of a physiologically relevant level of EGF (5 ng/mL). HPV16 early transcripts potentially encoding the oncoproteins E6, E7, and E5 were quantified to reveal increased viral transcript levels at 24 h, and significantly higher levels by 48 h post treatment (Fig 3.2). These data indicate EGF activation and likely EGFR signaling has a positive effect on HPV transcription in proliferating cells maintaining episomal HPV genomes.

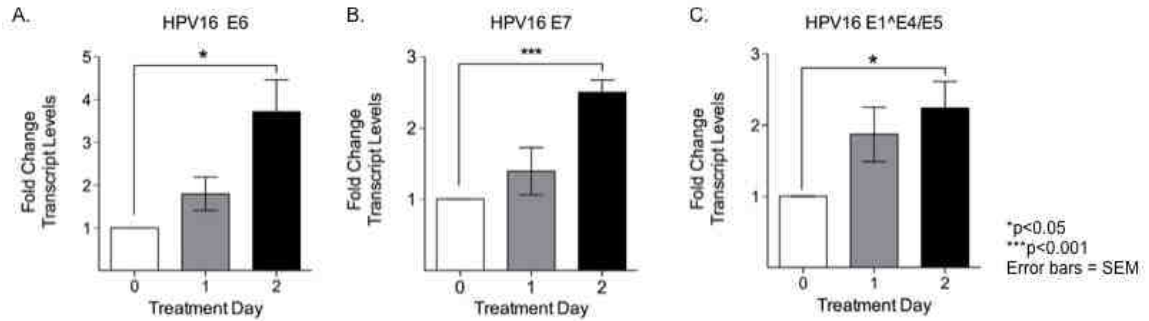


Figure 3.2 EGF stimulation results in increased viral transcription in HPV16-positive NIKS-SG3 cells.

Cells were incubated in the presence of 5 ng/mL EGF for the indicated times. Total RNA was analyzed by RT-qPCR for levels of HPV early transcripts E6 (A), E7 (B) or E1^{E4/E5} (C). Results were normalized to β -actin transcripts and are shown as fold-change over mock treated cells. Error bars = SEM, * $p < 0.05$, *** $p < 0.001$. Data summarizes 4 independent experiments.

3.3.2 HPV16 Infection Does Not Significantly Alter EGFR Expression or Signaling in Proliferating Cells

HPV infection is well documented to render cells less dependent upon EGF for proliferation or survival [132, 135, 150]. HPV early proteins E5, E6 and E7 have each been reported to enhance EGFR expression and/or downstream signaling in cells ectopically expressing high levels of these proteins [63-66, 72, 122]. However, whether the viral oncoproteins expressed from their natural promoters and in the physiologically relevant context of replicating HPV16 genomes can modulate EGFR signaling in proliferating human keratinocytes has not been investigated to our knowledge. We therefore sought to determine if HPV status conferred any differences in EGFR expression or signaling in isogenically matched NIKS cell lines.

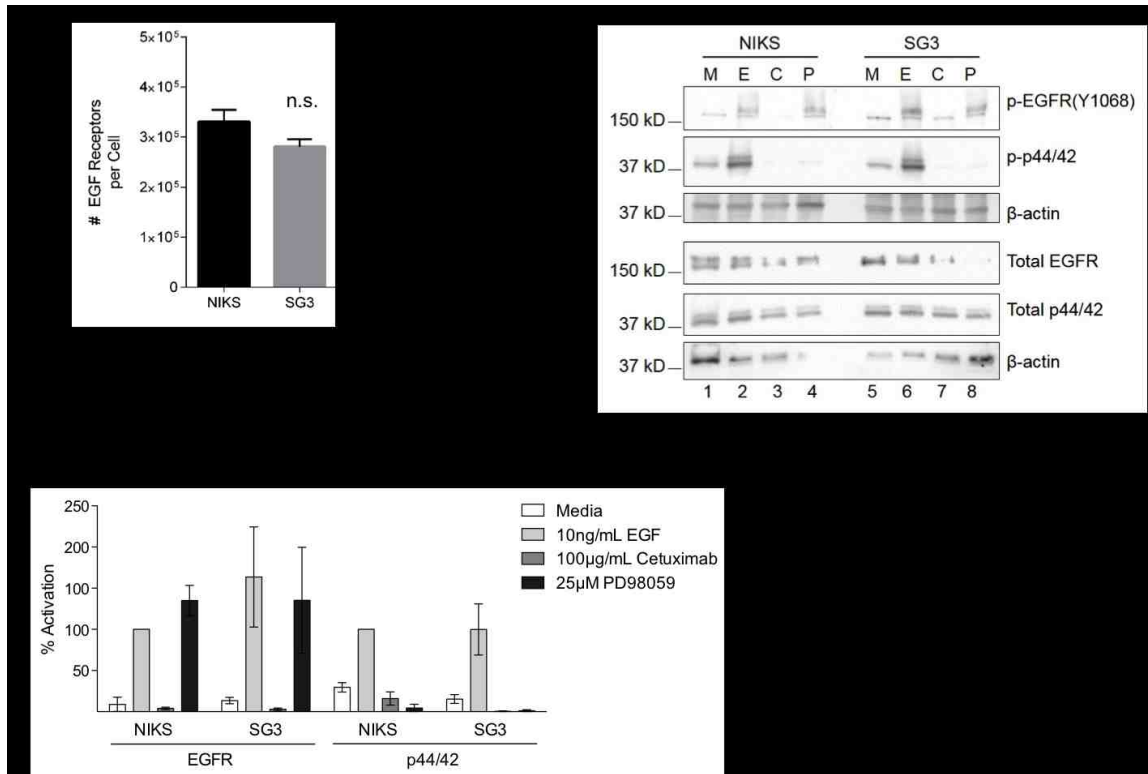


Figure 3.3 Cells maintaining HPV16 genomes do not exhibit significantly heightened EGFR signaling, and remain sensitive to EGFR pathway inhibition.

(A) The number of EGFR proteins on plasma membrane was quantified by flow cytometry. An average of three independent experiments is shown. (B) NIKS and NIKS-SG3 were serum-starved for 8h and treated with 100 µg/mL cetuximab or 25µM PD98059 before (4 hours/cetuximab or 1 hour/PD98059) and during exposure to 10 ng/ml EGF in serum-free media for 5 minutes. The results of three independent experiments are quantified in (C). M = media only, E = EGF only without inhibitor, C=Cetuximab, P=PD98059. Error bars = SEM.

Quantitative comparison of cell surface EGFR levels between the parental NIKS and NIKS-SG3 cells revealed slight, but not significantly lower, EGFR levels on the HPV16 positive NIKS cells (Figure 3.3A). A previous study noted that human foreskin keratinocytes (HFKs) transduced with a retroviral vector expressing HPV16 E6 had hyper-activated EGFR signaling in a ligand-dependent manner and sustained receptor activation in the absence of ligand [124]. We thus strove to determine whether the NIKS cells persistently infected with HPV16 acquired increased EGFR activity independent of receptor levels. EGFR contains multiple phosphorylation sites that direct downstream

signaling pathways and we chose to target phosphorylation at tyrosine residues 1173 and 1068 (Y1173 and Y1068, respectively), which are both capable of activating the Grb2/Sos signaling cascade that includes Ras/MAPK/MEK [151, 152]. Subconfluent, serum-starved NIKS and NIKS-SG3 cell lines were subjected to EGF stimulation. We observed heightened EGFR and downstream activation in some experimental replicates, measured by phospho-EGFR (Y1068 and Y1173) and phospho-44/42 (MEK1/2), in NIKS-SG3 cells as compared to parental HPV-negative NIKS cells upon ligand-induced activation (Fig 3.3B, lanes 2 and 5). However, no statistically significant differences were observed when replicates were averaged from multiple independent experiments (Fig 3.3C). These data suggest that HPV16 early gene expression may increase signaling downstream of EGFR, but this is not pronounced in proliferating cells.

3.3.3 HPV16-Positive Cells Are Sensitive to EGFR and MEK Inhibitors

To test the sensitivity of the cell lines to EGFR and MEK pathway inhibitors, we pretreated cells with the EGFR antagonist cetuximab, a monoclonal antibody that blocks ligand activation and induces receptor downregulation [153], or PD98059, a potent inhibitor of MEK1/2, prior to stimulation with EGF. Cetuximab inhibited EGF-mediated EGFR activation in both HPV-negative and HPV-positive cell lines as measured by detection of p-EGFR (Y1068) (Fig 3.3B lanes 3 and 6) and p-EGFR(Y1173) (data not shown), and completely diminished p-44/42 (MEK1/2) levels in the cell lines (Fig 3.3B lanes 3 and 6). Furthermore, treatment with PD98059 resulted in complete block of ERK1/2 phosphorylation in both cell lines (Fig 3.3B lanes 4 and 8). Therefore, HPV infection does not markedly alter sensitivity of NIKS-SG3 to EGFR/MEK inhibitors.

3.3.4 EGFR Signaling Dependency in HPV16-Positive Cells

Previous studies found that HPV16 early gene expression, in particular the E5 gene product, provides cells with growth factor independence [132, 135, 150]. Therefore, we expected the NIKS cells maintaining episomal HPV16 genomes would have a survival advantage compared to their uninfected parental NIKS cells when EGFR signaling was inhibited. The cell lines seeded at subconfluent densities were treated with increasing concentrations of inhibitors or vehicle for 7 days. Treatment media were refreshed every 2 days and cell viability was determined on day 7.

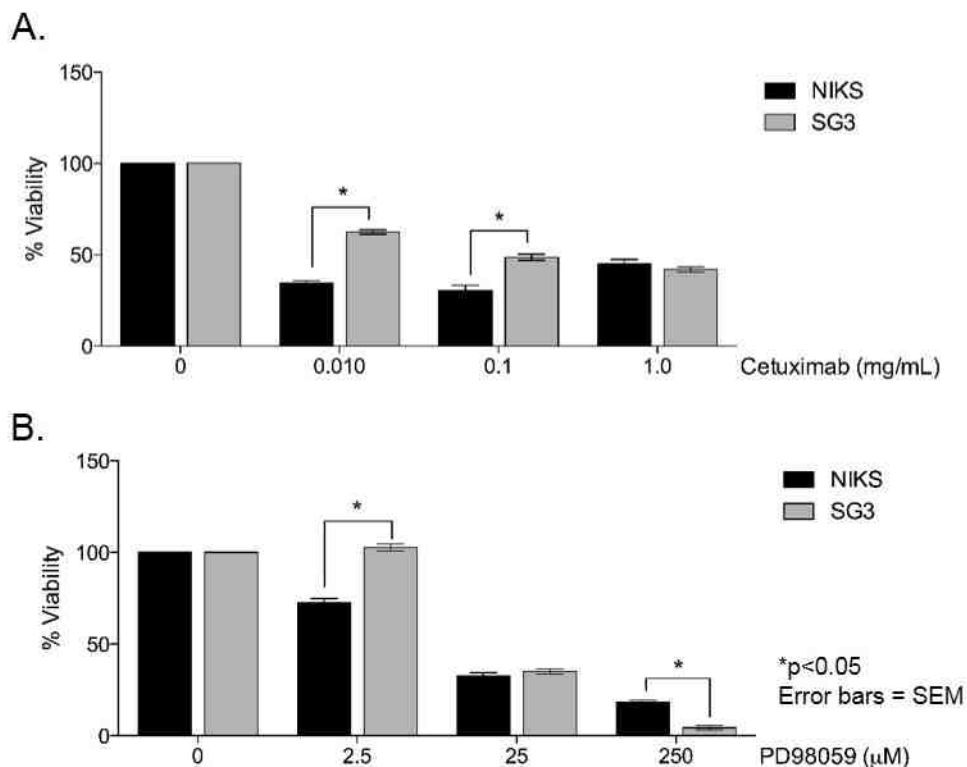


Figure 3.4 Dependence of HPV-positive and HPV-negative NIKS on EGFR and MEK1/2 signaling for cell survival.

NIKS and NIKS-SG3 cells were grown 7 days in the presence of cetuximab (10 µg/mL, 100 µg/mL, 1 mg/mL) (A) or PD98059 (2.5 µM, 25 µM, and 250 µM) (B). Data are the result of 3 independent experiments. Error bars = SEM. *p<0.05.

At the highest concentrations tested (1.0 mg/ml cetuximab), the HPV-negative and HPV-infected NIKS cells had similar viability (Fig. 3.4A). However, the NIKS-SG3 cells were less sensitive to the EGFR inhibitor at the lower concentrations tested (Fig. 3.4A). Viability in the presence of MEK1/2 inhibition was also evaluated. NIKS-SG3 cells exhibited significantly higher viability in the presence of low dose (2.5 μ M PD98059) MEK inhibitor than HPV-negative NIKS (Fig. 3.4B). There was no apparent difference in viability at moderate dosage of inhibitor which reduced NIKS viability to similar levels as the 0.1 mg/mL cetuximab treatment. However, we found that NIKS-SG3 cells were much more sensitive to higher doses of MEK1/2 inhibition than NIKS, and this was true across multiple independent experiments (Fig. 3.4B). These findings indicate the EGFR/MEK pathway is important for the proliferation of human keratinocytes whether they maintain HPV genomes or not, but show that HPV16 infection significantly reduces the dependence of the cells on EGFR and MEK1/2 signaling. This data supports our hypothesis that HPV affects the EGFR pathway and agrees with previous studies indicating that HPV infection partially imparts growth factor independence to infected cells [132, 135, 150].

3.3.5 EGFR/MEK Inhibition Has Antiviral Effects

As EGFR pathway activation resulted in increased HPV transcription in cells maintaining episomal viral genomes (Fig. 3.2), we predicted that inhibiting EGFR signaling would have a negative effect on viral activities. Cells were grown in the presence of 100 μ g/mL cetuximab, the intermediate concentration tested in Fig 3.4A, and total early viral transcript levels were assessed (Fig 3.5A). EGFR inhibition resulted in a marked

decrease in HPV16 E6, E7 and E1^{E4/E5} transcript levels by 24 h treatment. Inhibition of the MEK1/2 signaling pathway by PD98059 produced similar downregulation of early viral transcripts (Fig. 3.5B). However, inhibition of PI3K, which is often mutated in HPV-positive cancers, with BKM120 did not alter expression levels of viral early transcripts (Fig. 3.5C) [154].

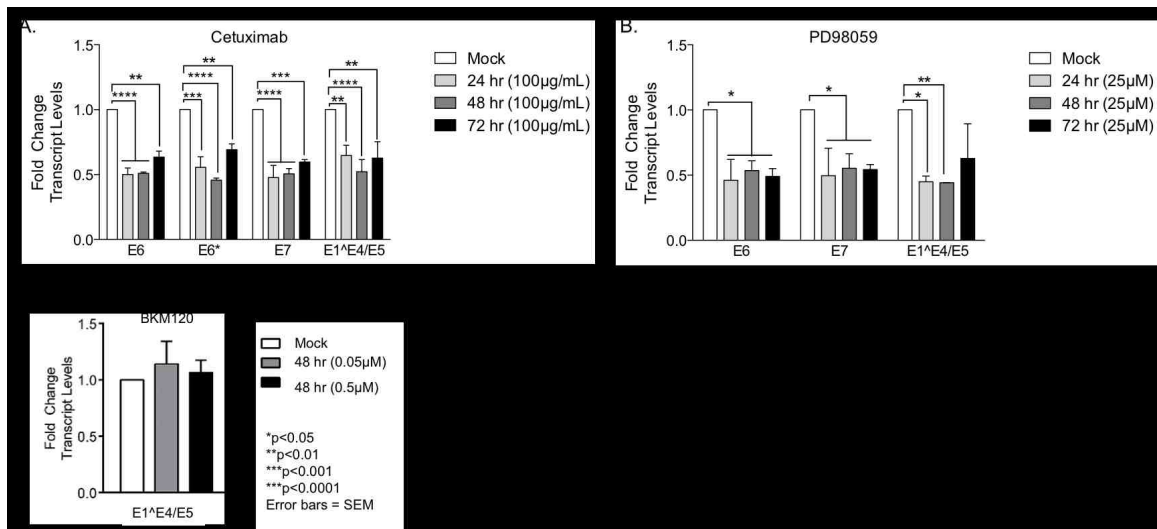


Figure 3.5 Inhibition of EGFR signaling decreases viral early transcript levels in NIKS cells maintaining episomal HPV16 genomes.

NIKS-SG3 cells were treated with 100 µg/ml cetuximab, 25 µM PD98059, or 0.5 or 0.05µM BKM120. mRNA was harvested at indicated time points and RT-qPCR performed for HPV early transcripts for cetuximab (A), PD98059 (B), or BKM120 treated cells (48 hours treatment) (C). Data were normalized to β-actin transcript levels. Mock = vehicle only. Data analyzed by 2-way ANOVA (multiple comparisons). Error bars = SEM, *p<0.05, **p<0.01, ***p<0.001, ****p<0.0001. Graphed are the results of 2 independent experiments performed in duplicate.

As early HPV gene expression is needed for viral genome maintenance (reviewed in [18] and [17]), we surmised viral DNA replication might also be negatively impacted by reduced EGFR/MEK signaling. We detected a statistically significant decrease in viral genome copies by 48 hours post-exposure to either inhibitor, and levels continued to diminish over six days of treatment (Fig 6). Together, these data indicate that cetuximab

has anti-viral effects in cells harboring episomal HPV genomes. MEK inhibition resulted in almost identical decrease of viral transcription and genome levels while PI3K inhibition had no effect on viral transcript levels. These data indicate that EGFR signal transduction through the MEK/ERK pathway is responsible for mediating the viral effects, and further support our hypothesis that EGFR signaling modulates HPV16 early transcription.

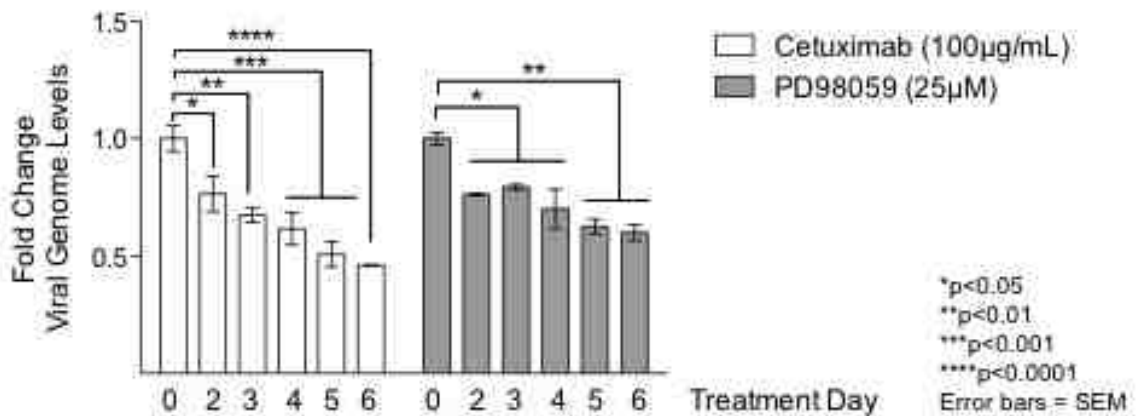


Figure 3.6 Inhibition of EGFR and MEK signaling decreases viral genome copy numbers in NIKS cells maintaining episomal HPV16 genomes.

NIKS-SG3 cells were treated with 100 µg/ml cetuximab or 25 µM PD98059. Total cellular DNA was harvested at indicated time points and qPCR performed for HPV16 LCR. Data were normalized to total µg DNA. Mock = vehicle only. Data analyzed by 2-way ANOVA (multiple comparisons). Error bars = SEM, *p<0.05, **p<0.01, ***p<0.001, ****p<0.0001. Graphed are the results of 2 independent experiments performed in duplicate.

3.3.6 HPV-Infection Does Not Significantly Alter p53 Levels in NIKS-SG3

We showed HPV16 early gene expression is responsive to activation or inhibition of EGFR signaling. Thus, we expected the levels of viral oncoproteins and oncoprotein activities to coincide with altered EGFR signaling. Specifically, we anticipated changes in E6/E7 RNA and protein to inversely correlate with p53 levels. E6 and E7 protein levels are notoriously difficult to detect in HPV infected precancerous cells, and a direct

relationship between E6 and E7 RNA levels and oncoprotein levels has not been determined. Therefore, we assayed cellular surrogates of E6 and E7 oncoprotein activities. E7 inactivation of pRb leads to increased p16 expression and p16 is a widely accepted surrogate of HPV infection [73-76]. Thus, we evaluated the levels of p53 and p16 in cells treated to activate or to inhibit EGFR signaling. The comparable levels of p53 in treated NIKS-SG3 and NIKS was somewhat surprising and suggests that HPV16 E6 proteins are not robustly expressed in NIKS-SG3 cells. This is likely because this cell line contains only 1-10 copy(s) of the viral genome per cell [135]. Additionally, levels of E6 and E7 are kept tightly regulated by viral processes in non-transformed, undifferentiated cells, further explaining the lack of difference in p53 levels between NIKS and NIKS-SG3 (reviewed in [20]). Initial experiments showed no difference in p53 levels following EGFR activation or inhibition for 72 hours in NIKS-SG3 (data not shown). Because stimulation of p53 activity may be required to observe any virally mediated changes in p53 protein levels following incubation with EGF or cetuximab, we stimulated p53 activity by incubating cells with the DNA damaging agent, cisplatin. Cells were pretreated with EGF or inhibitor for 48 hours then cisplatin was added to induce DNA damage and enhance p53 levels and activation for the last 24 hours of treatment. Nevertheless, MTT assay results from cells treated with cisplatin and those without cisplatin exposure appeared similar. When normalized to β -actin levels, total p53 levels in untreated cells were not significantly altered in HPV-positive NIKS-SG3 cells as compared to HPV-negative NIKS cells (Fig. 3.7AB; compare lanes 1 and 2). We interpret this to mean that E6 levels are maintained at low levels in these cells and therefore p53 levels are not noticeably affected. Although EGF stimulation for 48 hours

led to a ~3.5-fold increase in E6 RNA (Fig. 3.2A), levels of p53 protein also increased on average, which is not consistent with our hypothesis that downregulation of viral transcript levels and presumed decrease in E6 protein would lead to decreased p53 levels (Fig 3.7AB; compare lanes 2 and 3). These results may be independent of viral functions and instead due to the fact that EGF treated cells are actively proliferative therefore initiate DNA damage repair machinery more robustly. Furthermore, while viral oncogene RNAs were reduced by 50% when cells were treated 48 hours with EGFR and MEK inhibitors, we detected no significant difference in p53 levels under similar conditions (Fig 3.7A).

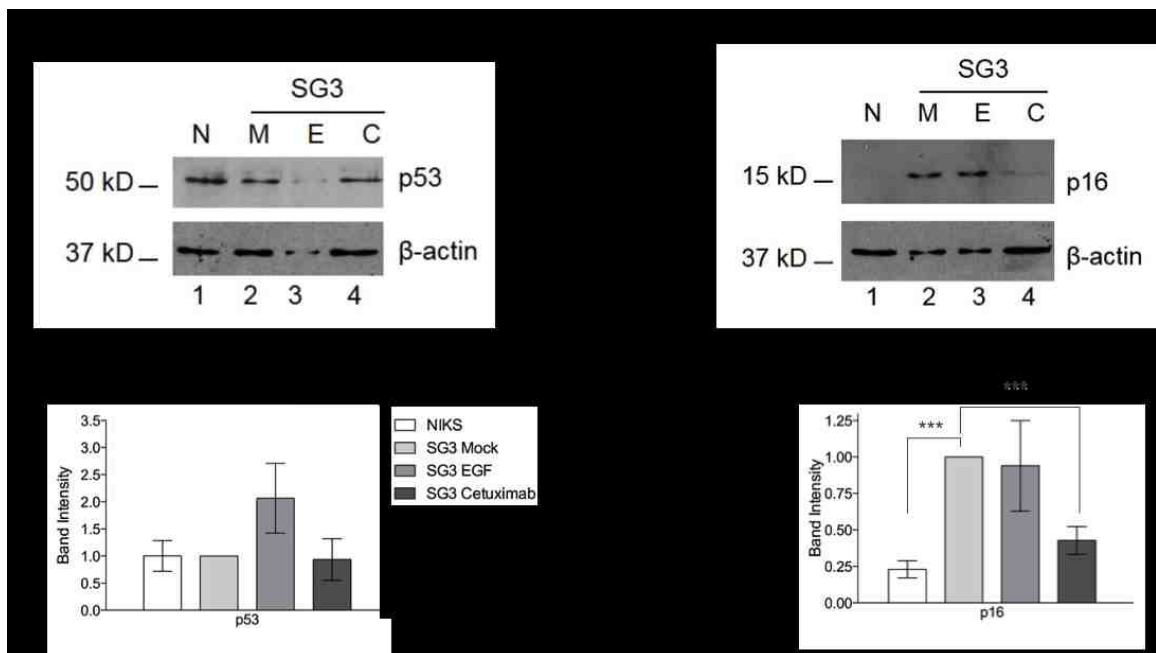


Figure 3.7 HPV-infection does not significantly alter p53 levels in NIKS-SG3 cells but increases levels of p16.

NIKS-SG3 cells were treated with cetuximab or EGF for 72 hours. Protein levels of p53, p21 (A), p16 (C) and β-actin were assessed by immunoblot in NIKS (N) or NIKS-SG3 treated with media alone (M), 10 ng/ml EGF (E), 100 μg/ml cetuximab (C); fold change of p53 and p21 levels (B) and p16 levels (C) were analyzed from three separate experiments. Error bars = SEM.

Interestingly, a significant upregulation of p16 was seen in mock-treated NIKS-SG3 cells as compared to NIKS suggesting more robust expression of active E7 protein in the NIKS-SG3 cells (Fig. 3.7CD; compare lanes 1 and 2). Although EGF exposure increased E7 transcripts by ~1.5 fold after 2 days, p16 levels were not significantly changed upon EGF stimulation (Fig 3.7CD; compare lanes 2 and 3). However, cetuximab treatment decreased p16 levels in NIKS-SG3 to near those in the parental cell line, NIKS (Fig. 3.7CD; compare lanes 1 and 4). This decrease in p16 levels corresponds with the downregulated E7 transcript levels seen following EGFR inhibition (Fig 3.7A) and indicates a corresponding reduction in E7 protein levels. Furthermore, these data indicate that inhibition of EGFR can have antiviral effects on infected cells even in cases of low levels of viral activity.

3.3.7 EGFR Inhibition Sensitizes HPV-Positive Cells to Apoptotic Stimuli

Cisplatin, a DNA cross-linking agent, induces the formation of DNA adducts that activate p53 leading to apoptosis in cells with normal tumor suppressor functions and catastrophic DNA damage in highly proliferative cells lacking wild-type p53 [155]. As another measure of viral oncoprotein depletion and tumor suppressor protein restoration, we sought to determine if cetuximab-induced reduction of viral oncogene expression levels could sensitize cells to DNA damaging agents. NIKS-SG3 cells were pretreated with cetuximab for two or six days prior to cisplatin exposure, were treated concurrently with cetuximab and cisplatin, or treated with cisplatin alone. Cell viability was determined at 72 hrs post cisplatin treatment at the timing indicated in Fig. 3.8A.

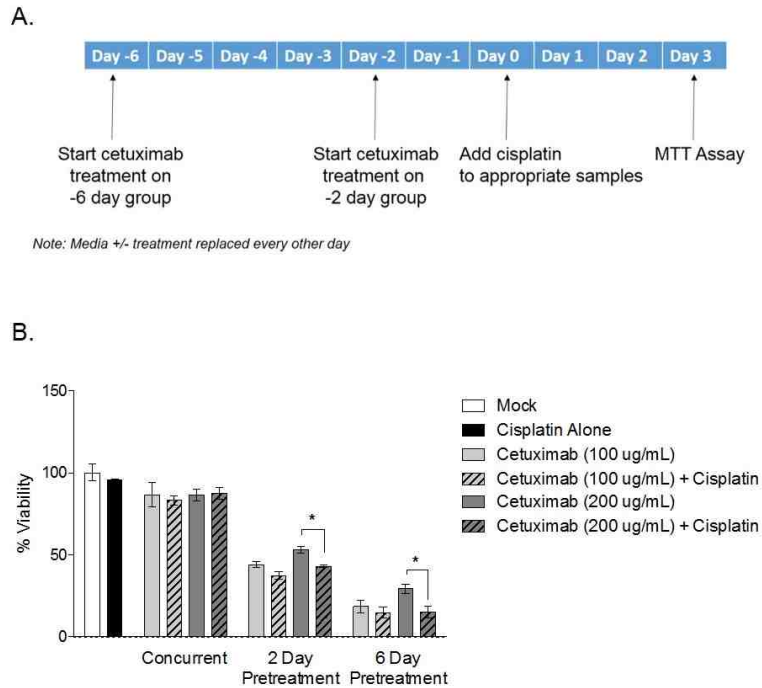


Figure 3.8 EGFR inhibitors sensitize HPV16-positive cells to apoptotic stimuli.

(A) Experimental design. (B) NIKS-SG3 cells were left untreated or exposed to cetuximab at the indicated concentrations for 6 or 2 days prior to, or concurrent with cisplatin treatment. Cell viability was determined by MTT assay 72 hr after cisplatin treatment. Error bars = SEM, * $p < 0.05$. Data are the result of 1 experiment performed in triplicate.

NIKS-SG3 cells treated only with cisplatin showed minimal loss of viability (Fig. 3.8B). Cells treated concurrently with cisplatin and cetuximab had only a slight reduction in viability as compared to media alone or cisplatin alone, concurrent delivery of cetuximab and cisplatin together showed no benefit over either agent alone. As expected from figure 3.4A, treatment with cetuximab alone resulted in ~50 – 75% loss of viability for 2- and 6 day pretreatment, respectively, when compared to the media only control. When cetuximab was administered as a neoadjuvant to cisplatin, further loss of viability was seen at both concentrations of EGFR inhibitor. Loss of viability in the neoadjuvant groups was significantly greater in the group receiving the higher dose of cetuximab. These results indirectly support our corollary hypothesis that EGFR inhibition has

antiviral effects that restore tumor suppressor activity. Surprisingly, we did not observe a dose response to cetuximab. As the MTT assay does not directly measure cell death, this experiment might be best repeated using a clonogenic assay to evaluate the effects of cetuximab. Testing the ability of cetuximab to sensitize cells to ionizing radiation rather than cisplatin would also be informative. Additionally, this loss of viability could be due to recovery of pRb functions as well, as we saw reduction of the p16 levels in HPV-positive NIKS-SG3 following cetuximab treatment (Fig 3.7AB). In continuing this work, it will be important to determine which viral and cellular components are most affected by cetuximab-induced HPV oncoprotein downregulation.

3.4 Discussion

HPVs are the infectious agent responsible for multiple types of squamous cell carcinomas including cervical, anogenital and oropharyngeal [5, 6 zur Hausen, 2009 #3649, 7, 139]. Most HPV infections resolve without medical intervention. However, persistent infection with HPV increases the potential of developing a pre-cancerous or malignant lesion. In this study we demonstrated that the EGFR pathway is important in the regulation of HPV16 oncogene transcription and maintenance of viral genome levels. Importantly, inhibition of this pathway has antiviral effects suggesting that EGFR activation plays a role in maintenance of infection and may be a critical vulnerability.

This work shows that positive feedback between EGFR signaling and HPV16 oncoproteins is subtle in preneoplastic cells. Unlike previous studies using ectopic overexpression of viral oncoproteins, our HPV-positive cell line did not exhibit the expected degree of EGFR pathway upregulation when measured by flow cytometry and

immunoblot in cells from subconfluent monolayers. We detected slightly lower levels of cell surface-associated EGFR in our HPV-positive cell line (Fig 3.3A). And while we occasionally observed heightened EGFR and ERK1/2 activation in NIKS-SG3 cells as compared to NIKS cells, overall, EGFR-signal transduction was not significantly elevated in HPV-positive cells (Fig 3.5BC). The HPV-positive NIKS-SG3 cells demonstrated higher viability when grown in the presence of EGFR and MEK inhibitors than did NIKS cells (Fig 3.4). This indicates that HPV infection imparts growth factor independence in proliferating cells that maintain episomal HPV genomes, agreeing with previous reports by other labs.

HPV16 E6 and E7 have been shown to upregulate EGFR signaling [122, 123]. Additionally, viral oncoprotein E5 increases recycling of EGFR augmenting membrane availability of the receptor [63-67, 72]. There are a number of caveats to those studies. Previous studies have examined the interaction between single HPV oncoproteins and the EGFR pathway, usually employing ectopic over-expression of the viral proteins. Additionally, many of the previous studies have used cell types not typically targeted by HPV in a natural infection. To our knowledge, ours is the first study examining the interplay between high-risk HPV and EGFR signaling to utilize relevant cell types carrying the entire HPV genome to model pre-neoplasia. Additionally, our use of isogenically matched HPV-negative and HPV-positive cell lines enables us to directly address differences due to viral effects in our model. Compared with the previously described effects of HPV16 oncoproteins on EGFR signaling, our data suggest that the effect of viral oncogenes on the EGFR pathway is subtle in proliferating cells modeling persistent infection. These results reinforce the importance of evaluating viral gene

function in the context of “normal” virus replication rather than in systems over-expressing a single or multiple viral genes.

We found that EGFR activation positively affected HPV oncogene transcript levels in NIKS-SG3 cells. NIKS-SG3 cells carry HPV16 genomes extrachromosomally in the background of a near-diploid immortalized human foreskin keratinocyte cell line. As this cell line is capable of carrying out late viral life-cycle events in the raft system [135], it represents persistently infected, preneoplastic keratinocytes. Previous studies have shown that EGFR signaling can modulate HPV early transcription in keratinocytes. Our findings agree with a previous study showing that EGFR activation by its cognate ligand resulted in increased HPV16 E6/E7 transcript levels in the SiHa cervical-carcinoma derived cell line as soon as 2 hours post ligand addition [130]. Another study demonstrated that 48-hr EGF exposure of PHK160b, a cell line derived from primary epidermal keratinocytes immortalized by transfection with wild-type HPV16 genome, resulted in down-regulation of HPV early transcripts E6/E7 as assayed by northern blot [134]. This effect of EGFR stimulation was seen concurrently with an EGFR activation-induced increase in cell proliferation and c-myc expression. Both of these previous studies utilize cell lines immortalized by HPV16 and harbor integrated viral genomes. SiHa cells contain 1.5 viral genomes by whole genome sequencing, the viral genome structure and copy number for the PHK160b cells is not published [156]. The differences reported by these authors could be due to differences in the LCR of the viral genomes or integration sites. Integration of HPV into the host genome is random although chromosomal fragile sites appear to be preferred [37, 157, 158]. Loss of the LCR upstream of viral genes could occur via a break in the viral DNA downstream of this

region prior to integration. Methylation of the viral LCR in integrated HPV genomes has also been shown to cause loss of function [157]. Additionally, insertion of the viral genome downstream of a strong host promoter could drive viral oncogene transcription even in the presence of a functional LCR [159, 160]. Further analysis of the differences in cellular genomes, proteomes and methylomes among these cell lines may help to reveal the molecular basis for these differing results.

We detected several antiviral effects of EGFR and MEK inhibition. Inhibition of EGFR signal transduction in NIKS-SG3 cells results in reduction of viral oncogene transcript levels, confirming our hypothesis that the EGFR pathway is important in the control of viral transcription (Fig 3.5A). We also discovered that this control of viral transcription is mediated through the MEK1/2 signaling pathway (Fig. 3.5B). Notably, we showed that inhibition of the EGFR pathway reduced the viral genome load in NIKS-SG3 cells (Fig. 3.6). The decrease in viral early transcript levels preceded the decreased genome levels (Fig. 3.5A and B compared with Fig. 3.6) suggesting that the loss of early protein expression results in the inability of the virus to replicate its genome. Transcripts thought to encode early viral proteins E1 and E2 are expressed from the same viral promoter as E5, E6 and E7 and are necessary for the replication and maintenance of viral genomes (reviewed in [18] and [17]). Therefore, an EGFR/MEK inhibitor-mediated decrease in early gene expression, including E1 and E2, might underlie the loss of viral genomes.

We detected antiviral effects of EGFR and MEK inhibition with regard to tumor suppressor functions. First, enhancement of viral E7 function following EGFR activation was observed in the NIKS-SG3 cell line by assessing cellular p16 levels (Fig. 3.7B). The

downregulation of p16 following cetuximab treatment further indicates that inhibition of EGFR activation downregulates E7 activities in actively infected cells and likely restores cell cycle regulation. Although RNAs with potential to encode E6 were downregulated with EGFR inhibition, we saw no change in p53 levels. This could be because E6 protein levels are low in NIKS-SG3 cells. However, our finding that pretreatment of HPV-positive cells with cetuximab sensitized cells to the DNA-damaging effects of cisplatin (Fig 3.8) indirectly suggests that p53 levels and/or function were increased in the context of EGFR inhibition and antiviral effects. DNA-damage induced apoptosis that results from cisplatin exposure can be p53-mediated [155] therefore recovery of cellular p53 in these cell lines may be responsible for the increase in cell death in the cetuximab-sensitized cells. A similar loss of cell viability was obtained by Woodworth *et al.* in HPV16 E6/E7 expressing cervical epithelial cells treated with the EGFR inhibitor erlotinib [161]. Although previous reports indicate that cisplatin can activate EGFR [162]; other studies have shown that cetuximab can inhibit this activity [163, 164]. Therefore, we do not believe this mechanism complicate our interpretation.

It might, nevertheless, be informative to repeat our experiment using ionizing radiation as the DNA damaging agent rather than cisplatin to avoid unintended EGFR activation. As we saw little HPV-associated downregulation of p53 in NIKS-SG3 cells, testing the ability of cetuximab to induce p53 recovery in a more robust system such as a preneoplastic cell line with higher HPV16 genome copies or an HPV-positive cancer cell line would also be beneficial. Our results are consistent with the findings of Meira, *et al.* who showed increased cytotoxicity in the HPV-positive CaSki cervical cancer cells in response to radiation or chemotherapy following pretreatment with cetuximab [165].

Although they did not investigate viral expression, their study suggests that the mechanism of sensitization is maintained even after oncogenic transformation. Our results are also in accord with Kimple *et al*, who found increased radiation sensitivity in cells expressing HPV16 E6 despite the effect of E6 to degrade p53. This suggests that low levels of normally functioning p53 in HPV-positive HNC cells could be activated by radiation, leading to cell death [166].

Taken together, the results of this study indicate that the EGFR pathway is important in the maintenance of HPV infection including expression of viral oncogenes and genome replication. This has implications in both active infections with high-risk HPV as well as HPV-positive carcinomas. We suggest that EGFR signaling enhances transcription of viral early genes enabling genome replication and persistent infection of the host cells. Our work also has significant implications regarding the importance of cofactors in the progression to HPV-associated cancers. Numerous predictive cofactors have been identified for cervical cancer including: parity, coinfection with other sexually transmitted infectious agents, and history of smoking [167, 168]. These cofactors may activate growth factor receptor pathways, possibly enhancing the expression of HPV oncogenes through mechanisms we have outlined herein, priming the cells for malignant transformation. In HPV infections and associated cancers, understanding the role of EGFR in maintaining viral oncoprotein levels may help to design more effective treatments and refine current treatment protocols. In productive infections, including cutaneous warts, genital warts, and recurrent respiratory papillomatosis (RRP), treatment with an EGFR or MEK inhibitor may be an alternative to current cryotherapy and surgical approaches, which result in high morbidity. In fact, several cases of RRP have

been successfully treated with the EGFR inhibitor erlotinib [169-171]. Additional clinical studies are needed to determine safety and long-term efficacy of these treatments. Cetuximab is already used in the treatment of HNSCC in conjunction with chemotherapy/radiation and some benefit has been shown for patients with advanced stage HPV-positive cancers over HPV-negative [172, 173]. However, previous clinical trials using concurrent cisplatin plus cetuximab or cetuximab as a monotherapy in cervical cancer have failed to show a therapeutic benefit for the use of EGFR inhibitors in their patient populations [174, 175]. It should be noted that cetuximab was given concurrently with cisplatin in these trials. Our data suggest cetuximab is likely to be more effective given as a neoadjuvant to induce antiviral effects prior to receiving chemoradiotherapy. Further investigation into the effect of EGFR/MEK inhibitors on viral activities driving HPV-positive cancers may be important in determining patient populations that will most benefit from these treatments.

3.5 Limitations of this study

While this study provides significant insight into the interplay between HPV and the EGFR pathway, it contains limitations. This study was carried out in a keratinocyte cell line harboring episomal HPV at low copy numbers. This cell line was selected due its ability to maintain episomal HPV genomes as well as recapitulate the viral life cycle in the organotypic raft system [135]. Therefore, we anticipated that this cell line, when grown in monolayer, would be an appropriate model for actively infected cells in the basal layer of the epidermis. In our study, these cells were maintained at subconfluent densities to avoid contact inhibition of growth. In our system, we failed to observe the

expected decrease in p53 levels in HPV-positive cells as compared to their parental cell line. However, a recent publication by Isaacson Wechsler *et al.* showed that in similar cells, growth to confluence was required for virally mediated downregulation of p53 levels [176]. For the most physiologically relevant model available, these cells should be grown in the organotypic raft system, which recapitulates stratified epidermis. Effects of EGFR activity on viral transcription can then be assessed at different points in the viral lifecycle. Additionally, as our cell lines did not robustly express E6 (based on the lack of observable downregulation of p53 levels), use of a more robust model system such as a cell line modeling an HPV-positive high-grade intraepithelial neoplasia or cancer cell line maintaining episomal genomes would be informative. Lastly, we showed that pretreatment of NIKS-SG3 cells sensitized cells to cisplatin, however the contribution of viral oncoprotein levels to this effect was not analyzed. This needs to be further evaluated, perhaps by siRNA inhibition of E6 and E7, to determine whether our result reflects viral oncoprotein downregulation or rather is a more general result of growth factor deprivation.

CHAPTER 4 - Evaluation of Anti-Viral Effects of the EGFR-Inhibitor Cetuximab in HPV-Positive Xenografts

Abstract

Head and neck cancer (HNC) is the 6th most common cancer worldwide. Historically, HNCs have been associated with a history of tobacco and alcohol use. However, there is a growing HNC patient population wherein their cancer is associated with human papillomavirus (HPV) infection. Approximately 30% of all oropharyngeal squamous cell carcinomas (OPSCCs) are HPV-positive, of these, HPV16 accounts for 90% of cases. Patients with HPV-positive OPSCC have a better prognostic outcome than patients with HPV-negative HNC. Numerous differences exist between HPV-positive and HPV-negative OPSCC yet the standard of care treatment is the same regardless of HPV-status. The EGFR inhibitor, cetuximab, is the only targeted therapy FDA approved for OPSCC. We have previously shown that inhibition of EGFR/MEK signaling by cetuximab downregulates viral oncogene expression *in vitro* in a model of preneoplasia. In this study, we sought to determine if cetuximab exhibited anti-viral effects *in vivo*, including downregulation of viral oncogene expression and restoration of the tumor suppressor p53, which is degraded by viral oncoprotein E6. Our study reveals that EGFR/MEK inhibition inhibits growth of HPV-positive xenografts and can lead to downregulation of viral oncogene expression *in vivo*. Furthermore, downregulation of the AP-1 transcription factor c-Fos appears to be associated with the antiviral effects. Administration of the MEK inhibitor, trametinib, exhibited dramatic antiviral effects in xenografts from a moderately cetuximab resistant HNC cell line indicating that treatments targeted downstream of EGFR may also be a viable therapeutic target in HPV-positive OPSCC.

4.1 Introduction

Head and neck cancer (HNC) is the 6th most commonly diagnosed cancer worldwide with over 60,000 incident cases every year [177]. Over 95% of HNC are squamous cell carcinomas (HNSCC). HNSCC are most commonly associated with heavy tobacco and alcohol use [178]. Incident cases of HNSCC attributed to these traditional risk factors have declined in the past 30 years, possibly due to public awareness of the risks of tobacco use. However, total numbers of HNSCC have not shown an equivalent pattern of decline [87, 179]. The reason behind this discrepancy is the rise in the number of HPV-associated HNSCC [87, 88, 179]. Currently, it is estimated that ~30-56% of HNSCC are HPV-positive and HPV16 alone is involved in ~90% of HPV-associated oropharyngeal SCCs (OPSCC) [88].

HPVs are the most commonly acquired sexually transmitted infectious agents and the majority of sexually active individuals will become infected at some point in their lifetimes [81]. Oncogenic, or the so called “high-risk” HPVs are the causative agent of numerous cancers including cervical, head-and-neck, anal, vulvar, and cancers of other anogenital sites [5-7, 139].

High-risk HPVs encode three oncoproteins: E5, E6, and E7. E6 and E7 are each able to induce cellular immortalization when overexpressed *in vitro* and are found expressed at high levels in HPV-positive cancers [39-42]. These proteins have multiple activities in the viral lifecycle, the outcomes of which are enhancement of cellular proliferation and inhibition of cellular differentiation [140]. These functions are achieved in part through association with and degradation of host cell cycle check point proteins including p53, degraded by E6, and pRb, which is degraded by E7 [43, 44, 58, 141, 142].

Genetic differences between HPV-positive HNSCCs and HPV-negative HNCs include disparities in the mutational landscapes, chromosomal abnormalities and gene-expression profiles [180-184]. HPV-positive HNSCCs harbor fewer mutations than their HPV-negative counterparts, an aspect attributed to HPV oncoprotein expression. Importantly, HPV-positive HNSCCs maintain wild-type *TP53* [182, 184]. The dissimilarities in these cancers is also highlighted by disparate patient outcomes; patients with HPV-positive OPSCCs tend to respond more favorably to treatment and have a better prognosis compared to patients with HPV-negative HNCs [185-187]. Although distinct genetic backgrounds likely play a role in outcome, the specific molecular mechanisms imparting the biological differences between HPV-positive and HPV-negative OPSCCs are not well defined.

Current standards of care for the primary, nonsurgical management of previously untreated, locally advanced HNSCC were developed during the era when HPV-negative disease predominated. Despite the contrasts between these cancers, the standard of care for locally advanced HNSCC (stage III-IVb), regardless of HPV involvement, is concurrent cisplatin-radiotherapy [188]. Notably, HPV status is a major independent and positive prognostic factor for patients with HNSCC, and these standards are likely to represent overtreatment. In a multivariate analysis of RTOG 0129, where patients with locally advanced HNSCC were treated with cisplatin-radiotherapy (RT), those with HPV positive tumors had a 58% reduction in risk of death compared with patients with HPV-negative tumors (hazard ratio 0.42; 95% CI 0.27-0.66) [187]. Moreover, in the Bonner trial, patients with HPV positive oropharyngeal tumors disproportionately benefitted from the addition of cetuximab, a chimeric monoclonal antibody against the epidermal growth

factor receptor (EGFR), to RT [91, 189]. In particular, the latter finding has been viewed as a clinical paradox: in the context of chemoradiation, why is EGFR targeting more effective in HPV-positive vs. HPV-negative tumors, when the purported target, EGFR, demonstrates significantly lower expression in HPV-positive vs. HPV-negative tumors?

Previous studies have shown that HPV16 oncoproteins upregulate EGFR signaling. Expression of E6 and E7 is reported to upregulate EGFR levels in cells [122, 123]. HPV16 E5 is also associated with upregulated EGFR signaling and recycling of the receptor to the cell membrane following activation-induced internalization [63-67, 72]. The fact that all three of these oncoproteins function to enhance signaling through this pathway suggest the EGFR signaling pathway must be important in the viral lifecycle. Interestingly, the AP-1 family of transcription factors, which is modulated by EGFR signaling, is important in regulating transcription of HPV early genes [127, 128, 130, 131, 190]. In particular, cFos expression increases transcription of HPV16 oncogenes [128, 130, 131] and levels of cFos can be controlled by EGFR activity (reviewed in [125]). De Wilde *et al.* showed that levels of AP-1 transcription factors are differentially expressed in HPV-transformed cells as compared to normal and precancerous tissues, and that cFos and JunB, specifically, are upregulated in cancerous cells [126]. Lastly, suppression of HPV oncogene transcription can be mediated by downregulation of cFos and JunB levels [191, 192].

Suppression of E6 and E7 levels in HPV-positive cancer cell lines by siRNA is reported to induce apoptosis and have anti-tumorigenic effects. siRNA knockdown of HPV E6 alone or in conjunction with E7 in HeLa and SiHa cells resulted in increased p53 levels and induction of cellular senescence and apoptosis *in vitro* [77, 78]. Furthermore,

recent studies reported that *in vivo* siRNA knockdown of E6/E7 results in delayed tumor growth, p53 recovery, and radiosensitization of SiHa and HeLa xenograft tumors [79, 80]. Together, these data demonstrate that decreasing levels of E6 and E7 proteins in HPV-positive cancers has therapeutic effects.

As EGFR signaling is upregulated by HPV oncoproteins, we previously hypothesized that HPV establishes a positive feedback loop with the EGFR pathway resulting in upregulation of viral transcription and that inhibition of EGFR signaling would have antiviral effects including downregulation of E6 and E7 expression and recovery of p53 levels and activity. In chapter 3, we showed that activation of EGFR signaling positively affected transcriptional activity of early genes including E6 and E7 in a cell line containing episomal HPV16 genomes. Furthermore, we demonstrated that blocking EGFR activation with cetuximab had antiviral effects including decreased viral oncogene transcript levels and sensitization of cells to cisplatin. Studies from other labs undertaken while we were conducting these experiments have shown that cetuximab is able to decrease HPV-positive xenograft tumor growth rate [193, 194]. As HPV-positive HNSCC do not typically overexpress EGFR and the ADCC component of cetuximab's mechanism of action is impeded in the immunocompromised animals used in these studies, the mechanism behind cetuximab's antitumor effects in these cohorts are not well understood. Based on our previous studies, we questioned if downregulation of viral oncogenes following cetuximab treatment might contribute to the antitumor effects in these xenografts. We hypothesized that cetuximab-mediated EGFR inhibition would downregulate viral oncogene expression in xenografts from cell lines maintaining viral LCR-mediated control of viral transcription. Furthermore, we postulated that this

downregulation of viral oncoproteins would restore wild-type p53 expression and downregulate p16 expression.

Herein we describe the effects of cetuximab treatment on viral oncogene expression levels, viral activities, and related cellular targets in xenografts from four HPV-positive cell lines. Different viral responses to cetuximab were seen among the cell lines used. We observed decreased E6 and E7 RNA expression levels in two cell lines treated with cetuximab or the MEK1/2 inhibitor, trametinib, and downregulation of viral oncogene expression appeared to correlate with the ability of the drug to modulate levels of AP-1 transcription factors, cFos and JunB. We also describe the histological effects of cetuximab treatment on xenografts with disparate viral responses.

4.2 Methods

4.2.1 Cell Culture

SiHa and CaSki cells, derived from HPV16-positive cervical cancers, were obtained from ATCC and maintained in MEM or RPMI-1640 containing 10% fetal calf serum (FCS), respectively. UM-SCC47 and UM-SCC104 cell lines, derived from HPV16-positive HNSCCs, were obtained from Dr. Thomas Carey's laboratory (U. Michigan) and authenticated by STR profiling (Table 2.1). HNSCC cell lines were maintained in DMEM containing 10% FCS. All cell lines were grown at 37°C, 5% CO₂. Cell lines and HPV status for each is listed in Table 4.1.

Table 4.1 List of HPV-Positive Cancer Cell Lines Used

Cell Line	HPV Status (Variant) ^a	Source	Viral Genome Copy Number qPCR ^b	Viral Genome Copy Number WGS ^c	References
SiHa	HPV16 (EUR)	Cervical	0.397	2	[156, 195]
CaSki	HPV16 (EUR)	Cervical (small bowel metastasis)	122	831.6	[156, 196]
UM-SCC-47	HPV16 (AFR2a)	Lateral tongue	21.1	47	[156, 197]
UM-SCC-104	HPV16 (EUR)	Floor of mouth	2.86	1.1	[156, 198]

^aHPV variant: (EUR) European; (ASN) Asian; (AFR) African. Nomenclature is based on variants in E6 and LCR regions by the IARC HPV Variant Study Group [199].

^bViral copy number as measured by real-time PCR. Copy number reflects the ratio of HPV16 E6 to Endogenous retrovirus 3 gene (ERV3).

^cViral copy number as determined by whole-genome sequencing (WGS).
Adapted from [199]

4.2.2 Xenograft Preparation

Cell lines derived from HPV-positive cervical cancers (SiHa, CaSki) or HNSCC (UM-SCC47, UM-SCC104) were trypsinized and resuspended in appropriate cell culture media. To establish xenografts, cells ($1-2 \times 10^6$) mixed 1:1 with Matrigel (BD Biosciences) were injected subcutaneously into flanks of 8-10 week old, female NOD/SCID-gamma (NSG) mice. Once tumors were palpable, they were measured by caliper, stratified by size, and animals randomized into treatment and control groups. Cetuximab (1, or 5 mg/kg) or 0.9% saline control was administered 3x/week by i.p. injection. Trametinib (1 mg/kg) or vehicle control (10% Cremophor EL, 10% PEG 400) was administered daily by oral gavage. Tumors were measured by caliper 3x/week and volumes calculated using the formula: length x width x width/2. Xenografts were

harvested when the control group reached 1 cm in size. Tumors were surgically removed, divided for histology, RNA, and protein extraction and flash frozen in liquid nitrogen. The Institutional Animal Care and Use Committee of the University of New Mexico Health Sciences Center (Albuquerque, NM) approved all animal procedures.

4.2.3 RNA Extraction

Total RNAs were extracted from frozen tumor portions using Direct-zol RNA MiniPrep kit (Zymo) according to manufacturer's protocol. Briefly, frozen tissues were weighed, thawed in TriReagent (at least 1ml Trizol per 100mg tissue) (Sigma) and homogenized using a Pro200 rotary homogenizer (Pro Scientific). Lysates were held at 4°C overnight. Non-soluble material removed by centrifugation (12K x g for 10 minutes at 4°C) and supernatant was transferred to a fresh tube. An equal volume of 100% ethanol was added to supernatant to precipitate nucleic acids. Solution was added to Zymo column and washed. Following wash steps, RNA was eluted in RNase-free dH₂O. DNA was removed by DNase treatment (TURBO DNA-free, Ambion). Quality and concentration of RNA was determined by spectrometry (Nanodrop, BioRad) and agarose gel electrophoresis as described in [138].

4.2.4 RT-qPCR

cDNA was prepared from 0.2 (UM-SCC47, 5 mg/kg cetuximab cohort) – 0.5 mg of total RNA using M-MLV reverse transcriptase and random hexamer primers (Applied Biosystems). 25ng of template was used for each qPCR reaction (10ng for UM-SCC47, 5mg/kg cetuximab cohort). Sequences and concentrations of primers and probes as well as PCR cycle profiles are provided in Table 2.1. For hydrolysis probes, iQ master mix (BioRad) was used. E6, E7, and cFos primer sets were run with SsoFast Evagreen master

mix (BioRad). JunB primers were obtained from Applied Biosystems and used with TaqMan Fast Advanced Master Mix (Applied Biosystems). All qPCR reactions were run on CFX96 thermocycler (BioRad) and data analyzed using BioRad CFX Manager (version 3.1.1517.0823). Cq values for targets were normalized to human B-actin expression levels using the ΔCq method.

4.2.5 Immunohistochemistry

Formalin-fixed paraffin embedded (FFPE) blocks were sectioned at 5 μm thickness and transferred to charged slides (Fisher Scientific). Sections were deparaffinized in Citrisolv (Fisher Scientific) and rehydrated through 70% ethanol followed by 10 minutes in dH_2O (for H&E) or 1X PBS (for IHC). For manually stained IHC slides, antigen retrieval was performed by boiling slides in appropriate buffer for indicated times (see Table 2.3). Blocking was performed in 5% normal horse serum (Vector Labs), 1 hour at room temperature. The following antibodies were used for IHC: total-EGFR (Cell Signaling), phospho-EGFR(Y1173) (Cell Signaling), phospho-p44/42 (Cell Signaling), Ki-67 (BD Biosciences/Thermo Scientific), p16^{INK4a} (Roche/Ventana, performed by UNM Human Tissue Repository), p53-D07 (Novocastra, performed by MD Anderson Research Park Histology Core), human mitochondria marker (Chemicon, performed by MD Anderson Research Park Histology Core). Manually stained sections were incubated with primary antibody in blocking solution overnight at 4°C in a humidified chamber (see Table 2.4 for antibody concentrations). Slides were washed in TBS-T, and incubated with biotinylated anti-mouse/rabbit secondary antibody (VECTASTAIN Elite Universal ABC Kit, Vector Labs) for 30 minutes followed by 30 minutes incubation with ABC reagent. Sections were incubated with DAB (Vector Labs) for 15 minutes. Slides were counter stained

with hematoxylin, dehydrated and cleared in Citrisolv. Coverslips were mounted with Permount mounting media.

4.2.6 Histological Evaluation

Blinded sections were evaluated and all HALO analysis was performed by a certified pathologist (Dr. Donna Kusewitt of the UNM Comprehensive Cancer Center). IHC stained tissues were assigned a score between 0-3 based on epithelial staining intensity with 0 representing the lowest intensity and 3 representing the strongest. For evaluation of tissue morphology, Aperio-scanned H&E-stained slides and the HALO (Indica Labs) morphometry system were used. The entire tumor mass was outlined to obtain the total tumor area. HALO was then trained to recognize viable tumor epithelium, keratin, stroma, large blood vessels, and background (no tissue) within the tumor. Necrotic areas within the tumor epithelium were outlined by hand for exclusion in calculations. HALO was reprogramed for each cell line because of vastly different morphologies. HALO determined the area of these components and percentage of the entire tumor occupied by these areas was calculated by the pathologist. Areas of tumor epithelium were confirmed by IHC for human mitochondrial marker (shown in Supp Figs 1 and 2). Ki67 IHC slides were also scanned into Aperio and analyzed using HALO. HALO was trained to recognize epithelium and then to identify Ki67-positive nuclei in that epithelium. Positive nuclei were classified as strongly (+3), moderately (+2), or weakly (+1) positive (considered background). The number of strongly and moderately positive nuclei (+2, +3) were normalized to the area of the epithelium.

4.2.7 RNAscope® - RNA in situ hybridization

FFPE sections were stained according to manufacturer's protocol (2.5 HD Detection Kit – Brown) using a probe to high-risk HPV E6/E7 (hrHPV 7, Advanced Cell Diagnostics). Briefly, fresh cut sections were deparaffinized in xylenes (2 x 5 minutes each) and washed in 100% ethanol (2 x 1 minutes each). Exogenous peroxidase was quenched by incubation with 3% H₂O₂ (Advanced Cell Diagnostics) for 15 minutes then washed with dH₂O. Slides were submerged in sub-boiling temp Antigen Retrieval Buffer (Advanced Cell Diagnostics) for 15 minutes followed by washing in dH₂O then 100% ethanol. Tissues were encircled with a hydrophobic pen and slides were allowed to dry overnight. Slides were incubated in protease (Advanced Cell Diagnostics) 30 minutes, 40°C then washed in dH₂O. High risk HPV E6/E7 probe was hybridized for 2 hours at 40°C. AMP steps 1- 4 were performed for recommended lengths of time at 40°C, with 2 minute washes in 1x Wash Buffer (Advanced Cell Diagnostics) between each amplification step. The final two AMP steps (5 and 6) were performed at ambient temperature for recommended times, slides were washed with 1x Wash Buffer after each step. Signal detection was performed with DAB (Advanced Cell Diagnostics) for 10 minutes at ambient temperature. Tissues were counterstained with 50% Gil's hematoxylin solution, coverslipped and allowed to dry overnight. Slides were digitally scanned (Aperio Slide Scanner) and analyzed using HALO software by Dr. Kusewitt.

4.2.8 Statistical Analysis

All statistics for growth curves and RT-qPCR experiments were performed in GraphPad Prism version 6.0g for Mac. Growth curves were compared by multiple t-tests (unpaired). RT-qPCR data were compared by t-test. Correlation between tumor size and

transcript expression levels was determined by Spearman's r test. Statistical outliers were determined for each experimental group using Grubb's outlier test (GraphPad Prism) and outliers were removed from the datasets. Semi-quantitative histology results were compared using the Mann-Whitney test. Error bars represent the standard error of the mean (SEM) for each group. p -values of less than 0.05 were considered to be statistically significant.

4.3 Results

4.3.1A Effect of Cetuximab Treatment on Viral Oncogene Expression in UM-SCC47 Tumor Xenografts

The UM-SCC47 cell line is derived from an HPV16-positive lateral tongue lesion and produces moderately differentiated xenograft tumors. It was recently described as moderately resistant to cetuximab by dose response *in vitro* as compared to other HNSCC cell lines [200]. Consistent with this, we found treatment with a 1 mg/kg dose of cetuximab 3x/week for 4 weeks had no effect on tumor growth rate in the UM-SCC47 tumor-bearing cohort (Fig 4.1A) and no change in E6 or E7 expression levels was observed (Fig 4.1B).

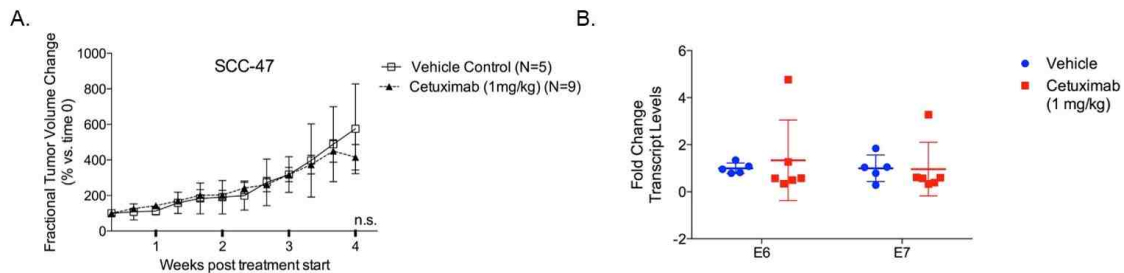


Figure 4.1 Low-dose cetuximab does not affect tumor growth or viral oncogene levels in SCC47 xenografts.

NSG mice bearing SCC47 xenografts implanted subcutaneously were given cetuximab (1 mg/kg) or vehicle only (0.9% saline) 3x/week. Tumors were measured 3x/week by caliper and percent growth from treatment start (time=0) are shown in (A). RNA from homogenized tumor sections was analyzed by RT-qPCR for expression levels of viral oncogenes E6 and E7 and transcript levels were normalized to human β -actin transcript levels. The average expression levels of normalized E6 and E7 from the vehicle tumors was set to 1 and data shown as fold-change compared to control (B). Error bars = SEM, statistical significance assessed by Student t-test.

However, a dosage of cetuximab at 5 mg/kg significantly inhibited tumor growth over 3.5 weeks (Fig 4.2A, final tumor weights shown in 4.2B). We observed that the amount of RNA recovered from the high-dose cetuximab treated tissues was low as compared to

yield from other tumors of the same weight. For this reason, cDNA from 10ng of total RNA template was used for each RT-qPCR reaction. Due to the low amount of template, levels of E6 and E7 transcripts had C_q values of >30 , near the detection limit for the assay, and β -actin levels for these were also low but within the detection range (data not shown). When E6 and E7 transcript levels were normalized to β -actin, we observed no change in viral oncogene transcript levels in tumors between vehicle and cetuximab treated mice (Fig 4.2C). There was no correlation between E6/E7 expression levels and tumor growth or final tumor weight (Fig 4.2D, E). This indicates that cetuximab has anti-tumor effects independent of the level of viral oncogene expression.

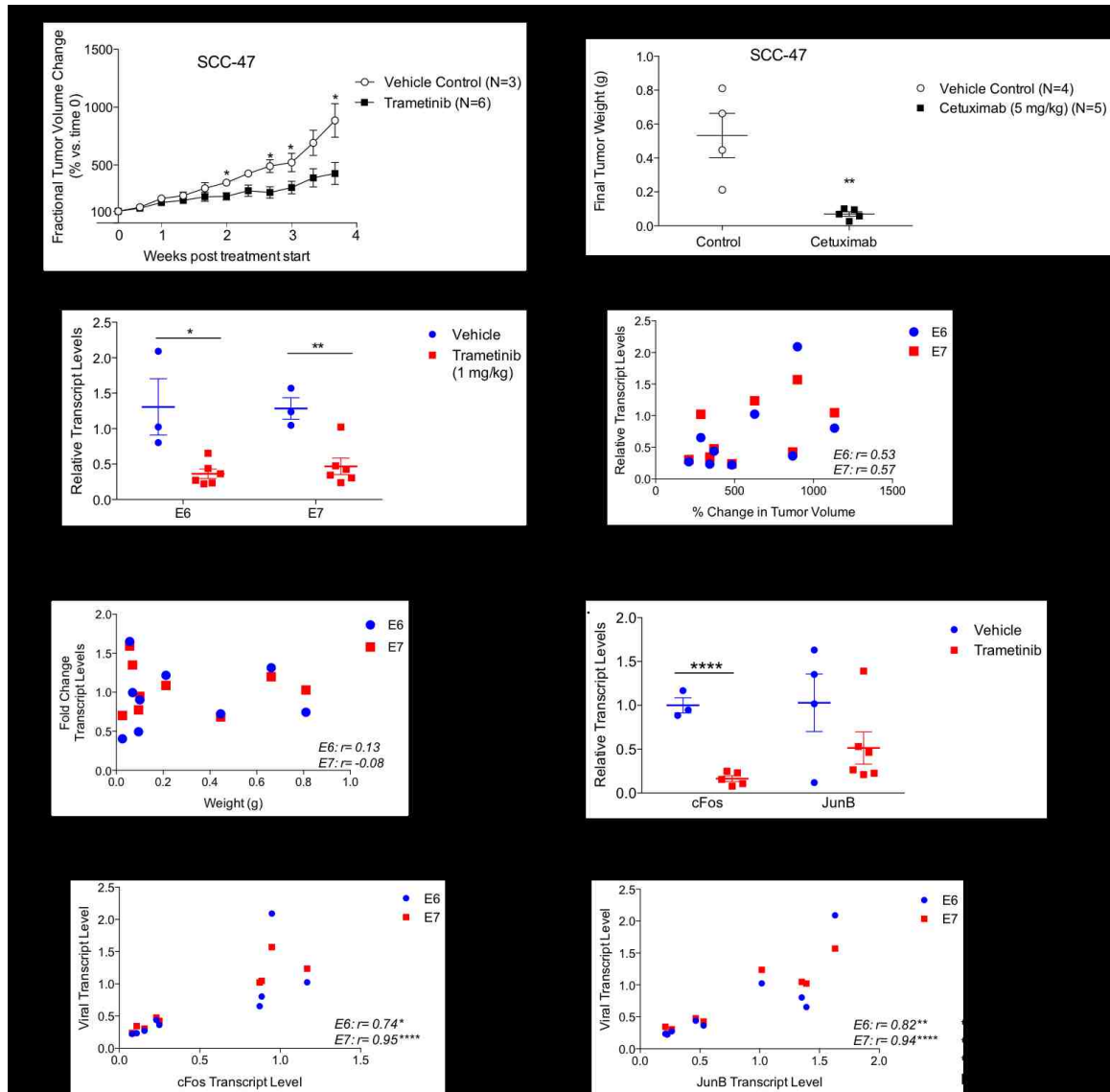


Figure 4.2 Cetuximab delays tumor growth independent of normalized viral oncogene expression levels in SCC47.

NSG mice bearing SCC47 xenografts implanted subcutaneously were given cetuximab (5 mg/kg) or vehicle only (0.9% saline) by i.p injection 3x/week. Tumors were measured 3x/week by caliper and percent growth from treatment start (time=0) are shown in (A). Final tumor weights (in grams) at necropsy are shown (B). RNA from homogenized tumor sections was analyzed by RT-qPCR for expression levels of viral oncogenes E6 and E7, and AP-1 transcription factors cFos and JunB. Transcript levels were normalized to human β -actin transcript levels. The average expression levels of normalized target from the vehicle tumors was set to 1 and data shown as fold-change compared to control. Relative expression levels of E6 and E7 are shown in (C). Relative expression levels of E6 and E7 transcripts were plotted against the change in tumor volume over the course of treatment (D) or the final tumor volume (E) and linear correlation assessed by Spearman's r test. Relative expression levels of cFos and JunB are shown in (F). Relative levels of E6 and E7 transcripts were plotted against the expression levels of cFos (G) and JunB (H) and linear correlation assessed by Spearman's r test. Error bars = SEM, Statistical significance assessed by Student t-test, * $p \leq 0.05$, ** $p \leq 0.01$.

There is compelling evidence that EGFR signaling controls AP-1 transcription factors that subsequently regulate HPV oncogene expression. Many studies have shown that the AP-1 family of transcription factors is important in regulating transcription of HPV early genes [127-129, 131]. Another study demonstrated that EGFR-activation can mediate upregulation of AP-1 transcription factors leading to enhanced HPV early gene expression [130]. Several additional groups have shown that expression levels of several AP-1 transcription factors, including cFos and JunB, are dysregulated in HPV-positive cervical cancer [126, 131, 192]. Unexpectedly, we observed no significant change in the levels of either cFos or JunB transcription factor RNA in the tumors from cetuximab-treated mice (Fig 4.2F). An explanation for this finding may be due to the fact that ERK1/2 activation in SCC47 cells is partially resistant to EGFR inhibition. Indeed, a previous study reported that, treatment of SCC47 cells *in vitro* with cetuximab and/or trastuzimab, which targets ErbB2, failed to inhibit ERK1/2 activation [201]. There was no significant correlation between E6/E7 transcript levels (Fig. 4.2G, H), which were also unchanged by cetuximab treatment.

4.3.1B UM-SCC47 Biomarker Detection by Histology and IHC

The SCC47 high-dose cetuximab cohort was selected for histological analysis. As mentioned previously, SCC47 is an HPV16-positive cell line that yields moderately differentiated tumors. Treatment of SCC47 xenografts with high dose (5mg/kg) cetuximab resulted in significant reduction of tumor growth as compared to controls (Fig 4.2A, B) but produced no noticeable change in viral oncogene RNA levels (Fig 4.2C).

As expected, SCC47 xenograft tumors treated with cetuximab showed an average of less than half of the total epithelial area as compared to the control group (Fig 4.3A

and B). Untreated xenografts appeared moderately differentiated with stratified epithelium surrounding areas of accumulated keratin. Intermediate layers of epithelium in the untreated group were markedly thickened, indicating hyperplasia (Fig 4.3A). Cetuximab treatment induced further differentiation of epithelium in treated tumors, as seen by few stratified layers of epithelium and higher levels of keratin deposits in H&E stained sections (Fig 4.3A and B). In fact, the bulk of the cetuximab treated tumors was composed of keratin deposits and not epithelium (Fig 4.3B). Additionally, tumors exposed to cetuximab had more than twice the stromal makeup compared to control tumors. None of the tumors exhibited signs of necrosis. The high ratio of keratin to epithelium explains the low RNA yield obtained from the cetuximab treated tumors.

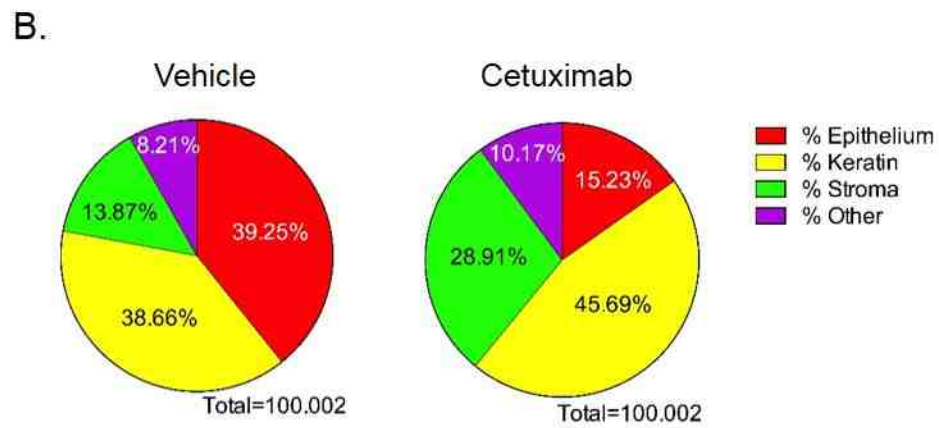
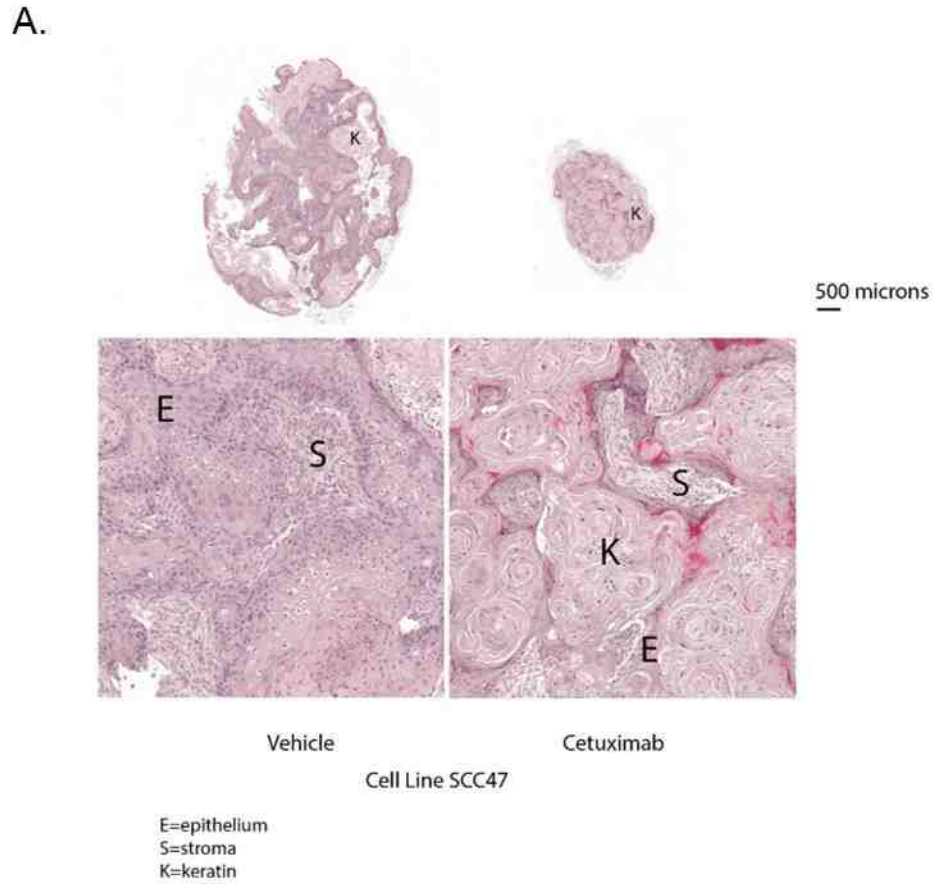


Figure 4.3 Cetuximab treatment induces differentiation and morphologic changes in SCC47 xenografts.

FFPE sections of xenografts from cetuximab and control tumors were H&E stained, representative images for vehicle and cetuximab sections are shown (A). Slides were scanned using an Aperio slide scanner and percent tumor composition determined using HALO software. Results are summarized in (B).

The IHC results reported in Figures 16-17 are summarized in Table 2. Tumors from mice treated with cetuximab showed slightly decreased EGFR staining and importantly, phospho-EGFR staining was lower in those receiving EGFR inhibitor than in untreated controls (Table 2 and Fig 4.4A and B). This indicates that cetuximab diminished the total and active levels of EGFR. EGFR staining in both groups was largely restricted to the cell periphery indicating localization of the receptor to the plasma membrane. In the well-differentiated epithelium, only the basal layer of cells were EGFR-positive while the majority of the thickened epithelium in the untreated tumors stained positive for EGFR (Fig 4.4A).

Table 4.2 IHC Scores for UM-SCC47 5mg/kg Cetuximab Cohort

Total EGFR	Vehicle ^b			1	3	2.75	0.2063
	Cetuximab ^c			4	1	2.2	
phospho-ERK	Vehicle				4	3	0.0079
	Cetuximab		2	3		1.6	
p53	Vehicle			1	3	2.75	0.0476
	Cetuximab			5		2	

Interestingly, cetuximab treatment also led to decreased intensity of phospho-ERK1/2 by approximately half in SCC47 xenografts compared to that in vehicle treated controls (Fig 4.4C). It should be noted that there was extensive staining of the upper

layers of epithelium with this ERK1/2 antibody, which may be a staining artifact. Staining for ERK1/2 in tumors from the cetuximab treated animals was restricted to these upper layers while tumors from control animals exhibited staining throughout multiple epithelial layers. The decreased ERK1/2 staining in tumors from the cetuximab-treated group seems contradictory to the report of sustained ERK1/2 activity in SCC47 cells in monolayer culture even after cetuximab or trastuzimab treatment [201]. Together, these data suggest that cetuximab deprives the tumor cells of growth factor stimulation resulting in differentiation.

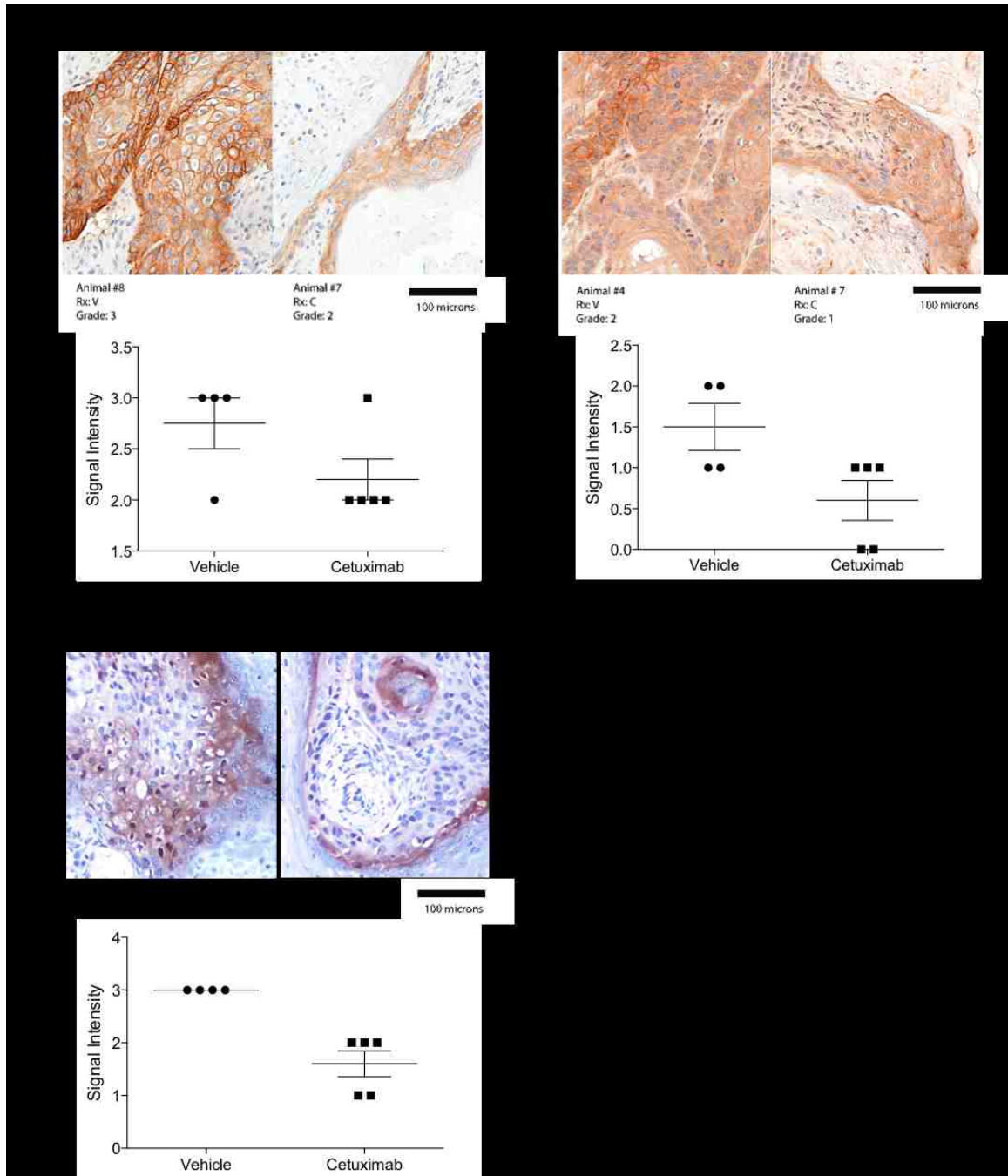


Figure 4.4 Cetuximab decreases levels of active EGFR and ERK1/2 in SCC47 xenografts.

FFPE sections from cetuximab treated and control tumors were stained by IHC for total EGFR (A), phospho-EGFR(Y1173) (B), and phospho-ERK1/2 (C). Representative images of each treatment group are shown for each target. Staining intensity was scored from 0-3, with 3 indicating the strongest signal.

To evaluate the effects of cetuximab on viral activity, we analyzed levels of p16^{INK4a}, p53, and Ki67. Expression of p16 is often elevated in HPV-positive cancers and

p16 detection is commonly used as a surrogate marker of HPV-positive tumors [73-76]. Surprisingly, even though we measured no change in viral oncogene expression in tissue extracts by RT-qPCR, we did observe decreased p16 staining in cetuximab treated xenografts (Fig 4.5A). In cetuximab treated tumors, p16 staining was restricted to the basal layers of epithelium (Fig 4.5A). Conversely, control tumors exhibited staining throughout the basal and intermediate layers of epithelium.

Both control and treatment groups contained epithelium with p53-positive nuclei, but p53 staining intensity was higher in the control group than in the cetuximab treated cohort (Fig 4.5B). Additionally, in untreated tumors, nuclei in the upper layers of the epithelium stained positive for p53 expression while nuclei in the lower layers of epithelium were negative. The cetuximab treated xenografts contained mostly basal cells and only few of those exhibited p53 expression. The p53 staining pattern in the untreated xenograft tumor group is reminiscent of that observed when the W12E cervical cancer cell line, which maintains episomal HPV16 genomes, was cultured as differentiated epithelium in the raft system [202, 203]. Staining for p53 in these tissues is restricted to cells in the upper layers of epithelium, suggesting recovery of p53 levels as viral oncogene expression is downregulated concomitant with cellular differentiation.

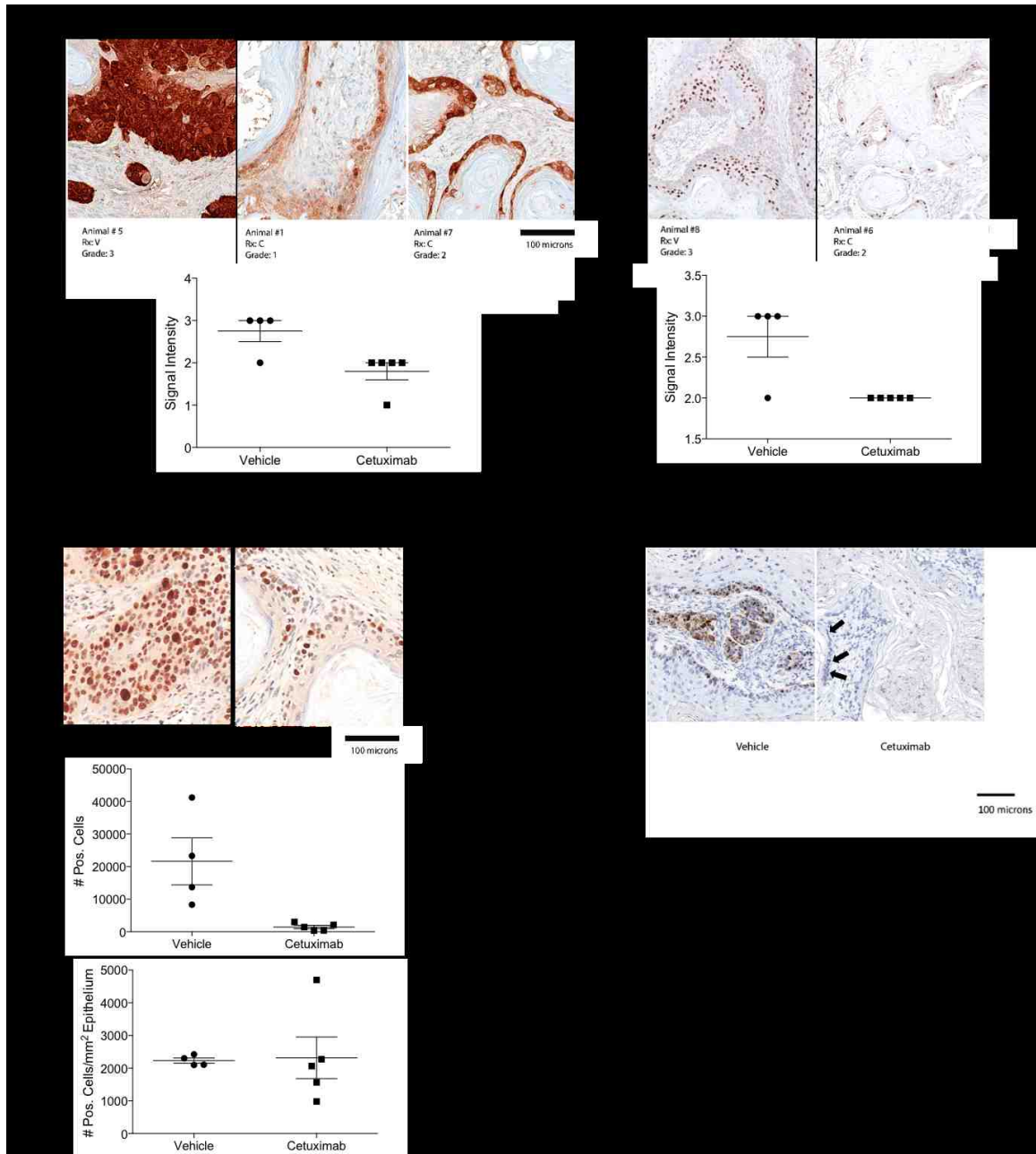


Figure 4.5 E6/E7 expression and p53 levels change concomitant with cellular differentiation in SCC47.

FFPE sections were stained by IHC for p16^{INK4a} (A) and p53 (D07) (B) and staining intensity was scored from 0-3, with 3 indicating the strongest signal and scores are summarized in graphs. (C) IHC for Ki67. Slides were scanned using an Aperio slide scanner and staining analyzed using HALO software. Number of total Ki6-positive cells for each tumor are shown in the top graph while number of Ki-67-positive cells normalized to epithelial area for each tissue section is shown in the bottom graph. (D) RNA ISH was performed to determine spatial expression of HPV E6 and E7, black arrows represent areas of E6/E7 positive nuclei. Representative images of each treatment group are shown for each target.

Proliferative ability of the epithelial cells in each tumor was assessed by Ki67 expression (Fig 4.5C). Only cells in basal and intermediate layers of epithelium stained positive for Ki67. Overall, cetuximab treated xenografts contained significantly fewer Ki67 positive cells as compared to those in the control. However, when the number of Ki67-positive nuclei was normalized to the total epithelial area in the section, the difference in proliferating cells between the treatment groups was no longer significant (Fig 4.5C). The p16, p53, and Ki67 staining patterns in these tissues suggest differentiation-dependent downregulation of viral oncogene expression.

To assess the spatial expression patterns of E6/E7 we used RNAscope (Advanced Cell Diagnostics), a method of RNA *in situ* hybridization, in a selection of tissues from each group. In the untreated group, expression of E6/E7 was only seen in the basal layers of the differentiated epithelium, which correlates with high p16 and Ki67 expression, and lack of p53 staining in these layers (Fig 4.5D). E6/E7 RNA positive nuclei were difficult to detect in cetuximab treated groups, but were identified in cells in the basal layer albeit with lower staining intensities (Fig 4.5D). These data indicate that concurrent with increased differentiation, cetuximab treatment leads to lower expression of HPV oncogenes in SCC47 xenografts. At present, we cannot determine if lower E6/E7 RNA levels are the cause or result of increased differentiation in cetuximab-exposed tumors. The reason for the discrepancy between our E6/E7 ISH and RT-qPCR data is not clear. The method for RT-qPCR normalization may be at fault. Our RT-qPCR data is normalized to β -actin expression levels. Since E6/E7 expression in vehicle treated tumors is confined to the basal layers of epithelium, β -actin RNAs from the upper layers of epithelium may dilute out the relative E6/E7 transcripts in the untreated tissues. This

underscores the importance of evaluating targets by multiple methods and highlights one of the limitations of using tumor homogenates to measure gene expression and protein levels.

4.3.1C Effect of Trametinib Treatment on Viral Oncogene Expression in UM-SCC47 Tumor Xenografts

Data from our laboratory has indicated that MEK1/2 is a critical factor for EGFR-mediated regulation of viral transcript levels (described in Chapter 3). Therefore, we hypothesized that directly targeting MEK1/2 in these tumors would have an antiviral effect in SCC47 xenografts. To test this theory, we treated a cohort of animals bearing SCC47 xenografts with 1mg/kg trametinib. The delay in tumor growth in the treatment cohort was statistically significant as compared to the control group (Fig 4.6A). In agreement with our hypothesis, trametinib treatment significantly blunted viral oncogene transcript levels in xenografts (Fig 4.6B). The levels of E6/E7 expression were only moderately correlated with tumor growth (Fig 4.6C).

We quantified cFos and JunB RNA levels to determine if inhibition of MEK1/2 significantly altered their expression. Whereas we detected no change in the expression of either AP-1 transcription factor when tumors were exposed to cetuximab, levels of cFos and JunB RNA were significantly reduced in the trametinib treated tumors (Fig 4.15A). Additionally, there was a strong positive correlation between transcript levels of cFos and JunB and E6/E7 RNAs (Fig 4.6B, C). Taken together, these results indicate MEK inhibition effectively inhibits viral oncogene transcription in tumors from SCC47 cells. Furthermore, the strong correlation between levels of the AP-1 transcription factors

cFos and JunB and viral oncogene RNAs may suggest MEK exerts its antiviral effect via these transcription factors.

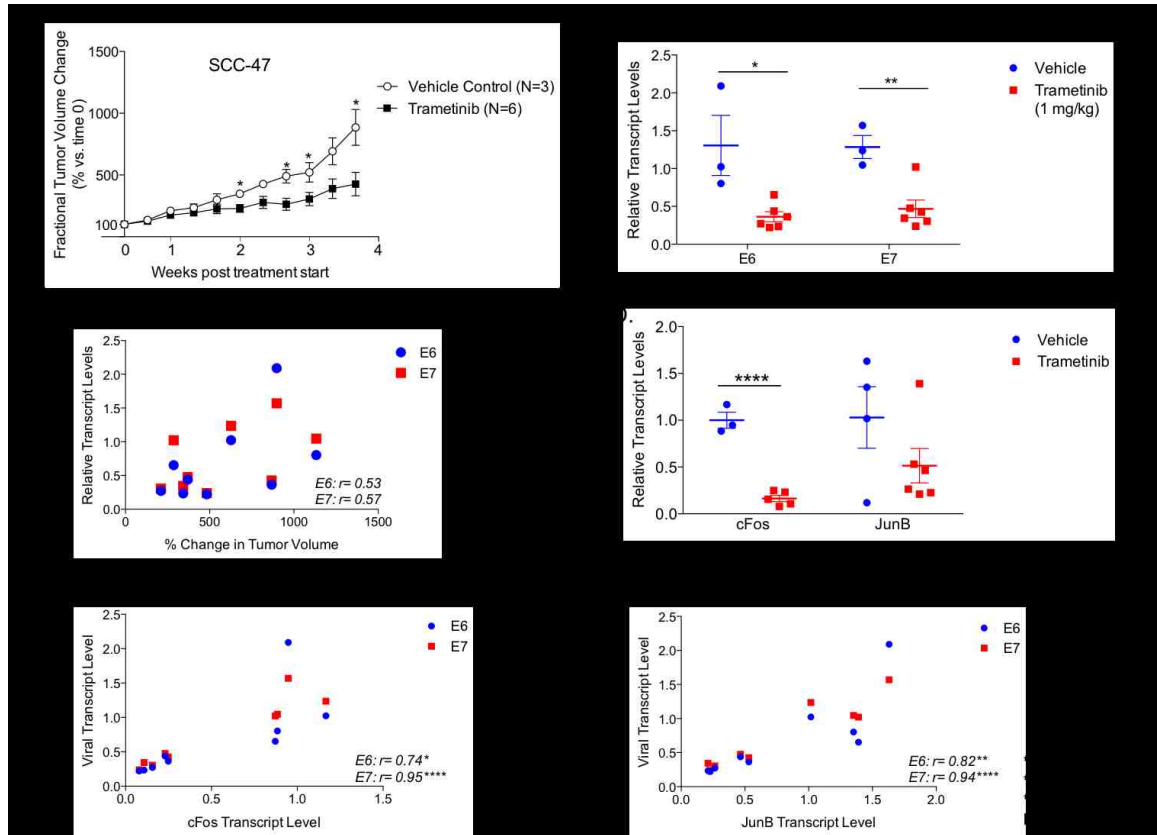


Figure 4.6 Trametinib produces antitumor effects concomitant with downregulation of viral oncogene expression in SCC47 xenografts.

NSG mice bearing SCC47 xenografts implanted subcutaneously were given the MEK inhibitor trametinib (1 mg/kg) or vehicle only (10% Cremophor EL, 10% PEG 400) daily by oral gavage. Tumors were measured 3x/week by caliper and percent growth from treatment start (time=0) are shown in (A). RNA from homogenized tumor sections was analyzed by RT-qPCR for expression levels of viral oncogenes E6 and E7, and AP-1 transcription factors cFos and JunB. Transcript levels were normalized to human β -actin transcript levels. The average expression levels of normalized target from the vehicle tumors was set to 1 and data shown as fold-change compared to control. Relative expression levels of E6 and E7 are shown in (B). Relative levels of E6 and E7 transcripts were plotted against the change in tumor volume over the course of treatment and linear correlation assessed by Spearman's r test (C). Relative expression levels of cFos and JunB are shown in (D). Relative levels of E6 and E7 transcripts were plotted against the expression levels of cFos (E) and JunB (F) and linear correlation assessed by Spearman's r test. Error bars = SEM, statistical significance assessed by Student t-test, * $p \leq 0.05$, ** $p \leq 0.01$, **** $p \leq 0.0001$.

In summary, the SCC47 cell line produces moderately differentiated xenografts in which EGFR/MEK signal inhibition produces antitumor and antiviral effects. A

summary of the data obtained from the SCC47-cetuximab cohort is shown in Supplemental Table 1. While 1mg/kg dose of cetuximab had no inhibitory effect on tumor growth, an increased dose of 5mg/kg significantly reduced tumor growth rate. However, we observed no overall change in E6 or E7 RNA levels in tumor homogenates from cetuximab treated animals at either dose when compared to controls. Levels of cFos and JunB also remained unchanged in treated animals. Cetuximab treatment decreased total and phospho-EGFR and phospho-ERK1/2 levels in tumors as compared to controls. In untreated tumors, high levels of p16 and Ki67 staining in the lower layers of epithelium corresponded with areas of E6/E7 RNA expression. p53-positive cells in these tumors were restricted to upper epithelial cell layers lacking E6/E7 RNA. Cetuximab treatment induced differentiation as evidenced by fewer stratified layers of epithelium and increased keratin deposits. There was no overall change in the number of Ki67-positive cells/mm² epithelium in response to cetuximab treatment indicating that the remaining cells were capable of proliferating. In contrast to results from cetuximab treated animals, administration of trametinib resulted in diminished tumor growth along with significantly decreased E6 and E7 transcript levels, which were tightly correlated with reduced levels of cFos and JunB RNA. Indicating that MEK inhibition is important in controlling viral gene expression in tumors from this cell line.

4.3.2A Effect of Cetuximab Treatment on Viral Oncogene Expression in UM-SCC104 Tumor Xenografts

The SCC104 cell line is derived from a recurrent HPV16-positive floor-of-mouth SCC and contains 1 viral genome [156, 199]. The integrated viral genome contains one breakpoint within the E2 ORF indicating that the LCR is maintained upstream of E6 and

E7 genes [156]. This cell line was derived from a tumor that had been twice resected and previously treated with chemotherapy and radiation [198]. Because of its aggressive nature, cetuximab was used at a higher dose (5mg/kg, 3x/week) for xenografts derived from this cell line. These tumors grew very rapidly and we were only able to treat the animals for two weeks after tumors appeared before the control animals required euthanasia. However, cetuximab treatment significantly inhibited the growth of SCC104 xenografts (Fig 4.7A). The erratic growth curves for the UM-SCC104 xenografts reflect difficulty in measuring these tumors during growth using our previously determined criteria (described in the methods section) (Fig 4.7A). At ~3 weeks post-implantation, the tumors contracted in length and width and instead grew in height. As an additional comparison, final weights of the UM-SCC104 tumors are shown (Fig 4.7B). Contrary to our hypothesis, SCC104 xenografts responded to cetuximab treatment with heightened E6 and E7 expression (Fig 4.7C). There was also a significant negative correlation between E6/E7 levels normalized to β -actin and tumor growth in SCC104 xenografts (Fig 4.7D). These data suggest that the antitumor effects seen in this cohort are independent of downregulated viral oncogene expression.

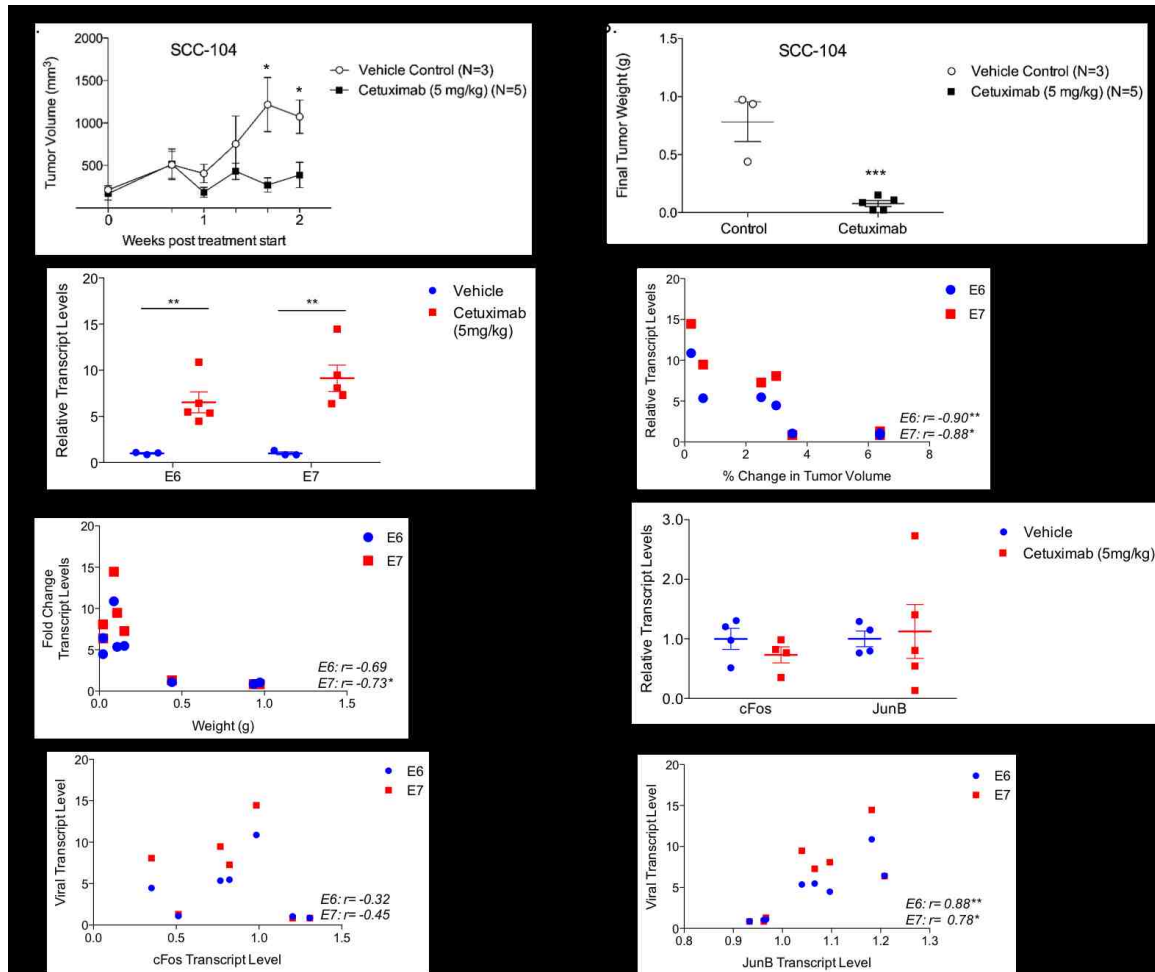


Figure 4.7 Cetuximab downregulates tumor growth rate while producing increased E6 and E7 transcript levels in SCC104 xenografts.

NSG mice bearing SCC104 xenografts implanted subcutaneously were given cetuximab (5 mg/kg) or vehicle only (0.9% saline) by i.p injection 3x/week. Tumors were measured 3x/week by caliper and percent growth from treatment start (time=0) are shown in (A). Final tumor weights (in grams) at necropsy are shown (B). RNA from homogenized tumor sections was analyzed by RT-qPCR for expression levels of viral oncogenes E6 and E7, and AP-1 transcription factors cFos and JunB. Transcript levels were normalized to human β -actin transcript levels. The average expression levels of normalized target from the vehicle tumors was set to 1 and data shown as fold-change compared to control. Relative expression levels of E6 and E7 are shown in (C). Relative expression levels of E6 and E7 transcripts were plotted against the change in tumor volume over the course of treatment (D) or the final tumor volume (E) and linear correlation assessed by Spearman's r test. Relative expression levels of cFos and JunB are shown in (F). Relative levels of E6 and E7 transcripts were plotted against the expression levels of cFos (G) and JunB (H) and linear correlation assessed by Spearman's r test. Error bars = SEM, Statistical significance assessed by Student t-test, * $p \leq 0.05$, ** $p \leq 0.01$, *** $p \leq 0.001$.

The levels of cFos were not significantly altered in cetuximab treated mice as compared to vehicle-only controls and although JunB levels were slightly elevated, the

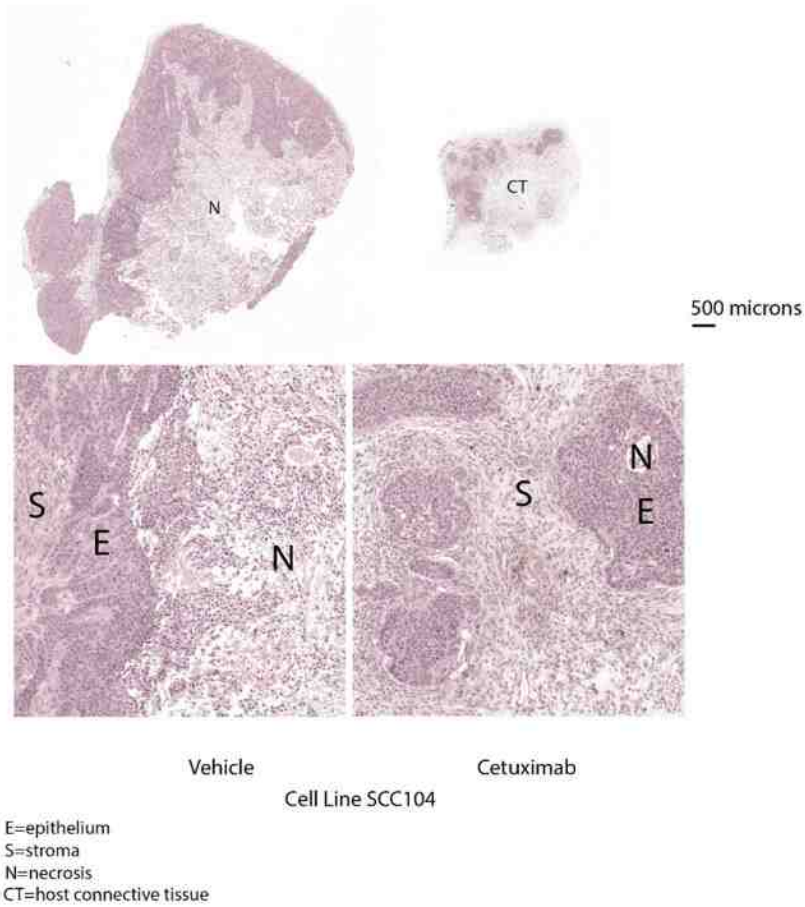
average was not statistically significant (Fig 4.7F). There was no correlation between cFos and viral oncogene transcript levels (Fig 4.7G). However, there was a moderate positive correlation between JunB RNA and E6/E7 transcript levels (Fig 4.7H). It should be noted that this cell line contains a deletion in *NOTCH1* that results in a truncated version of the protein [156]. Loss of function mutations in this gene are commonly associated with HPV-positive cervical cancer and HNC and have been shown to upregulate cFos expression [181, 184, 191, 204-208]. Conversely, exogenous expression of functional NOTCH1 in HeLa cells led to decreased E6/E7 expression by reducing cFos expression levels [191]. Therefore, the lack of antiviral response to cetuximab in SCC104 tumors may be due to the lack of EGFR-mediated control of AP-1 TF expression levels in this cell line.

14.3.2B UM-SCC104 Biomarker Detection by Histology and IHC

To further define the effects of EGFR inhibition on these xenografts we evaluated sections of these tumors histologically. Sections prepared from FFPE blocks were stained with H&E to first observe tissue morphology. Subsequent sections of the tumors were stained by IHC for total EGFR, phospho-EGFR(Y1173), phospho-ERK1/2, p16^{INK4a}, human mitochondria maker, p53, and Ki-67. SCC104 xenografts from vehicle treated mice were composed of poorly differentiated epithelium similar to the parental tumor as reported by Tang, *et al.* [198]. These cells form cystic or lobular epithelial structures in xenografts and tissues remained poorly differentiated even in the cetuximab treatment group with little to no evidence of stratification or keratinization (Fig 4.8A). The main morphological difference between tumor epithelium from cetuximab-treated mice as

compared to controls, was the size of the epithelial lobules which stain darker than the necrotic, stromal, or connective tissues also observed in the tumors (Fig 4.8A). Tumors from the cetuximab-treated group contained small or mixed lobules of epithelium while untreated tumors were composed of large lobules of epithelium. Cetuximab-treated mice had tumors with a higher percentage of stroma compared to epithelium than was present in the control groups (Fig 4.8B) but contained less total stromal area overall (average of 1.9mm^2 versus 6.81mm^2 for cetuximab and vehicle groups, respectively). Tumor vascularization was observed in tumors from both treated and vehicle control mice (Fig. 4.8B). Necrotic areas were evident in both groups but composed a higher percentage of the tumors in vehicle control than cetuximab-treated (Fig 4.8B). Tumors with larger lobules (control group) contained areas of necrosis usually at the center of the lobule. Conversely, the tumors composed of smaller epithelial lobules (cetuximab treated), tended to have a single area of necrosis near the center of the tumor mass. Analysis of tumor components by morphology (described in methods) revealed there was significantly more necrosis, both as total area of necrosis and as a percentage of total tumor area, in the tumors of vehicle-treated mice than in those of cetuximab-treated mice (Fig 4.8B). The increased necrosis in tumors of vehicle-treated mice was likely due to the large size of these tumors and consequent lack of an adequate blood supply.

A.



B.

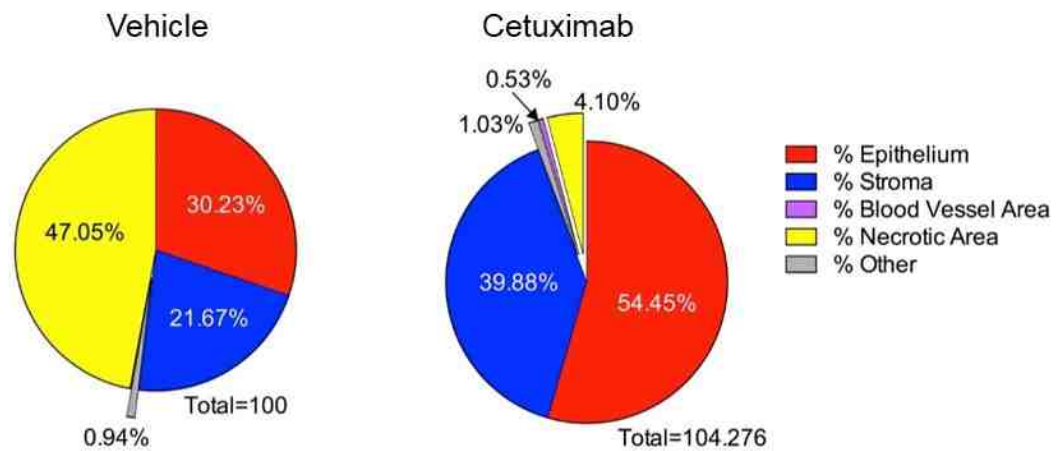


Figure 4.8 Cetuximab treatment induces morphologic changes in SCC104 xenografts.

FFPE sections of xenografts from cetuximab and control tumors were H&E stained, representative images for vehicle and cetuximab sections are shown (A). Slides were scanned using an Aperio slide scanner and percent tumor composition determined using HALO software. Results are summarized in (B).

The IHC results shown in Figures 4.9-4.10 are summarized in Table 3. Cellular staining for EGFR was diffuse in tumors from both treatment and control groups (Fig 4.9A). Levels of both total and phospho-EGFR were lower in cetuximab-treated tumors than vehicle controls indicating the drug efficiently reached the tumors (Fig 4.9A and B). Additionally, the intensity of phospho-ERK1/2 staining in tissues receiving EGFR inhibitor was reduced consistent with the drug interrupting upstream signaling to this pathway. Together, these data indicate that cetuximab was effective in inhibiting EGFR signaling and blunting the activity of the downstream effector ERK1/2.

Table 4.3 IHC Scores for UM-SCC104 5mg/kg Cetuximab Cohort

Total EGFR	Vehicle ^b			3		2	0.2063
	Cetuximab ^b		4	1		1.2	
phospho-ERK	Vehicle	1		2		1.25	0.0476
	Cetuximab	2	2	1		0.8	
p53	Vehicle ^d	3				0	n/a
	Cetuximab ^d	5				0	

^aSlides scored 0-3 based on staining intensity of tumor epithelium with 3 representing the strongest staining.

^bStaining in basal layers and around necrotic areas.

^cDiffuse staining.

^dNo or rare p53-positive nuclei in epidermis.

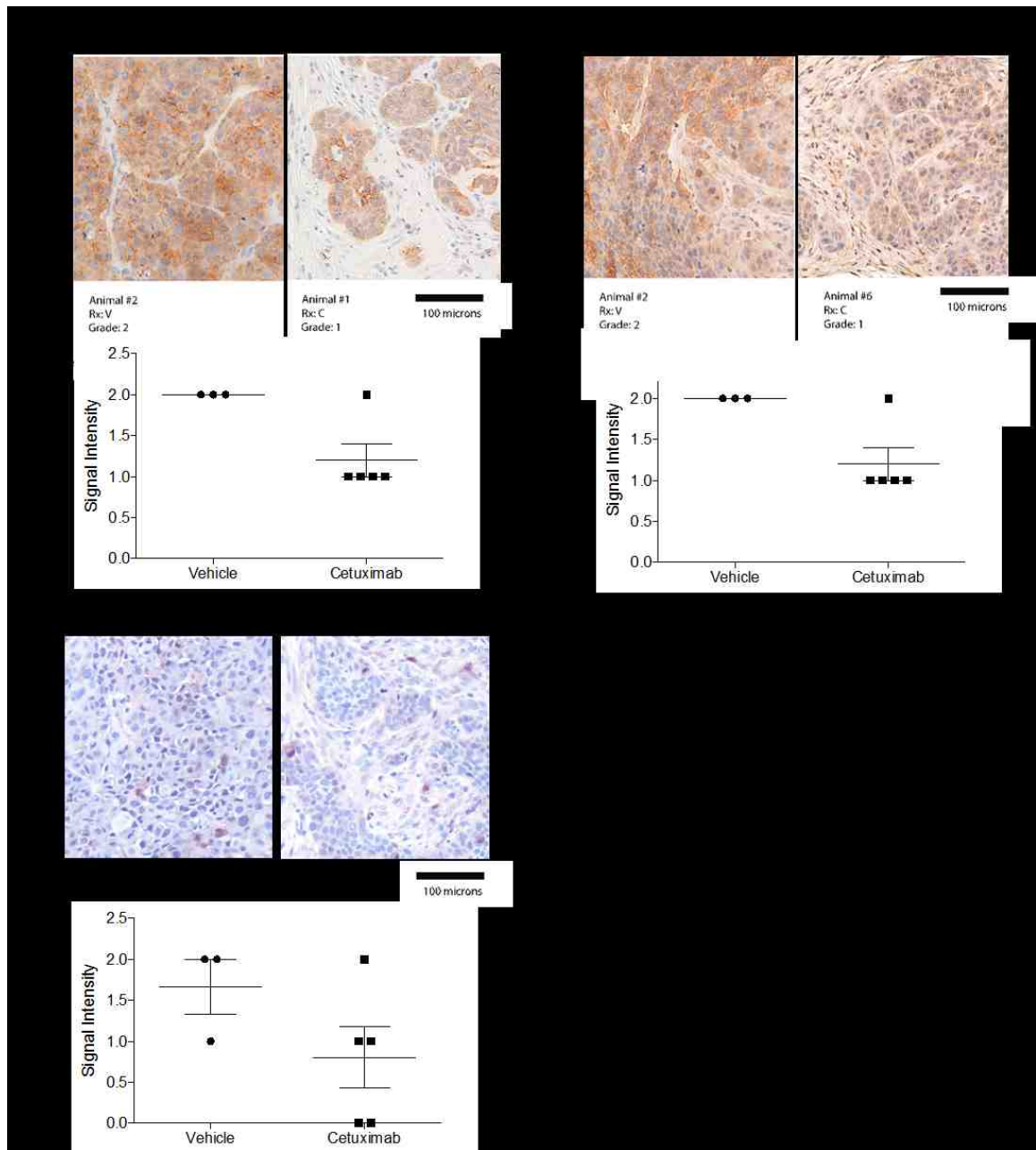


Figure 4.9 Cetuximab decreases levels of active EGFR and ERK1/2 in SCC104 xenografts.

FFPE sections from cetuximab treated and control tumors were stained by IHC for total EGFR (A), phospho-EGFR(Y1173) (B), and phospho-ERK1/2 (C). Representative images of each treatment group are shown for each target. Staining intensity was scored from 0-3, with 3 indicating the strongest signal.

As a surrogate marker of viral activity, we analyzed the levels of p16^{INK4a}, which is a well-documented marker of HPV-positive cancers [73-76]. The strength of p16

staining was slightly but consistently lower in the tumors from the treatment group compared to those in the control group (average intensity 2 vs 3, respectively) (Fig 4.10A). The decrease in p16 intensity in cetuximab-treated tumors is confounding since RT-qPCR revealed elevated E6/E7 levels in cetuximab-treated tumors and suggests that decreased p16 is independent of E7 levels.

Consistent with high levels of E6 expression, p53 was not detectable in either cetuximab or untreated tumors (Fig 4.10B). Tang, *et al.* reported that the SCC104 parental tumor contained ~10% p53-positive cells and a subsequent 50% loss of p53-positive cells was shown in cancer stem cell xenografts from this cell line [198]. This suggests the possibility that successive passaging of this cell line has resulted in selection of clones with lower p53 expression.

The total number of Ki-67-positive epithelial cells was significantly higher in tumors from untreated mice than those receiving cetuximab (Fig 4.10C). However, when the number of Ki-67-positive epithelial cells was normalized to epithelial area, the difference between the two groups was no longer significant (Fig 4.10C, lower panel). This indicates a possible selection for cells with higher proliferative capacity following cetuximab treatment, which would agree with our finding of elevated viral oncogene expression in these tumors (Fig 4.7B).

To gain spatial information about the expression of viral oncogene levels in these tissues, we performed RNAscope (Advanced Cell Diagnostics), a method of RNA *in situ* hybridization, for HPV E6/E7 (Fig. 4.10D). Staining was analyzed using HALO image analysis software (Indica) and the percentage of E6/E7 positive nuclei determined by dividing the number of positive nuclei by the total number of nuclei in each tissue

section. Due to their larger epithelial area, the total number of E6/E7-positive cells was slightly higher in tissues from the untreated group (Fig 4.10D). However, when the number of E6/E7 expressing cells was normalized to total epithelial area, a higher percentage of nuclei stained positive for E6/E7 RNA in tumors from the cetuximab treated mice, which is consistent with the heightened expression of E6 and E7 measured by RT-qPCR (Fig 4.7B).

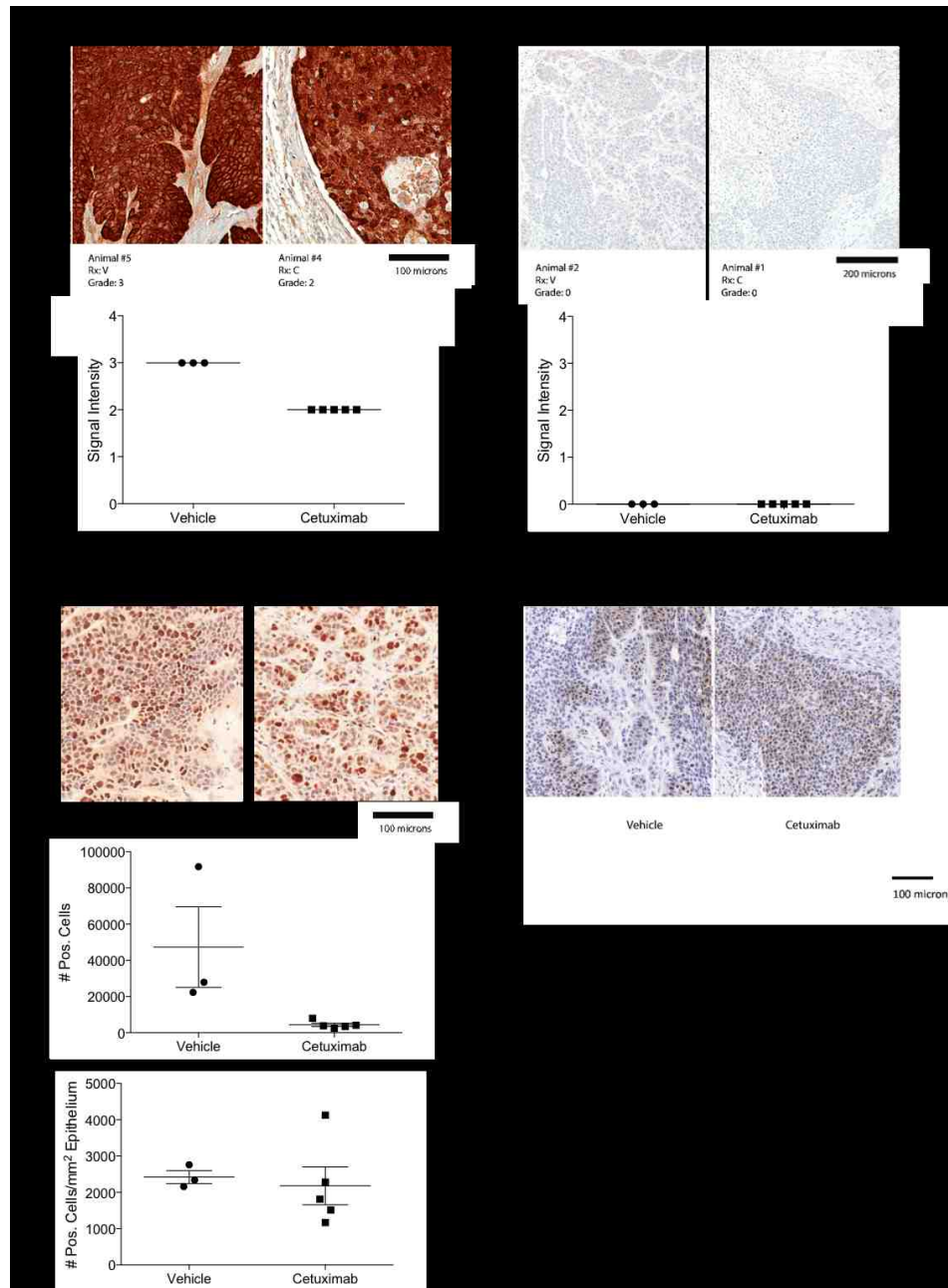


Figure 4.10 Cetuximab decreases p16 but not p53 or Ki-67 levels in SCC104 xenografts.

FFPE sections were stained by IHC for p16^{INK4a} (A) and p53 (D07) (B) and staining intensity was scored from 0-3, with 3 indicating the strongest signal and scores are summarized in graphs. (C) IHC for Ki67. Slides were scanned using an Aperio slide scanner and staining analyzed using HALO software. Number of total Ki6-positive cells for each tumor are shown in the top graph while number of Ki-67-positive cells normalized to epithelial area for each tissue section is shown in the bottom graph. (D) RNA ISH was performed to determine spatial expression of HPV E6 and E7. Representative images of each treatment group are shown for each target.

A data from the SCC104 xenografts is shown in Supplemental Table 2. Overall, in SCC104 xenografts, cetuximab was effective in downregulating levels of phospho-EGFR and phospho-ERK1/2. Cetuximab treatment led to decreased tumor growth and altered morphology. Epithelial lobules were smaller and necrosis was substantially reduced from 47% to 4% by cetuximab treatment. Cetuximab did not lead to reduced c-Fos or JunB RNA levels in xenograft tumors (Fig 4.7D). The lack of change in c-Fos and JunB levels may be due to the loss of functional Notch1 which normally inhibits expression of these genes and likely explains why HPV E6 and E7 levels were not diminished in response to cetuximab. Furthermore, the unchanged levels of p16, p53 and Ki67 reflect the maintenance of high expression of E6 and E7 in the tumors.

4.4 Discussion

HPV-positive HNSCC represents an increasing percentage of total cases of HNSCC (~30% of all HNSCC world-wide in 2014) [87, 88, 179]. While the prognosis for these HPV-positive patients is favorable, the current treatment modalities have high morbidity [154]. The current standard of care for HNSCC is the same regardless of HPV status, although there are clinical trials underway to determine the benefit of de-escalation of treatments. A more thorough understanding of the effects of current therapies on the viral oncogenes presumed to be driving these cancers will provide a basis for designing more effective therapies.

Cetuximab, a monoclonal antibody that inhibits EGFR activity is currently used in the treatment of both HPV-negative and HPV-positive HNSCC. As shown in chapter 3, HPV oncogene expression can be inhibited by EGFR inhibition. Previous studies have

shown that cetuximab can inhibit growth of HPV-positive xenografts [166, 193, 209]. However, the effect of cetuximab treatment on viral activities in these xenografts had not been investigated. Pogorzelski *et al.* evaluated the role of E6 and E7 in modulating the response of cells to cetuximab however this was done in HPV-negative cell lines transduced with E6 and E7. Therefore, the LCR elements which control normal viral transcription were not intact [210]. Here, we asked if EGFR inhibition *in vivo* produced antiviral effects including decreased viral oncogene expression levels, reinstatement of p53 expression, and diminished p16 levels indicative of restored pRb. We evaluated xenografts from two HPV-positive HNSCC cell lines thought to represent the two HPV-positive HNSCC subtypes, “classical” (CL) and “inflamed/mesenchymal” (IMS) [207] (data from these xenograft cohorts is summarized in Appendix B - Supplemental Tables 1 and 2). We also assessed the response of viral transcription to cetuximab treatment in xenografts from two HPV-positive cervical cancer cell lines (See supplemental data in Appendix B sections B.1 and B.2), one maintaining an intact LCR and the other lacking the viral control region upstream of integrated E6 and E7 [156]. In our study, cetuximab appears to suppress tumorigenicity through two different mechanisms: either in conjunction with or independent of antiviral effects. Our results show that EGFR and MEK1/2 inhibition has antitumor effects in xenografts from HPV-positive cancer cell lines. We observed decreased E6 and E7 RNA expression levels in two of the xenograft groups upon EGFR or MEK1/2 inhibition, and downregulation of viral oncogene expression appeared to correlate with the ability of the drug to reduce expression of AP-1 transcription factors, cFos and JunB.

In our study, cetuximab treatment reduced growth rate in xenografts from HPV-positive HNSCC cell lines (Figs. 4.2A and 3A) as well as HPV-positive cervical cancer cell lines (Supplemental Figs. 4A and 5A), however a higher dose of cetuximab was required to obtain an antitumor effect in the former group indicating possible moderate resistance to the drug. While EGFR inhibition downregulated viral oncogene levels as measured in tumor homogenates from SiHa xenografts (Supplemental Fig. 4B), E6 and E7 levels in SCC47 xenografts remained unchanged (Fig. 4.2B). However, the results from the SCC47 xenografts are misleading. Analysis of spatial expression of E6 and E7 by RNA ISH in SCC47 tumors revealed that these viral oncogenes are expressed differentially in the stratified epithelium of these tumors with the highest concentration of E6/E7 expression confined to the basal layers of epithelium (Fig. 4.5D). It is important to note that, for RT-qPCR, oncogene transcript levels were measured in a homogenized tissue sample and normalized to total levels of human β -actin transcripts, which are expressed throughout the epidermal layers, resulting in dilution of the E6 and E7 transcript levels. Growth of the cervical cancer cell line, W12E, in the organotypic raft system, which allows differentiation of epithelium reveals a similar pattern of viral oncogene expression, with E6 and E7 expressed in the basal cells and disappearance of detectable levels in the suprabasal layers [202, 203]. This suggests that the decreased E6/E7 levels might be mediated by cetuximab-induced differentiation in these tumors and not direct effects on viral transcription.

SCC47 is thought to represent the CL subtype of HPV-positive HNSCC described by Keck *et al.* [207]. The CL HPV-positive tumors are typically moderately differentiated and highly proliferative as compared to the IMS type. Prognosis for

patients with the CL type of tumor is also poorer than for the IMS type. To gain an idea of the effects of cetuximab treatment in this tumor type, we evaluated SCC47 tumors histologically. Cetuximab-mediated downregulation of total and phospho-EGFR was evident (Table 4.2 and Fig. 4.4A, B) as was decreased staining for phospho-ERK1/2 (Table 4.2 and Fig. 4.4C) indicating that cetuximab treatment inhibited EGFR activation and reduced downstream signaling through MEK. In agreement with data from Vermeer *et al.* showing sustained ERK1/2 activation following incubation with cetuximab and trastuzimab *in vitro*, levels of ERK1/2 activity were not completely diminished in SCC47 xenografts following cetuximab treatment [201]. The presence of Ki67-positive cells in these tumors (Fig. 4.4C) suggests that the remaining ERK activity is sufficient to sustain some tumorigenic activity. This indicates that there is possibly upregulation of other cellular pathways resulting in MEK/ERK activation. A recent publication reported enhanced expression of HER2 and HER3 in HPV-positive HNSCC and it thought to contribute to cetuximab resistance [211]. Levels of Her2/Her3 have not been reported for SCC47 cell line but if upregulation is present, it may contribute the remaining ERK activity observed. Together with the antiviral effects seen in SCC47 xenografts treated with the MEK inhibitor, trametinib, these data indicate that MEK inhibitors may have therapeutic value in HPV-positive HNSCC.

Restoration of functional p53 levels and thus cell cycle control is a goal in the treatment of HPV-positive cancers. *TP53* is mutated in many cancers (reviewed in [212]). However, presumably due to E6-mediated degradation of the p53 protein, HPV-positive cancers typically maintain wild type *TP53* [182, 184]. Previous studies have shown that suppression of E6 and E7 levels in HPV-positive cancer cell lines by siRNA

has anti-tumorigenic effects [77-80]. These studies additionally report restoration of p53 levels and induction of apoptosis. In the SCC47 xenografts, p53 expression was seen in the suprabasal layers of epithelium and coincided with downregulation of E6 and E7 expression (Fig. 4.5B and Table 4.2). Cetuximab treatment resulted in cellular differentiation concurrent with downregulation of E6 and E7 expression and recovery of p53. These data indicate that induction of epithelial differentiation in the CL HPV-positive tumor type through use of EGFR or downstream inhibitors may have therapeutic effects.

HPV-positive cancers typically express elevated p16 due to E7-mediated inactivation of pRb [73, 74]. We questioned if changes in viral oncogene expression would result in altered p16 expression as a surrogate readout of viral activity. Levels of p16, as detected by IHC, were markedly lower in cetuximab treated SCC47 tumors (Fig. 4.5C) and coincided with areas of decreased E6/E7 expression measured by RNA ISH (Fig. 4.5D) indicating that the reduction in viral gene expression correlates to lower viral oncoprotein levels. This is another indication of the antiviral effects of EGFR pathway inhibition in these tumors. The presence of remaining albeit diminished p16 and p53 levels following cetuximab treatment may indicate that low levels of E6 and E7 are still expressed in these cells. Further studies are needed to determine whether the cetuximab-associated reduction in viral oncoprotein levels in SCC47 xenografts is enough to increase sensitivity of these tumors to radiotherapy.

Histological evaluation of SCC47 xenografts from cetuximab and control groups revealed numerous morphological differences. Cetuximab treated tumors were smaller and therefore contained a smaller area of SCC and infiltrating stroma (Fig. 4.3A). Ki67

staining was markedly lower overall in cetuximab treated tumors (Fig. 4.3C, upper panel). However, when normalized to the area of epithelium in each section, the number of Ki67 positive cells was not significantly different (Fig. 4.3C, lower panel) indicating that decreased proliferative ability in the remaining cells could not account for differences in tumor size. SCC47 xenografts from cetuximab treated animals contained very little epithelia and the majority of the tumor was composed of stroma and keratin deposits indicating a strong inhibition of cellular proliferation and induction of differentiation. The members of the AP-1 transcription factor family are involved in epithelial differentiation and expression levels change concurrent with differentiation. No difference was observed for cFos or JunB levels in tumor homogenates, similar to what was seen with E6 and E7 (Figs. 4.2D and B). It is likely that we would also observe a similar change in expression patterns concurrent with cellular differentiation if c-Fos and JunB transcripts were measured by RNA ISH in these tumors. Taken together, it is clear that cellular differentiation and HPV oncogene expression are tightly linked in SCC47 xenografts. Whether the cetuximab-mediated cellular differentiation is preceded by a decrease in E6 and E7 levels or the cause of E6 and E7 downregulation is still unclear and may be difficult to tease out in this system.

In contrast to cetuximab treatment, administration of trametinib to animals bearing SCC47 xenografts resulted in significantly decreased levels of viral oncogene expression levels concomitant with cFos and JunB downregulation (Fig. 4.4A). Both SiHa-cetuximab and SCC47-trametinib xenografts exhibited strong correlation between E6/E7 expression levels and levels of cFos, indicating that these transcription factors might play an important role in facilitating the antiviral response observed (Fig. 4.4D-F

and Supplemental Fig. 4D-F). Histological comparison of SCC47-trametinib treated tumors with those treated with cetuximab will hopefully provide deeper insight into the mechanisms at play.

Cetuximab clearly exhibited antitumor effects independent of antiviral effects in SCC104 and CaSki xenografts. Despite significant suppression of tumor growth, viral oncogene RNA levels were elevated or remained unchanged in SCC104 and CaSki xenografts treated with cetuximab (Fig. 4.7A and Supplemental Fig. 5A). The increase in viral oncogene expression levels following cetuximab treatment might be attributed to two different mechanisms. It is possible that EGFR inhibition induced elevated expression of viral oncogenes in these tumors through activation of the promoter controlling transcription of E6 and E7. However, it is also plausible that EGFR inhibition instead created a selective pressure, which led to clonal growth of a cellular population with higher oncogene expression levels. CaSki cells contain only one transcriptionally active viral genome. This integrant lacks a portion of the LCR upstream of E6 and E7 in this active integrant and it is unclear what drives expression of these genes in this cell line. Preliminary data from our lab indicate upregulation of E6 and E7 expression without apparent selective clonal expansion in CaSki cells *in vitro* following only 48 hours treatment with cetuximab. This supports the idea that EGFR inhibition is facilitating upregulation of expression in the overall population of cells. Further analysis of transcriptional control of viral gene expression in CaSki cells may shed light on our results and help to understand the mechanism underlying viral oncogene upregulation following cetuximab treatment.

The other explanation for the increase in E6 and E7 transcript levels after cetuximab administration is selection for a subpopulation of cetuximab resistant cells that already express high levels of E6 and E7. SCC104 cells were originally described as a mixed population of cells containing a small subset of cancer stem cells (CSS) exhibiting high ALDH expression (2.32% of the total cell population) [198]. Tang *et al.* implanted NSG mice with SCC104 subpopulations expressing either high or low ALDH levels and only the CSS were able to produce tumors. However, the tumorigenicity of the remaining cells that comprised the majority of the original population and expressed moderate levels of ALDH, was not evaluated. It is unknown if the percentage of each cell group has changed after multiple rounds of culturing *in vitro*. In our study, cells were not sorted prior to implantation therefore the effects of cetuximab treatment on these distinct subsets of cells, if still present in the implanted population, are not known. Future studies could address the presence and proportion of each of the ALDH subsets in our SCC104 cell stocks and investigate whether these proportions change following xenograft development and cetuximab treatment and if E6 and E7 expression differs or remains similar among these groups. Interestingly, RNA ISH staining of tissues from these populations indicates that a higher percentage of cells from cetuximab treated SCC104 tumors stained strongly for E6/E7 expression than in the vehicle treated group (Fig. 4.10D). These data support the idea that cetuximab treatment selected for a subset of cells with strong viral oncogene expression in SCC104 xenografts.

Decreased E6/E7 RNA levels were not observed in CaSki, SCC104, or SCC47 xenograft homogenates by RT-qPCR following cetuximab treatment. Neither was there apparent downregulation of cFos or JunB expression in these tumors (Fig. 4.2A, 4.7A

and Supplemental Fig. 5A). Whether the failure of cetuximab to downregulate AP-1 contributed to the unchanged E6 and E7 levels in CaSki cells is unclear. As discussed earlier, the levels of cFos and JunB RNA as measured by RT-qPCR in SCC47 xenografts may not be representative of the true expression of these genes if they are expressed only in distinct layers of differentiated epidermal tissue. Additional methods including IHC and RNA ISH could be used to validate RT-qPCR results in the context of epithelial morphology and differentiation state. The fact that trametinib treatment induced significantly decreased E6, E7 and AP-1 RNA levels in SCC47 xenografts indicates that cFos and/or JunB may facilitate the antiviral effects in this cell line. As mentioned previously, SCC104 cells have a mutation in *NOTCH1* resulting in a truncated form of the protein [156]. In an exome sequencing study of 32 primary HNSCC tumors, *NOTCH1* mutations were seen in 15% of tumors analyzed including three out of four HPV-positive tumors [154, 184]. *NOTCH1* mutations have also been seen in a percentage of HPV-positive cervical cancers and are associated with elevated expression levels of AP-1 transcription factors, including cFos and JunB [126, 191]. Reintroduction of functional Notch1 was shown to decrease levels of AP-1 transcription factors concomitantly with a reduction in E6/E7 expression levels [191]. Whether inhibitors targeting another cellular pathway would be effective in changing AP-1 components in this cell line is unclear. Further assessment of the promoters controlling viral oncogene expression, whether they are cellular or viral, may provide insight and aid in determining effective means of downregulating E6 and E7 expression.

SCC104 cells are reported to express high levels of EGFR; therefore, the antitumor effects may be mediated via the high EGFR expression in this cell line.

Cetuximab-mediated downregulation of total and phospho-EGFR as well as phospho-ERK1/2 was apparent (Table 4.3 and Figs. 4.8B and C). The downregulation of these proteins indicates that cetuximab treatment successfully inhibited EGFR/MEK signaling. In SCC104 tumors, we were unable to detect p53, even in the cetuximab treated group (Fig. 4.10B). Low levels of p53 staining were seen even in the parental tumor [198]. The lack of detectable p53 in these tumors makes sense due to the relatively high levels of E6/E7 expression seen in this cell line [199]. Furthermore the lack of p53 recovery in tumors that received cetuximab corresponds to the upregulation in viral oncogene expression levels observed (Fig. 4.7B). While cetuximab-treated SCC104 tumors exhibited slightly less intense staining for p16, expression was still strong and diffuse in these tissues (Fig. 4.10A). The persistence of p16 and absence of p53 (Fig. 4.10B) supports the lack of E6/E7 downregulation seen by RT-qPCR (Fig. 4.7B) and RNA ISH (Fig. 4.10D).

Histological evaluation of SCC104 xenografts from cetuximab and control groups revealed smaller tumors and therefore contained a smaller area of SCC and infiltrating stroma (Fig. 4.8A). As in SCC47 tumors, cetuximab induced markedly lower overall Ki67 levels in SCC104 xenografts but this difference disappeared when the number of Ki67 cells was normalized to epithelial area (Fig. 4.10C). Therefore, decreased proliferative ability in the remaining cells could not account for differences in tumor size.

Cetuximab treated SCC104 tumors exhibited a higher ratio of epithelium to stroma, indicating inhibition of fibroblast recruitment (Fig. 4.7B). However, it should be noted that fibroblasts present in the cetuximab treated tumors from both cell lines exhibited less staining for SMA, a marker of activated cancer associated fibroblasts

(CAFs) (Supplemental Fig. 3A and B). CAFs have been reported to have multiple roles in promoting malignant progression including enhancing metastatic potential. Recruitment and activation of CAFs by cancer cells is thought to take place via paracrine signaling and the TGF- β family of molecules, among others, has been shown to be important (Reviewed in [213]). The decreased SMA staining in cetuximab treated tumors indicates that EGFR inhibition downregulated release of fibroblast recruitment and/or activation signals from the cancer cells.

It is interesting to note that SCC47s contain 47 integrated copies of the HPV16 genome whereas SCC104 cells harbor only 1 viral genome copy as measured by whole genome sequencing [156]. Likewise, CaSki cell lines have 831 genome copies as compared to 1.5 in SiHa. The viral LCR seems to be retained in the majority of the integrated genomes, including all of the viral integration sites in the cells harboring low viral genome numbers [156]. As CaSki and SCC104 both exhibited heightened viral oncogene expression following cetuximab administration, the susceptibility of the virus to EGFR inhibition is not solely based on the number of viral genomes present. Instead, downregulation of viral oncogene transcription seems to correlate with the ability of cetuximab to reduce cFos expression levels as discussed previously.

In HPV-associated cancers, understanding the role of EGFR in maintaining viral oncoprotein levels may help to design more effective treatments and refine current treatment protocols. Cetuximab is already used in the treatment of HNSCC in conjunction with chemotherapy/radiation and some benefit has been shown for patients with advanced stage HPV-positive cancers over HPV-negative [172, 173]. However, previous clinical trials using cisplatin plus cetuximab or cetuximab as a monotherapy in

cervical cancer have failed to show a therapeutic benefit for the use of EGFR inhibitors in their patient populations [174, 175]. Based on our results, we suggest that cetuximab is able to induce antiviral effects in a subset of HPV-positive cancers. However, the extent and importance of this effect in the clinical setting remains to be studied. Retrospective studies examining tumor differences including expression levels of viral oncogenes and genome integration status, *NOTCH1* status, c-Fos activity, and EGFR-signaling components between patients who had a favorable response to treatment may help to shed additional light and identify patient populations which might benefit from these therapies.

4.5 Limitations of This Study

Our study presents novel information regarding the mechanism of antitumor effects of cetuximab in HPV-positive cancers, however questions still remain. In the SCC47 xenografts, it is yet unclear whether cetuximab-induced differentiation is the effect or cause of viral oncoprotein downregulation. As discussed, histological evaluation of trametinib treated SCC47 tumors may shed some light on this question. Additionally, the small number of animals in each treatment group may present a concern as the sample sizes prohibit robust statistical analysis. Repetition of this study for a selection of the cell lines and treatments with larger cohort sizes may be necessary to increase statistical power and demonstrate reproducibility. In this study, we have attempted to utilize cell lines representing a range of HPV-positive cancers, however, this has made defining a mechanism of action difficult due to the differences and complexities of each cell line. Further analysis of multiple cell line as well as patient derived tumor xenografts for each

of the HNSCC HPV-positive cancer subtypes will be necessary to define the molecular mechanisms whereby cetuximab exerts antitumor effects in HPV-positive cancers.

Chapter 5 - Discussion and Future Directions

This study provides insight into the ability of EGFR signaling to influence HPV oncogene transcription both in preneoplasia as well as in a model of HPV-positive cancer. Transformation of cells by HPV has been reported to provide growth factor independence. The mechanisms by which this takes place have been studied using exogenous overexpression of viral proteins. Numerous studies have shown that expression of one or more HPV oncoproteins can increase EGFR levels and signaling potential [63-66, 72, 121-124]. In this work, we sought to define the extent of HPV-associated dysregulation of EGFR signaling and determine if EGFR signaling affected HPV early transcription in a model of preneoplasia. We also sought to determine if EGFR-associated control of viral transcription extended to HPV-positive cancer cell lines, wherein inhibitors could downregulate viral oncogene transcription in a xenograft model of HPV-positive cancer.

Inhibition of EGFR/MEK signaling led to antiviral effects in NIKS-SG3 including downregulated viral oncogene transcription and reduced viral genome burden in infected cells. NIKS-SG3 treated with cetuximab also exhibited increased sensitivity to apoptotic stimuli. In xenografts, antitumor effects of cetuximab occurred either concurrent with or independent of changes in viral oncogene expression, depending on the tumor line. EGFR/MEK downregulation of viral RNA levels was strongly correlated with the ability of the inhibitor to decrease levels of the AP-1 transcription factors cFos and JunB, suggesting that these proteins may play a role in mediating the effects of these inhibitors on viral oncogene expression.

We determined that EGFR signaling modulates HPV oncogene transcription in cells carrying episomal viral genomes and that these cells are still sensitive to EGFR/MEK inhibitors. EGFR activation of NIKS-SG3 cells produced heightened viral oncogene expression and increased protein levels of the HPV-associated biomarker p16. These results suggest that E7 protein levels were heightened concomitant with RNA transcripts. Conversely, inhibition of EGFR or MEK resulted in decreased viral transcript levels. Furthermore, the antiviral effects of EGFR/MEK inhibitors extended to decreased viral genome burden and increased sensitivity to DNA damage in treated cells. Together, this data suggests that the EGFR pathway is a therapeutic target for HPV infections. It also provides a possible mechanism to explain the therapeutic effects of EGFR inhibitors such as erlotinib on laryngeal papillomas in RRP [169-171]. This has implications for the treatment of numerous HPV-associated diseases, including cancer, cervical preneoplasias, RRP, and genital and cutaneous warts.

Evaluation HPV oncogene expression on EGFR pathway regulation in a model of preneoplasia yielded surprising results. Contrary to previous reports, we discovered that EGFR expression was slightly lower in HPV-positive NIKS-SG3 than their parental cell line. The activation level of the EGFR pathway was not significantly enhanced by HPV infection, as we did not detect reproducible upregulation of phospho-EGFR in unstimulated cells. NIKS-SG3 are stably transfected with wild-type HPV16 genomes that are maintained episomally. These cells are capable of recapitulating the viral lifecycle and producing late viral proteins when grown in the organotypic raft system. Furthermore, NIKS-SG3 cells are reported to exhibit growth factor independence, indicating viral dysregulation of growth factor signaling pathways [135]. In agreement

with this, we observed that viral infection did contribute a degree of resistance to EGFR/MEK inhibition as seen by sustained viability in the presence of inhibitors. Indicating that viral activities did alter dependence on this pathway but the effect was subtle and differences in activation levels were not detectable in our system.

We also discovered that viral proteins did not significantly alter p53 levels in NIKS-SG3 when grown in subconfluent monolayers. This hindered our ability to evaluate the cellular effects of viral transcriptional downregulation. It should be noted that a previous publication by colleagues using a similar cell line, reported enhanced viral oncogene expression and activity when cells were grown to confluence [176]. For the most biologically relevant model available, our results should be confirmed in the organotypic raft culture system, which would allow recapitulation of epithelial differentiation and enable analysis of the effect of EGFR activation and inhibition on the full viral lifecycle. One drawback of this model is that cells cannot be continuously treated with EGF in the raft system as it prohibits cellular differentiation. It would be possible, however, to grow epidermal equivalents and allow them to differentiate prior to addition of EGF. This would enable investigation of the effect of EGF stimulation in an active infection. Our study further reinforces the importance of studying viral-host protein interactions under the most biologically relevant conditions possible.

EGFR activation-induced upregulation of viral transcription has many implications in HPV disease and progression to cancer. Numerous cofactors have been implicated in the progression from HPV infection to malignancy. These include lifetime number of sexual partners, parity, coinfection with other STIs, tobacco use, and long-term oral contraceptive use [89, 214-218]. Many of these cofactors possess the ability to

induce inflammation and activation of growth factor signaling pathways. Cervical malignancies typically arise from cells of the transformation zone, an area of metaplastic epithelium at the interface between the endo- and ectocervix [51, 86, 219]. The extensive remodeling of cervical tissue that occurs during pregnancy may result in heightened growth factor expression, increasing viral oncogene expression levels and exacerbating the chance of cellular transformation [220]. This may partially explain why women with high parity are at a higher risk of developing cervical cancer.

Chronic inflammation is considered a risk factor in cancer development [221] and STIs have been shown to initiate an inflammatory response in the genital tract. Coinfection with other STI's including *C. gonorrhoea* and HSV-2 has been shown to increase the risk of HPV-associated cancer, possibly by stimulating inflammation [89, 218]. However, inflammatory causes do not have to be infectious. In fact, exposure to seminal fluid itself has been implicated in activating release of inflammatory cytokines from immortalized ectocervical cells in vitro [222]. While some studies have shown that inflammatory cytokines can inhibit HPV gene expression in vitro, this seems to be context dependent and this has not been examined in vivo [36, 223, 224]. Additionally, we previously showed that nitric oxide or mainstream (MS) tobacco smoke exposure led to heightened HPV oncogene expression, DNA damage and mutation rates in HPV-positive cancer cells in vitro [137, 225]. Alam, *et al*, also reported that exposure to benzo[a]pyrene, a major component of MS tobacco smoke, activated the MEK pathway and enhanced HPV oncogene expression and virion production in vitro [226]. Further investigation into the effects of these factors on the tissue milieu may provide insight into the mechanisms that underlie progression to cancer in HPV infected cells.

In our xenograft model, cetuximab inhibited tumor growth either concurrent with or independent of changes in viral RNA levels. Viral oncogene expression was downregulated in SiHa xenografts treated with cetuximab. However, administration of cetuximab in animals bearing SCC104 or CaSki xenografts resulted in higher E6 and E7 RNA levels. It is unclear whether EGFR inhibition in these tumors upregulated viral transcription or selected for a subpopulation of cells with heightened oncogene expression. Interestingly, trametinib but not cetuximab was able to induce significant downregulation of viral oncogene levels in SCC47. In all cell lines, downregulation of cFos and JunB by EGFR/MEK inhibition was seen concomitantly with decreased E6 and E7 levels. Whether this relationship is causative has yet to be determined.

The UM-SCC47 xenografts represent an interesting subset of HPV-positive cancers. Untreated tumors from this cell line were moderately differentiated and RNA ISH revealed downregulation of viral transcript levels in suprabasal layers. This indicates that differentiation events are tied to viral transcription, similar to a natural productive infection. In the upper layers of epithelium from untreated SCC47 tumors, downregulation of E6/E7 transcript levels and proliferative activity, as seen by Ki67 staining, corresponded with increased levels of nuclear p53. Cetuximab treatment further enhanced differentiation in SCC47 xenografts, resulting in tumors containing very little epithelium. The epithelial cells that remained following cetuximab treatment contained comparatively low levels of E6/E7 expression, as visualized by RNA ISH, when compared to basal cells in the untreated tumors. Downregulation of viral RNA levels was seen concomitant with cellular differentiation; however, it is unclear whether the decreased viral transcription is the cause or effect of cellular differentiation. Future work

should investigate the fate of these remaining cells following exposure to radiochemotherapy. Cetuximab treatment and differentiation may have sensitizing effects on these cells resulting in apoptosis. Conversely, the cetuximab resistant cells could represent a population of cancer cells with prior resistance to cetuximab or cells with acquired resistance, either of which are more resistant to therapy. Determining the fate of these remaining cells following radiochemotherapy may provide insight into the development of resistance to EGFR inhibitors.

The ability of trametinib to significantly inhibit viral transcription in SCC47 cells while cetuximab did not suggests that the MEK/ERK pathway may not be sufficiently inhibited by cetuximab. A previous report indicated that SCC47 cells sustained ERK activation in the presence of cetuximab or trametinib in vitro [201]. Our cetuximab tissues showed downregulated but not abolished ERK signaling suggesting possible activation of this signaling node by another pathway. Investigation of the histological features of these tumors and comparison with cetuximab treated tumors may shed some light on the different effects seen by these two inhibitors.

The UM-SCC104 cell line, which responded to cetuximab with upregulated HPV oncogene transcript levels in the xenograft system, contains a NOTCH1 mutation. This mutation is commonly seen in cervical cancers and is also seen in 14-15% of HNSCC [154, 184, 207]. While Notch1 appears to play a beneficial role in the early stages of the HPV lifecycle, by initiating cellular differentiation, loss of this protein appears to support progression to malignancy [191, 208, 227]. Additionally, loss of Notch1 is associated with upregulation of cFos expression [126, 191, 208]. In each of our xenograft lines, the ability of the treatment to downregulate levels of cFos in the tumor appeared to

correspond to downregulation of E6/E7 expression. Whether mutations in Notch1 affect the response to EGFR inhibition should be further investigated. Possible dysregulation of this and other associated pathways should be considered when determining the efficacy of EGFR/MEK inhibitor therapy in HPV-positive tumors.

Our study revealed that EGFR/MEK inhibition produced antiviral effects by downregulating E6/E7 expression in subsets of HPV-positive xenografts. However, further studies will need to be conducted to determine what viral oncoprotein downregulation ultimately means in terms of treatment benefit. Cetuximab was able to reduce growth of all of our xenograft lines, regardless of viral response. Whether downregulation of viral protein levels in the responding tumors results in heightened sensitivity to chemoradiotherapy has yet to be determined. While numerous cancers contain mutated p53, HPV-associated cancers typically do not. Reinstatement of p53 levels by decreasing E6/E7 expression should sensitize tumors to chemoradiotherapy and numerous groups have shown this *in vitro* [79, 209, 228, 229]. This remains to be studied in the clinic. In fact, our lab is involved in a new clinical trial to determine if administration of cetuximab as a neoadjuvant prior to chemotherapy or radiation downregulates E6/E7 expression and increases radiosensitivity in HPV-positive HNSCC. Data from this study will help to further understand the extent of EGFR-mediated control of HPV oncogene expression *in vivo*.

EGFR or MEK1/2 inhibition resulted in decreased E6 and E7 RNA levels in SiHa and SCC47 xenografts indicating that viral transcription can be modulated by EGFR-pathway signaling. However, we did not investigate whether EGFR activation increased viral oncoprotein levels in this system. Cisplatin, a platinum-based chemotherapeutic

commonly used in the treatment of HPV-associated cancers, has been reported to activate EGFR [162]. The effect of cisplatin-induced EGFR activation on viral activities and how this might affect treatment outcome has yet to be investigated. However, this could have significant implications in response to therapy and should be studied further.

Previously, HNSCC were classified based solely on anatomic site, stage, and HPV-status. However, a recent study analyzed gene expression profiles from an extensive panel of HNSCC patient tumors including 44% HPV-positive tumors. The authors discovered three distinct gene expression profiles which, when HPV-status is factored in, creates five subtypes of HNSCC [207]. The authors argue that there are two subsets of HPV-positive HNSCC, a classical type (CL) and an inflamed/mesenchymal (IMS) subset. CL HPV-positive HNSCCs contain upregulation of the polyamine degradation pathway, which is correlated with high levels of cell proliferation. These tumors also contain many of the copy number variations and mutations associated with HPV-positive HNSCC including PIK3CA. Interestingly, over 40% of the CL HPV-positive tumors studied were keratinizing, indicating a higher degree of differentiation. The phenotypic characteristics of these tumors are similar to the SCC47 xenografts. SCC47 tumors have a rapid growth rate, are moderately differentiated, and tumors contain keratin deposits indicating this cell line might be representative of the CL HPV-positive HNSCC subtype. Better understanding of the mechanism behind the cetuximab-associated differentiation in SCC47 xenografts and resulting reaction of these tumors to chemoradiotherapy may help to inform whether these patients are good candidates for EGFR/MEK inhibitors.

In contrast to HPV-positive CL tumors, HPV-positive IMS tumors express more mesenchymal markers, including vimentin and matrix metalloproteinases, while expression of epithelial markers, including cadherins and cytokeratins, is downregulated. Expectedly, these tumors appear poorly differentiated morphologically. IMS tumors also exhibited heightened expression of immune response genes including *CD8*, indicating immune involvement. Follow-up studies revealed the presence of infiltrating CD8+ lymphocytes in tumor sections. Interestingly, these patients had a higher 5-year overall survival than the CL HPV-positive subgroup possibly owing to immune response. Cetuximab's therapeutic effects are hypothesized to partially depend on an effective immune response [120]. It would be interesting to determine if these patients have a better response to cetuximab therapy than those with CL HPV-positive tumors. The delineations set forth by Keck, *et al.* are crucial in designing effective therapeutic interventions that will best target each subtype. Additional research into how these distinct subsets respond to individual therapies is needed.

As the single most prevalent sexually transmitted infectious agent, human papillomaviruses present a significant health problem. Cancers attributed to HPV infection represent 5% of all cancers worldwide [5]. In addition to the well-established relationship between high-risk HPVs and cervical cancer, infection with these viruses is now associated with a growing number of head and neck cancers [5-7]. While the greatest burden of cervical cancer falls on the developing world, the highest number of incident cases of HPV-positive HNSCC is found in developed countries including the U.S.

There are effective vaccines that protect against the HPV types that cause 70% of all cervical cancer and 90% of all HPV-associated head and neck cancers. However, overall public health benefit is hindered by low uptake. In the U.S., currently only 40% of females and <30% of males of the target age have received the full three dose series of the vaccine [8]. Furthermore, the high cost of the vaccine limits its usage in developing countries where it would be most beneficial in preventing cervical cancer. Although the PAP screening program has been very successful in decreasing the incidence of cervical cancer in the U.S. and other developed countries, there is no mechanism in place for screening of women in developing countries. Furthermore, there is currently no clinically available method of screening for oral HPV infections. Therefore continued research into mechanisms that underlie HPV-associated malignant progression is imperative.

The growing number of HPV-positive HNSCC creates a new patient population that will benefit from enhanced therapeutic approaches. Understanding of the pathways regulating viral oncogene expression is imperative in designing effective therapies. While this work focused on HPV16, mechanisms of viral transcriptional control are similar for other oncogenic HPV types that have been studied [20]. The work herein described the antiviral effects of EGFR/MEK inhibitors on HPV-positive cells both in vitro and in vivo and sets the stage for future work to determine if the downregulation of viral activities translates to increased sensitivity to chemoradiotherapy. Results of these studies may help to design more effective treatments and refine current treatment protocols for HPV-associated diseases.

LIST OF APPENDICES

Appendix A – List of abbreviations

Appendix B – Supplemental Xenograft Data

Appendix C - References

Appendix A – Abbreviations

DMEM – Dulbecco’s modified eagle medium

DMSO – dimethylsulfoxide

dsDNA – double stranded DNA

EGF – epidermal growth factor

EGFR – epidermal growth factor receptor

ERK1/2 – extracellular signal-regulated kinase-1/2

HPV – human papillomavirus

HNC – head and neck cancer

HNSCC – head and neck squamous cell carcinoma

IB – immunoblot

IHC – immunohistochemistry

LCR – long control region

MAPK – mitogen-activated protein kinase

MEK1/2 – mitogen-activated protein kinase kinase-1/2

NBF – neutral buffered formalin

NSG – NOD/SCID-gamma

OPSCC – oropharyngeal squamous cell carcinoma

PBS – phosphate buffered saline

PI3K – phosphoinositide 3-kinase

RT-qPCR - reverse transcription quantitative polymerase chain reaction

SCC – squamous cell carcinoma

SEM – standard error of the mean

SFM – serum-free media

TBS-T – Tris buffered saline + 0.1% Tween-20

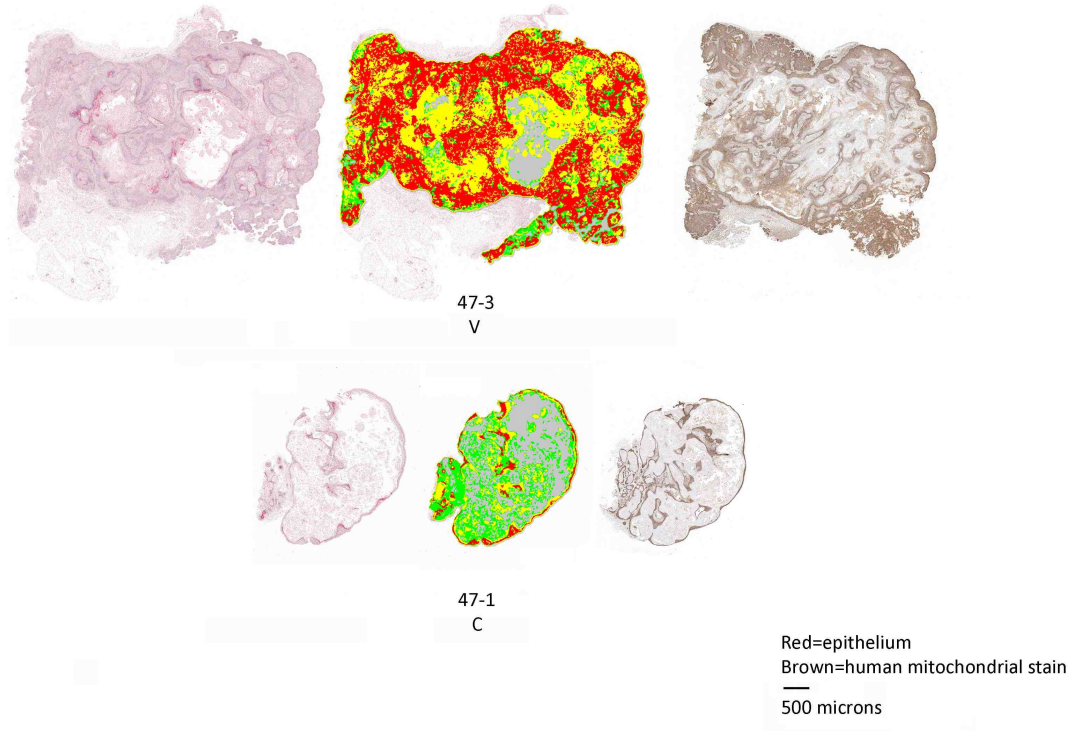
TF – transcription factor

TGF- α – transforming growth factor alpha

URR – upstream regulatory region

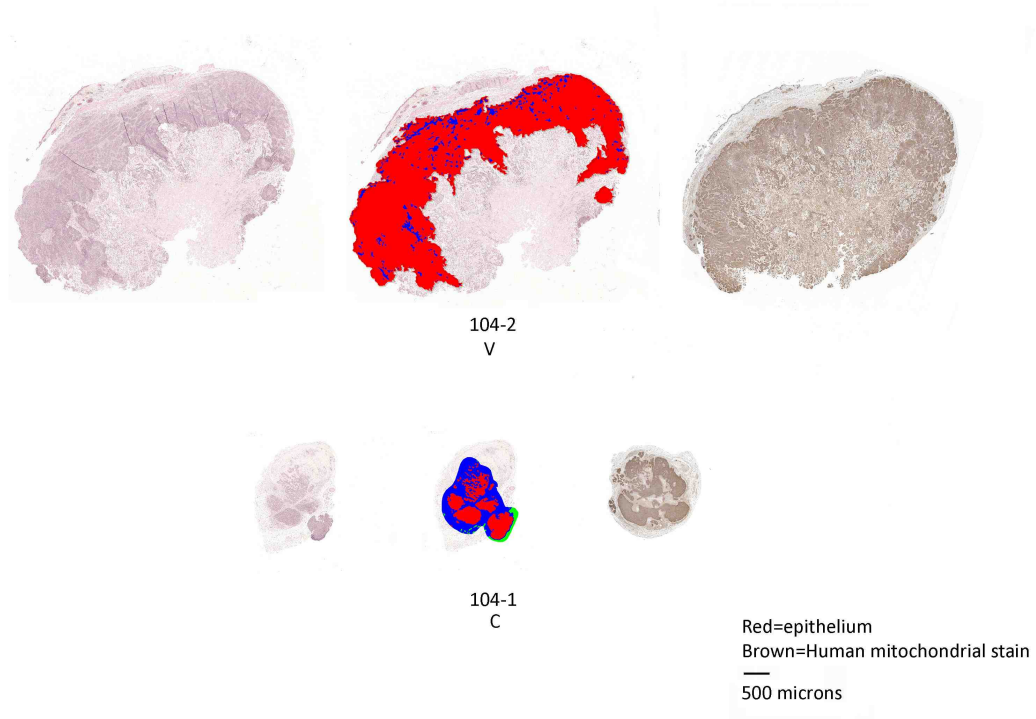
WT – wild type

Appendix B – Supplemental Xenograft Data



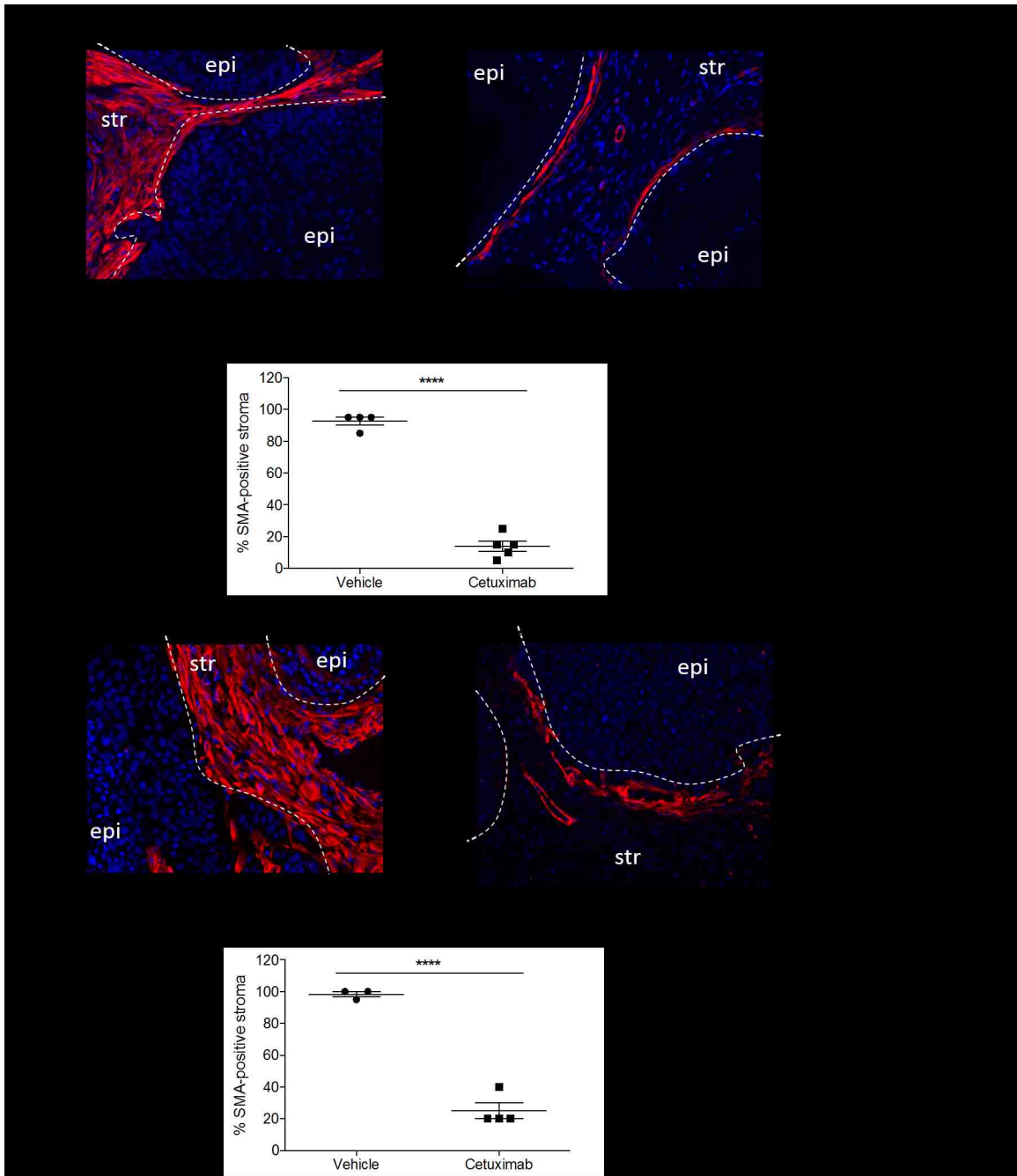
Supplemental Figure 1 Determination of epithelial area in SCC47 xenograft sections.

Scans of representative FFPE sections of xenografts from vehicle control tumors (top) and cetuximab treated tumors (bottom). Unmarked scans of H&E stained sections are shown (left). Center images depict scans of the same H&E slide with areas marked as epithelium (red), keratin (yellow), and stroma (green) determined by morphology. Percent composition was determined for each tumor and averages are shown in Fig. 4.3. Human mitochondrial marker IHC stained sections (right) were used to confirm epithelial areas. All histology was performed by a certified pathologist (Dr. D. Kusewitt) using Aperio ImageScope software.



Supplemental Figure 2 Determination of epithelial area in SCC104 xenograft sections.

Scans of representative FFPE sections of xenografts from vehicle control tumors (top) and cetuximab treated tumors (bottom). Unmarked scans of H&E stained sections are shown (left). Center images depict scans of the same H&E slide with areas marked as epithelium (red), and stroma (blue) determined by morphology. Percent composition was determined for each tumor and averages are shown in Fig. 4.8. Human mitochondrial marker IHC stained sections (right) were used to confirm epithelial areas. All histology was performed by a certified pathologist (Dr. D. Kusewitt) using Aperio ImageScope software.



Supplemental Figure 3 Cetuximab treatment leads to lower levels of smooth muscle actin (SMA) in tumor infiltrating fibroblasts.

Tumor sections from NSG mice bearing xenograft tumors from SCC47 (A) or SCC104 (B) cell lines were stained for SMA, a marker of activated tumor associated fibroblasts. Nuclei are stained with DAPI (blue) and SMA is shown in red. Representative images are shown for each xenograft group. Percent of stroma staining positive for SMA in sections from each tumor are shown in the graphs. Error bars = SEM, statistical significance assessed by Student t-test, ****p<0.001.

Supplemental Table 1 Summary of SCC47 xenograft data

	Average Untreated	Average Cetuximab	Figure
Tumor weight at necropsy (in grams)	0.07	0.440	4.2B
% Epithelium	39.25	15.23	4.3
% Necrosis	0	0	4.3
% Stroma	13.87	28.91	4.3
% SMA-positive stroma	92.50	14.00	Supp. Fig. 3
% Keratin	38.66	45.69	4.3
EGFR IHC score	2.75	2.2	4.4A
Phospho-EGFR IHC score	1.67	0.8	4.4B
Phospho-ERK1/2 IHC score	3	1.6	4.4C
Ki67-positive epithelium cells (total)	21,633.75	1452.60	4.5C
Ki67-positive cells (normalized to epithelial area)	784.55	760.96	4.5C
E6 relative RNA level	1.00	0.89	4.2C
E7 relative RNA level	1.00	1.07	4.2C
E6/E7 ISH	Staining sparse and low intensity	Strong staining in basal cells only, no staining in upper epithelium	4.5D
p16 IHC score	2.75	1.8	4.5A
p53 IHC score	2.75	2	4.5B
cFos relative RNA level	1.00	1.78	4.2F
cFos:E6 Spearman's <i>r</i> : -0.67			4.2G
cFos:E7 Spearman's <i>r</i> : -0.53			4.2G
JunB relative RNA level	1	1.11	4.2F
JunB:E6 Spearman's <i>r</i> : -0.67			4.2H
JunB:E7 Spearman's <i>r</i> : -0.48			4.2H

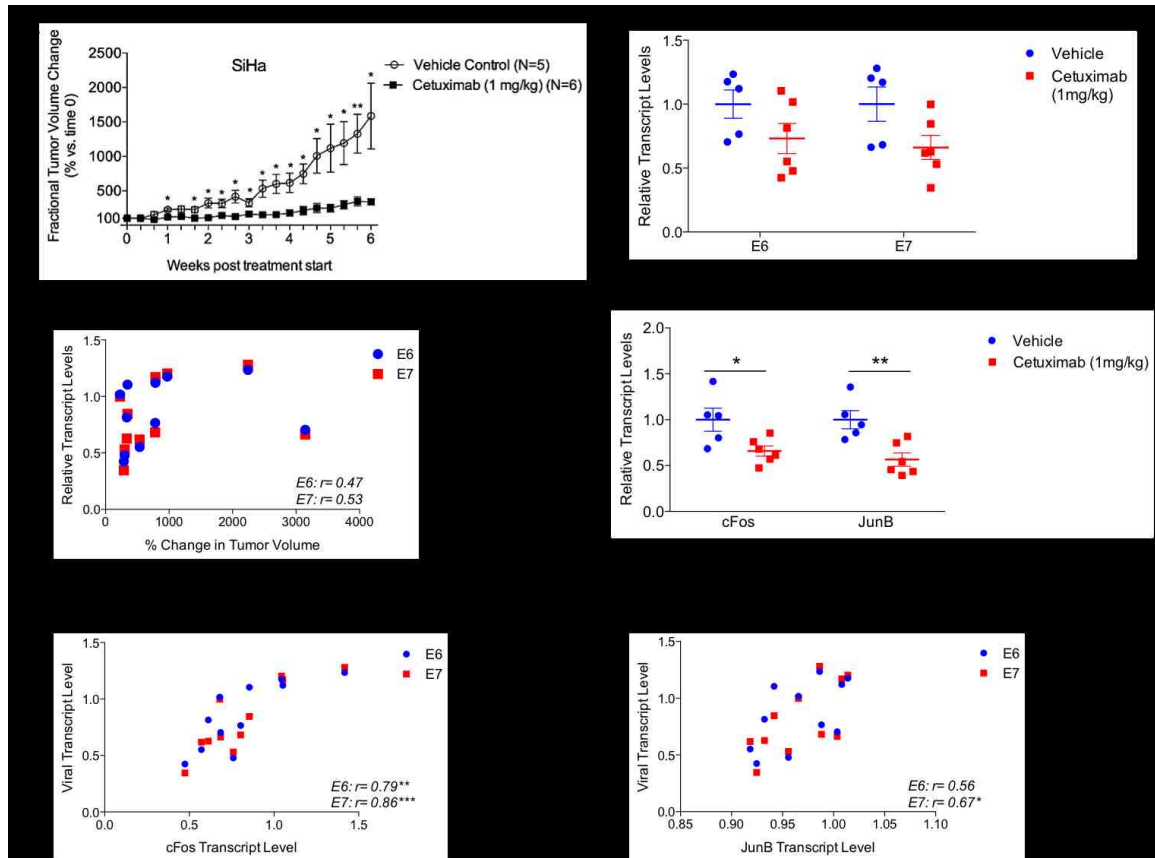
Supplemental Table 2 Summary of SCC104 xenograft data

	Average Untreated	Average Cetuximab	Figure
Tumor weight at necropsy (in grams)	0.78	0.078	4.7A, B
% Epithelium	30.23	54.45	4.8
% Necrosis	47.05	4.1	4.8
% Stroma	21.67	39.88	4.8
% SMA-positive stroma	98.00	25.00	Supp. Fig. 3
% Keratin	0	0	4.8
EGFR IHC score	2	1.2	4.9A
Phospho-EGFR IHC score	2	1.2	4.9B
Phospho-ERK1/2 IHC score	1.25	0.8	4.9C
Ki67-positive epithelium cells (total)	36,315	4,333	4.10C
Ki67-positive cells (normalized to epithelial area)	650	584	4.10C
E6 relative RNA level	1.00	6.52	4.7C
E7 relative RNA level	1.00	9.13	4.7C
E6/E7 ISH	High/Diffuse	High/Diffuse	4.1D
p16 IHC score	3	2	4.10A
p53 IHC score	0	0	4.10B
cFos relative RNA level	1.00	0.73	4.7F
cFos:E6 Spearman's <i>r</i> : 0.88			4.7G
cFos:E7 Spearman's <i>r</i> : 0.78			4.7G
JunB relative RNA level	1.00	1.12	4.7F
JunB:E6 Spearman's <i>r</i> : -0.32			4.7H
JunB:E7 Spearman's <i>r</i> : -0.45			4.7H

B.1 Effect of Cetuximab Treatment on Viral Oncogene Expression in SiHa Tumor Xenografts

SiHa cells contain 1.5 integrated copies of the HPV16 genome and whole genome sequencing has shown that the intact LCR is still located upstream of viral genes [156]. A previous study found that cetuximab treatment reduces the growth rate of SiHa xenografts in mice [194]. In our study, cetuximab (1mg/kg, 3x/week) treatment of mice with SiHa xenografts resulted in diminished tumor growth and this was highly evident as early as 2 weeks post treatment start (Supplemental Fig. 4A). Xenografts were harvested at 6 weeks post treatment, when control tumors reached the maximum volume allowed in our study. Cetuximab treated xenografts increased in size <2-fold from the starting volume while tumors in the control group increased by an average of 15x their original volume. E6 and E7 transcript levels in the xenograft tumors harvested at 6-weeks post

treatment were evaluated by RT-qPCR and normalized to human β -actin expression levels. Based on group averages, viral oncogene transcript levels were downregulated in cetuximab treated xenografts but this difference was not statistically significant (Supplemental Fig. 4B). When normalized levels of E6 and E7 transcripts were plotted against the change in tumor volume over the course of treatment, we observed no significant correlation between the levels of either E6 or E7 oncogene transcript and tumor volume (Supplemental Fig. 4C). This suggests that final tumor size is not directly associated with levels of viral oncogene expression. However, we cannot rule out a role for cetuximab-mediated oncogene suppression in the antitumor effects seen. There may be a threshold level of E6/E7 expression required to drive survival and or maintenance of tumor size in SiHa xenografts treated with cetuximab. In which case, the modest downregulation of E6/E7 expression observed may have been enough to have a significant impact on tumor growth rate.



Supplemental Figure 4 Cetuximab delays tumor growth and decreases viral oncogene expression along with c-Fos and JunB expression levels in SiHa xenografts.

NSG mice bearing SiHa xenografts implanted subcutaneously were given cetuximab (1 mg/kg) or vehicle only (0.9% saline) by i.p injection 3x/week. Tumors were measured 3x/week by caliper and percent growth from treatment start (time=0) are shown in (A). RNA from homogenized tumor sections was analyzed by RT-qPCR for expression levels of viral oncogenes E6 and E7, and AP-1 transcription factors cFos and JunB. Transcript levels were normalized to human β -actin transcript levels. The average expression levels of normalized target from the vehicle tumors was set to 1 and data shown as fold-change compared to control. Relative expression levels of E6 and E7 are shown in (B). Relative levels of E6 and E7 transcripts were plotted against the change in tumor volume over the course of treatment and linear correlation assessed by Spearman's r test (C). Relative expression levels of c-Fos and JunB are shown in (D). Relative levels of E6 and E7 transcripts were plotted against the expression levels of c-Fos (E) and JunB (F) and linear correlation assessed by Spearman's r test. Error bars = SEM, statistical significance assessed by Student t-test, * $p \leq 0.05$, ** $p \leq 0.01$, *** $p \leq 0.001$.

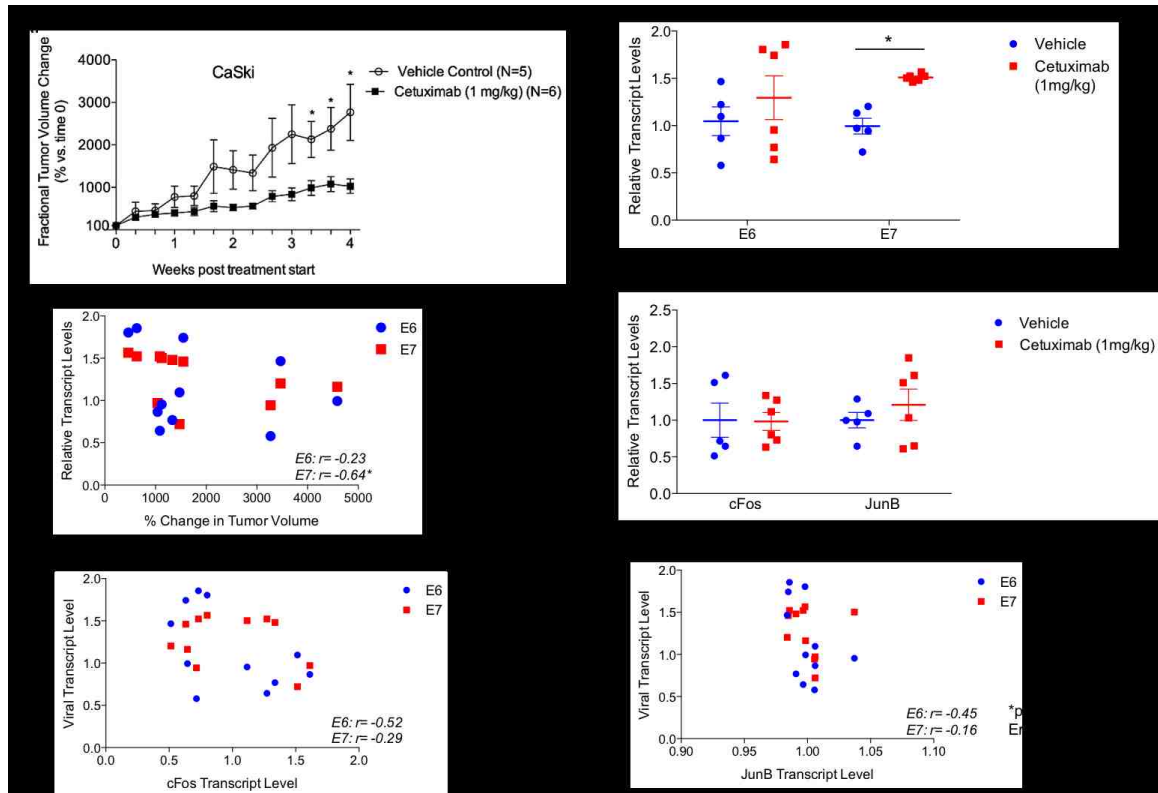
When the data in each group are averaged, expression of both cFos and JunB was downregulated in cetuximab treated animals (Supplemental Fig. 4D). In each tumor, we compared the levels of viral transcripts to the levels of AP-1 c-Fos and JunB RNA levels and found there was a strong positive correlation between levels of c-Fos expression and

E6 and E7 transcript levels in each tumor (E6: $r=0.79$, $p\leq 0.01$; E7: $r=0.86$, $p\leq 0.001$) (Supplemental Fig. 4E) and a modest correlation between JunB and E6/E7 transcript levels (E6: $r=0.56$, n.s.; E7: $r=0.67$, $p\leq 0.01$) (Supplemental Fig. 4F). These results indicate that cetuximab treatment leads to reduced viral oncogene transcript levels in SiHa xenografts, in agreement with our original hypothesis. The concurrent downregulation of transcript levels of AP-1 transcription factors c-Fos and JunB in cetuximab treated cells suggest that these proteins may be associated with the diminished E6 and E7 levels observed in these tissues. As noted previously, the integrated viral genome has been reported to contain the intact LCR, containing AP-1 binding sites, upstream of the E6 and E7 genes in SiHa cells indicating that this region may still control viral transcription [156].

B.2 Effect of Cetuximab Treatment on Viral Oncogene Expression in CaSki Tumor Xenografts

CaSki cells contain >800 integrated HPV16 genomes with numerous genomic translocations ([156] and others). However, only one of the viral genomes, located on a derivative of chromosome 14, is transcriptionally active [23]. There are two viral genomes integrated within chromosome 14, the first contains a viral breakpoint within the E6 gene and is therefore likely not the source of E6 and E7 expression [156]. The second integrated genome is likely the transcriptionally active site observed previously and it contains a breakpoint within the viral LCR, suggesting this region may not be influencing viral oncogene transcription in this cell line. CaSki tumors grew faster than SiHa xenografts and the tumors had to be harvested at 4 weeks post treatment start. Cetuximab treatment resulted in 2.5x decreased tumor growth rate in CaSki xenografts as

compared to the vehicle control group; however, this was less dramatic than in the SiHa cohort (Supplemental Fig. 5A). We detected no change in E6 RNA expression levels upon cetuximab treatment in CaSki xenografts (Supplemental Fig. 5B). Surprisingly, levels of E7 increased while the tumors grew slowly following cetuximab treatment (Supplemental Fig. 5B). The remarkably similar levels of E7 RNA found in cetuximab treated, slow growing tumors might be indicative that there was a selection for cells with higher E7 expression levels. Furthermore, there was a moderate negative correlation between normalized levels E7 transcripts and change in tumor volume over the course of treatment the tumors from the cetuximab treated group were expressing relatively higher levels of E7 than those from the control group (Supplemental Fig. 5C). These results suggest that the decrease in tumor growth rate is not associated with E6 and E7 expression levels.



Supplemental Figure 5 Cetuximab produces antitumor effects independent of viral oncogene expression in CaSki xenografts.

NSG mice bearing CaSki xenografts implanted subcutaneously were given cetuximab (1 mg/kg) or vehicle only (0.9% saline) by i.p injection 3x/week. Tumors were measured 3x/week by caliper and percent growth from treatment start (time=0) are shown in (A). RNA from homogenized tumor sections was analyzed by RT-qPCR for expression levels of viral oncogenes E6 and E7, and AP-1 transcription factors cFos and JunB. Transcript levels were normalized to human β -actin transcript levels. The average expression levels of normalized target from the vehicle tumors was set to 1 and data shown as fold-change compared to control. Relative expression levels of E6 and E7 are shown in (B). Relative levels of E6 and E7 transcripts were plotted against the change in tumor volume over the course of treatment and linear correlation assessed by Spearman's r test (C). Relative expression levels of c-Fos and JunB are shown in (D). Relative levels of E6 and E7 transcripts were plotted against the expression levels of c-Fos (E) and JunB (F) and linear correlation assessed by Spearman's r test. Error bars = SEM, Statistical significance assessed by Student t-test, * $p \leq 0.05$.

We observed no statistically significant differences in c-Fos or JunB expression between cetuximab and vehicle groups (Supplemental Fig. 5D). Neither did we find a significant correlation between E6 or E7 transcript levels and either of the AP-1 transcription factors evaluated (Supplemental Fig. 5E, F). These data together suggest that expression of c-Fos and JunB is not altered by EGFR inhibition. In fact, cetuximab

treatment led to similarly increased E7 RNA levels in xenografts. Analysis of gene expression profiles by RNAseq and proteomic profiling would be useful in better understanding the signaling pathways differentially activated in this cell line. Histological analysis of tumors from vehicle and treated animals will also be useful in determining the mechanisms behind the reaction of these tumors specifically, it would be important to determine if cetuximab treated tumors contain cells with sustained phospho-EGFR and heightened E7 expression.

Appendix C - References

1. Javier, R.T. & Butel, J.S. The History of Tumor Virology. *Cancer Research* **68**, 7693-7706 (2008).
2. Rous, P. A Sarcoma of the Fowl Transmissible by an Agent Separable from the Tumor Cells. *Journal of Experimental Medicine* **13**, 397-411 (1911).
3. Van Epps, H.L. Peyton Rous: father of the tumor virus. *Journal of Experimental Medicine* **201**, 320 (2005).
4. Martin, G.S. The road to Src. *Oncogene* **23**, 7910-7917 (2004).
5. de Martel, C., Ferlay, J., Franceschi, S., Vignat, J., Bray, F., Forman, D. & Plummer, M. Global burden of cancers attributable to infections in 2008: a review and synthetic analysis. *The Lancet Oncology* **13**, 607-615 (2012).
6. Giuliano, A.R., Nyitray, A.G., Kreimer, A.R., Pierce Campbell, C.M., Goodman, M.T., Sudenga, S.L., Monsonogo, J. & Franceschi, S. EUROGEN 2014 roadmap: Differences in human papillomavirus infection natural history, transmission and human papillomavirus-related cancer incidence by gender and anatomic site of infection. *International Journal of Cancer* **136**, 2752-2760 (2015).
7. zur Hausen, H. The search for infectious causes of human cancers: Where and why? *Virology* **392**, 1-10 (2009).
8. Markowitz, L.E., Hariri, S., Lin, C., Dunne, E.F., Steinau, M., McQuillan, G. & Unger, E.R. Reduction in human papillomavirus (HPV) prevalence among young women following HPV vaccine introduction in the United States, National Health and Nutrition Examination Surveys, 2003-2010. *Journal of Infectious Disease* **208**, 385-393 (2013).
9. Bernard, H.U., Burk, R.D., Chen, Z., van Doorslaer, K., zur Hausen, H. & de Villiers, E.M. Classification of papillomaviruses (PVs) based on 189 PV types and proposal of taxonomic amendments. *Virology* **401**, 70-79 (2010).
10. de Villiers, E.M., Fauquet, C., Broker, T.R., Bernard, H.U. & zur Hausen, H. Classification of papillomaviruses. *Virology* **324**, 17-27 (2004).
11. Steinberg, B.M., Auborn, K.J., Brandsma, J.L. & Taichman, L.B. Tissue site-specific enhancer function of the upstream regulatory region of human

- papillomavirus type 11 in cultured keratinocytes. *Journal of Virology* **63**, 957-960 (1989).
12. Schmitt, A., Rochat, A., Zeltner, R., Borenstein, L., Barrandon, Y., Wettstein, F.O. & Iftner, T. The primary target cells of the high-risk cottontail rabbit papillomavirus colocalize with hair follicle stem cells. *Journal of Virology* **70**, 1912-1922 (1996).
 13. Egawa, K. Do human papillomaviruses target epidermal stem cells? *Dermatology* **207**, 251-254 (2003).
 14. Meyers, C., Frattini, M.G., Hudson, J.B. & Laimins, L.A. Biosynthesis of human papillomavirus from a continuous cell line upon epithelial differentiation. *Science* **257**, 971-973 (1992).
 15. Ozbun, M.A. & Meyers, C. Human papillomavirus type 31b transcription during the differentiation-dependent viral life cycle. *Current Topics in Virology* **1**, 203-217 (1999).
 16. Ozbun, M.A. & Meyers, C. Two novel promoters in the upstream regulatory region of human papillomavirus type 31b are negatively regulated by epithelial differentiation. *Journal of Virology* **73**, 3505-3510 (1999).
 17. Zheng, Z.M. & Baker, C.C. Papillomavirus genome structure, expression, and post-transcriptional regulation. *Frontiers in Bioscience* **11**, 2286-2302 (2006).
 18. Kadaja, M., Silla, T., Ustav, E. & Ustav, M. Papillomavirus DNA replication — From initiation to genomic instability. *Virology* **384**, 360-368 (2009).
 19. Frattini, M.G. & Laimins, L.A. The role of the E1 and E2 proteins in the replication of human papillomavirus type 31b. *Virology* **204**, 799-804 (1994).
 20. Graham, S. Human papillomavirus: gene expression, regulation and prospects for novel diagnostic methods and antiviral therapies. *Future Microbiology* **5**, 1493-1506 (2010).
 21. Skiadopoulos, M.H. & McBride, A.A. Bovine papillomavirus type 1 genomes and the E2 transactivator proteins are closely associated with mitotic chromatin. *Journal of Virology* **72**, 2079-2088 (1998).
 22. You, J., Croyle, J.L., Nishimura, A., Ozato, K. & Howley, P.M. Interaction of the Bovine Papillomavirus E2 Protein with Brd4 Tethers the Viral DNA to Host Mitotic Chromosomes. *Cell* **117**, 349-360 (2004).

23. Van Tine, B.A., Dao, L.D., Wu, S.Y., Sonbuchner, T.M., Lin, B.Y., Zou, N.X., Chiang, C.M., Broker, T.R. & Chow, L.T. Human papillomavirus (HPV) origin-binding protein associates with mitotic spindles to enable viral DNA partitioning. *Proceedings of the National Academy of Sciences United States of America* **101**, 4030-4035 (2004).
24. Tan, S.-H., Bartsch, D., Schwarz, E. & Bernard, H.-U. Nuclear matrix attachment regions of human papillomavirus type 16 point toward conservation of these genomic elements in all genital papillomaviruses. *Journal of Virology* **72**, 3610-3622 (1998).
25. McBride, A.A., Oliveira, J.G. & McPhillips, M.G. Partitioning viral genomes in mitosis: same idea, different targets. *Cell Cycle* **5**, 1499-1502 (2006).
26. Doorbar, J., Ely, S., Sterling, J., McLean, C. & Crawford, L. Specific interaction between HPV-16 E1—E4 and cytokeratins results in collapse of epithelial cell intermediate filament network. *Nature (London)* **352**, 824-827 (1991).
27. Doorbar, J. The papillomavirus life cycle. *Journal of Clinical Virology* **32S**, S7-S15 (2005).
28. Ozburn, M.A. & Meyers, C. Temporal usage of multiple promoters during the life cycle of human papillomavirus type 31b. *Journal of Virology* **72**, 2715-2722 (1998).
29. Thierry, F. & Yaniv, M. The BPV1-E2 *trans*-acting protein can be either an activator or a repressor of the HPV18 regulatory region. *European Molecular Biology Organization Journal* **6**, 3391-3397 (1987).
30. Thierry, F., Dostatni, N., Arnos, F. & Yaniv, M. Cooperative activation of transcription by bovine papillomavirus type 1 E2 can occur over a large distance. *Molecular and Cellular Biology* **10**, 4431-4437 (1990).
31. Smotkin, D. & Wettstein, F.O. Transcription of human papillomavirus type 16 early genes in a cervical cancer and a cancer-derived cell line and identification of the E7 protein. *Proceedings of the National Academy of Sciences United States of America* **83**, 4680-4684 (1986).
32. Grassmann, K., Rapp, B., Maschek, H., Petry, K.U. & Iftner, T. Identification of a differentiation-inducible promoter in the E7 open reading frame of human papillomavirus type 16 (HPV-16) in raft cultures of a new cell line containing high copy numbers of episomal HPV-16 DNA. *Journal of Virology* **70**, 2339-2349 (1996).

33. Soeda, E., Ferran, M.C., Baker, C.C. & McBride, A.A. Repression of HPV16 early region transcription by the E2 protein. *Virology* **351**, 29-41 (2006).
34. Francis, D.A., Schmid, S.I. & Howley, P.M. Repression of the integrated papillomavirus E6/E7 promoter is required for growth suppression of cervical cancer cells. *Journal of Virology* **74**, 2679-2686 (2000).
35. Arias-Pulido, H., Peyton, C.L., Joste, N.E., Vargas, H. & Wheeler, C.M. Human Papillomavirus Type 16 Integration in Cervical Carcinoma In Situ and in Invasive Cervical Cancer. *Journal of Clinical Microbiology* **44**, 1755-1762 (2006).
36. Stanley, M.A., Pett, M.R. & Coleman, N. HPV: from infection to cancer. *Biochemical Society Transactions* **035**, 1456-1460 (2007).
37. Thorland, E.C., Myers, S.L., Gostout, B.S. & Smith, D.I. Common fragile sites are preferential targets for HPV16 integrations in cervical tumors. *Oncogene* **22**, 1225-1237 (2003).
38. Yu, T., Ferber, M.J., Cheung, T.H., Chung, T.K., Wong, Y.F. & Smith, D.I. The role of viral integration in the development of cervical cancer. *Cancer Genetics and Cytogenetics* **158**, 27-34 (2005).
39. Bedell, M.A., Jones, K.H. & Laimins, L.A. The E6-E7 region of human papillomavirus type 18 is sufficient for transformation of NIH 3T3 and Rat-1 cells. *Journal of Virology* **61**, 3635-3640 (1987).
40. Münger, K., Phelps, W.C., Bubb, V., Howley, P.M. & Schlegel, R. The E6 and E7 genes of the human papillomavirus type 16 together are necessary and sufficient for transformation of primary human keratinocytes. *Journal of Virology* **63**, 4417-4421 (1989).
41. Pirisi, L., Yasukmoto, S., Feller, M., Doniger, M., Doniger, J. & DiPaolo, J.A. Transformation of human fibroblasts and keratinocytes with human papillomavirus type 16 DNA. *Journal of Virology* **61**, 1061-1066 (1987).
42. Sedman, S., Barbosa, M., Vass, W., Hubbert, N., Haas, J., Lowry, D. & Schiller, J. The full-length E6 protein of human papillomavirus type 16 has transforming and trans-activating activities and cooperates with E7 to immortalize keratinocytes in culture. *Journal of Virology* **65**, 4860-4866 (1991).
43. Scheffner, M., Werness, B.A., Huibregtse, J.M., Levine, A.J. & Howley, P.M. The E6 oncoprotein encoded by human papillomavirus types 16 and 18 promotes the degradation of p53. *Cell* **63**, 1129-1136 (1990).

44. Werness, B.A., Levine, A.J. & Howley, P.M. Association of human papillomavirus types 16 and 18 E6 proteins with p53. *Science* **248**, 76-79 (1990).
45. Scheffner, M., Huibregtse, J.M., Vierstra, R.D. & Howley, P.M. The HPV-16 E6 and E6-AP Complex Functions as a Ubiquitin-Protein Ligase in the Ubiquitination of p53. *Cell* **75**, 495 - 505 (1993).
46. Vande Pol, S.B. & Klingelutz, A.J. Papillomavirus E6 oncoproteins. *Virology* **445**, 115-137 (2013).
47. Glaunsinger, B.A., Lee, S.S., Thomas, M., Banks, L. & Javier, R. Interactions of the PDZ-protein MAGI-1 with adenovirus E4-ORF1 and high-risk papillomavirus E6 oncoproteins. *Oncogene* **19**, 5270-5280 (2000).
48. Lee, S.S., Glaunsinger, B., Mantovani, F., Banks, L. & Javier, R.T. Multi-PDZ domain protein MUPP1 is a cellular target for both adenovirus E4-ORF1 and high-risk papillomavirus type 18 E6 oncoproteins. *Journal of Virology* **74**, 9680 - 9693 (2000).
49. Watson, R.A., Thomas, M., Banks, L. & Roberts, S. Activity of the human papillomavirus E6 PDZ-binding motif correlates with an enhanced morphological transformation of immortalized human keratinocytes. *Journal of Cell Science* **116**, 4925-4934 (2003).
50. Tomaic, V., Gardiol, D., Massimi, P., Ozbun, M., Myers, M. & Banks, L. Human and primate tumour viruses use PDZ binding as an evolutionarily conserved mechanism of targeting cell polarity regulators. *Oncogene* **28**, 1-8 (2009).
51. Doorbar, J., Egawa, N., Griffin, H., Kranjec, C. & Murakami, I. Human papillomavirus molecular biology and disease association. *Reviews in Medical Virology* **25 Suppl 1**, 2-23 (2015).
52. Klingelutz, A.J., Foster, S.A. & McDougall, J.K. Telomerase activation by the E6 gene product of human papillomavirus type 16. *Nature (London)* **380**, 79-82 (1996).
53. Oh, S.T., Kyo, S. & Laimins, L.A. Telomerase activation by human papillomavirus type 16 E6 protein: induction of human telomerase reverse transcriptase expression through Myc and GC-rich Sp1 binding sites. *Journal of Virology* **75**, 5559-5566 (2001).

54. Veldman, T., Horikawa, I., Barrett, J.C. & Schlegel, R. Transcriptional activation of the telomerase hTERT gene by human papillomavirus type 16 E6 oncoprotein. *Journal of Virology* **75**, 4467-4472 (2001).
55. Liu, X., Roberts, J., Dakic, A., Zhang, Y. & Schlegel, R. HPV E7 contributes to the telomerase activity of immortalized and tumorigenic cells and augments E6-induced hTERT promoter function. *Virology* **375**, 611-623 (2008).
56. Veldman, T., Liu, X., Yuan, H. & Schlegel, R. Human papillomavirus E6 and Myc proteins associate in vivo and bind to and cooperatively activate the telomerase reverse transcriptase promoter. *Proceedings of the National Academy of Sciences United States of America* **100**, 8211-8216 (2003).
57. Dyson, N., Howley, P.M., Münger, K. & Harlow, E. The human papillomavirus-16 E7 oncoprotein is able to bind to the retinoblastoma gene product. *Science* **243**, 934-936 (1989).
58. Boyer, S.N., Wazer, D.E. & Band, V. E7 protein of human papilloma virus-16 induces degradation of retinoblastoma protein through the ubiquitin-proteasome pathway. *Cancer Research* **56**, 4620-4624 (1996).
59. Hickman, E.S., Picksley, S.M. & Vousden, K.H. Cells expressing HPV16 E7 continue cell cycle progression following DNA damage induced p53 activation. *Oncogene* **9**, 2177-2181 (1994).
60. Stöppler, H., Hartmann, D., Sherman, L. & Schlegel, R. The human papillomavirus type 16 E6 and E7 oncoproteins dissociate cellular telomerase activity from the maintenance of telomere length. *The Journal of Biological Chemistry* **272**, 13332-13337 (1997).
61. Spardy, N., Duensing, A., Hoskins, E.E., Wells, S.I. & Duensing, S. HPV-16 E7 Reveals a Link between DNA Replication Stress, Fanconi Anemia D2 Protein, and Alternative Lengthening of Telomere-Associated Promyelocytic Leukemia Bodies. *Cancer Research* **68**, 9954-9963 (2008).
62. Roman, A. & Munger, K. The papillomavirus E7 proteins. *Virology* **445**, 138-168 (2013).
63. Tsai, T.C. & Chen, S.L. The biochemical and biological functions of human papillomavirus type 16 E5 protein. *Archives of Virology* **148**, 1445-1453 (2003).
64. Straight, S.W., Hinkle, P.M., Jewers, R.J. & McCance, D.J. The E5 oncoprotein of human papillomavirus type 16 transforms fibroblasts and effects the

- downregulation of the epidermal growth factor receptor in keratinocytes. *Journal of Virology* **67**, 4521-4532 (1993).
65. Crusius, K., Auvinen, E., Steuer, B., Gaissert, H. & Alonso, A. The Human Papillomavirus Type 16 E5-Protein Modulates Ligand-Dependent Activation of the EGF Receptor Family in the Human Epithelial Cell Line HaCaT. *Experimental Cell Research* **241**, 76-83 (1998).
 66. Crusius, K., Rodriguez, I. & Alonso, A. The human papillomavirus type 16 E5 protein modulates ERK1/2 and p38 MAP kinase activation by an EGFR-independent process in stressed human keratinocytes. *Virus Genes* **20**, 65-69 (2000).
 67. Venuti A., F.P., L. Nasir, A. Corteggio, S. Roperto, M. S. Camp, G. Borzacchiello Papillomavirus E5: the smallest oncoprotein with many functions. *Molecular Cancer* **10**, 1-18 (2011).
 68. Tomakidi, P., Cheng, H., Kohl, A., Komposch, G. & Alonso, A. Modulation of the epidermal growth factor receptor by the human papillomavirus type 16 E5 protein in raft cultures of human keratinocytes. *European Journal of Cell Biology* **79**, 407-412 (2000).
 69. Lai, C., Henningson, C. & DiMaio, D. Bovine papillomavirus E5 protein induces oligomerization and trans-phosphorylation of the platelet-derived growth factor B receptor. *Proceedings of the National Academy of Sciences United States of America* **95**, 15241-15246 (1998).
 70. DiMaio, D., Petti, L. & Hwang, E.-S. The E5 transforming proteins of the papillomaviruses. *Seminars in Virology* **5**, 369-379 (1994).
 71. Nilson, L.A., Gottlieb, R.L., Polack, G.W. & DiMaio, D. Mutational analysis of the interaction between the bovine papillomavirus E5 transforming protein and the endogenous beta receptor for platelet-derived growth factor in mouse C127 cells. *Journal of Virology* **69**, 5869-5874 (1995).
 72. Wetherill, L.F., Holmes, K.K., Verow, M., Muller, M., Howell, F., Harris, M., Fishwick, C., Stonehouse, N., Foster, R., Blair, G.E., Griffin, S. & Macdonald, A. High-Risk Human Papillomavirus E5 Oncoprotein Displays Channel-Forming Activity Sensitive to Small-Molecule Inhibitors. *Journal of Virology* **86**, 5341-5351 (2012).
 73. Jung, Y.-S., Qian, Y. & Chen, X. Examination of the expanding pathways for the regulation of p21 expression and activity. *Cell Signaling* **22**, 1003-1012 (2010).

74. Tam, S.W., Shay, J.W. & Pagano, M. Differential Expression and Cell Cycle Regulation of the Cyclin-dependent Kinase 4 Inhibitor p16^{Ink4}. *Cancer Research* **54**, 5816-5820 (1994).
75. Sano, T., Oyama, T., Kashiwabara, K., Fukuda, T. & Nakajima, T. Expression status of p16 protein is associated with human papillomavirus oncogenic potential in cervical and genital lesions. *American Journal of Pathology* **153**, 1741-1748 (1998).
76. Reimers, N., Kasper, H.U., Weissenborn, S.J., Stutzer, H., Preuss, S.F., Hoffmann, T.K., Speel, E.J., Dienes, H.P., Pfister, H.J., Guntinas-Lichius, O. & Klussmann, J.P. Combined analysis of HPV-DNA, p16 and EGFR expression to predict prognosis in oropharyngeal cancer. *International Journal of Cancer* **120**, 1731-1738 (2007).
77. Butz, K., Ristriani, T., Hengstermann, A., Denk, C., Scheffner, M. & Hoppe-Seyler, F. siRNA targeting of the viral E6 oncogene efficiently kills human papillomavirus-positive cancer cells. *Oncogene* **22**, 5938 - 5945 (2003).
78. Sima, N., Wang, S., Wang, W., Kong, D., Xu, Q., Tian, X., Luo, A., Zhou, J., Xu, G., Meng, L., Lu, Y. & Ma, D. Antisense targeting human papillomavirus type 16 E6 and E7 genes contributes to apoptosis and senescence in SiHa cervical carcinoma cells. *Gynecologic Oncology* **106**, 299-304 (2007).
79. Jung, H.S., Rajasekaran, N., Song, S.Y., Kim, Y.D., Hong, S., Choi, H.J., Kim, Y.S., Choi, J.S., Choi, Y.L. & Shin, Y.K. Human Papillomavirus E6/E7-Specific siRNA Potentiates the Effect of Radiotherapy for Cervical Cancer in Vitro and in Vivo. *International Journal of Molecular Science* **16**, 12243-12260 (2015).
80. Nishida, H., Matsumoto, Y., Kawana, K., Christie, R.J., Naito, M., Kim, B.S., Toh, K., Min, H.S., Yi, Y., Matsumoto, Y., Kim, H.J., Miyata, K., Taguchi, A., Tomio, K., Yamashita, A., Inoue, T., Nakamura, H., Fujimoto, A., Sato, M., Yoshida, M., Adachi, K., Arimoto, T., Wada-Hiraike, O., Oda, K., Nagamatsu, T., Nishiyama, N., Kataoka, K., Osuga, Y. & Fujii, T. Systemic delivery of siRNA by actively targeted polyion complex micelles for silencing the E6 and E7 human papillomavirus oncogenes. *Journal of Controlled Release* (2016).
81. Satterwhite, C.L., Torrone, E., Meites, E., Dunne, E.F., Mahajan, R., Banez Ocfemia, M.C., Su, J., Xu, F. & Weinstock, H. Sexually Transmitted Infections Among US Women and Men: Prevalence and Incidence Estimates: 2008. *Sexually Transmitted Diseases* **40**, 187-193 (2013).
82. Arbyn, M., de Sanjose, S., Saraiya, M., Sideri, M., Palefsky, J., Lacey, C., Gillison, M., Bruni, L., Ronco, G., Wentzensen, N., Brotherton, J., Qiao, Y.L.,

- Denny, L., Bornstein, J., Abramowitz, L., Giuliano, A., Tommasino, M. & Monsonego, J. EUROGIN 2011 roadmap on prevention and treatment of HPV-related disease. *International Journal of Cancer* **131**, 1969-1982 (2012).
83. Woodhall, S., Ramsey, T., Cai, C., Crouch, S., Jit, M., Birks, Y., Edmunds, W.J., Newton, R. & Lacey, C.J. Estimation of the impact of genital warts on health-related quality of life. *Sexually Transmitted Infections* **84**, 161-166 (2008).
84. Cubie, H.A. Diseases associated with human papillomavirus infection. *Virology* **445**, 21-34 (2013).
85. Gillison, M.L., Alemany, L., Snijders, P.J.F., Chaturvedi, A., Steinberg, B.M., Schwartz, S. & Castellsague, X. Human Papillomavirus and Diseases of the Upper Airway: Head and Neck Cancer and Respiratory Papillomatosis. *Vaccine* **30**, F34-54 (2012).
86. Stanley, M. Pathology and epidemiology of HPV infection in females. *Gynecologic Oncology* **117**, S5-10 (2010).
87. Chaturvedi, A.K., Anderson, W.F., Lortet-Tieulent, J., Curado, M.P., Ferlay, J., Franceschi, S., Rosenberg, P.S., Bray, F. & Gillison, M.L. Worldwide trends in incidence rates for oral cavity and oropharyngeal cancers. *Journal of Clinical Oncology* **31**, 4550-4559 (2013).
88. Gillison, M.L., Castellsague, X., Chaturvedi, A., Goodman, M.T., Snijders, P.J.F., Tommasino, M., Arbyn, M. & Franceschi, S. Eurogin Roadmap: Comparative epidemiology of HPV infection and associated cancers of the head and neck and cervix. *International Journal of Cancer* **134**, 497-507 (2014).
89. Trottier, H., E. L. Franco The epidemiology of genital human papillomavirus infection. *Vaccine* **24S1**, S1/4-S1/15 (2006).
90. Wirth, L.J. Cetuximab in Human Papillomavirus-Positive Oropharynx Carcinoma. *Journal of Clinical Oncology* (2016).
91. Rosenthal, D.I., Harari, P.M., Giralt, J., Bell, D., Raben, D., Liu, J., Schulten, J., Ang, K.K. & Bonner, J.A. Association of Human Papillomavirus and p16 Status With Outcomes in the IMCL-9815 Phase III Registration Trial for Patients With Locoregionally Advanced Oropharyngeal Squamous Cell Carcinoma of the Head and Neck Treated With Radiotherapy With or Without Cetuximab. *Journal of Clinical Oncology* (2015).

92. Wheeler, C.M., Kjaer, S.K., Sigurdsson, K.n., Iversen, O.Ä., Hernandez, ÄêAvila, M., Perez, G., Brown, D.R., Koutsky, L.A., Tay, E.H., Garc√#a, P., Ault, K.A., Garland, S.M., Leodolter, S., Olsson, S.Ä., Tang, G.W.K., Ferris, D.G., Paavonen, J., Steben, M., Bosch, F.X., Dillner, J., Joura, E.A., Kurman, R.J., Majewski, S., Mu√±oz, N., Myers, E.R., Villa, L.L., Taddeo, F.J., Roberts, C., Tadesse, A., Bryan, J., Lupinacci, L.C., Giacoletti, K.E.D., James, M., Vuocolo, S., Hesley, T.M. & Barr, E. The Impact of Quadrivalent Human Papillomavirus (HPV; Types 6, 11, 16, and 18) L1 Virus-Like Particle Vaccine on Infection and Disease Due to Oncogenic Nonvaccine HPV Types in Sexually Active Women Aged 16-26 Years. *The Journal of Infectious Diseases* **199**, 936-944 (2009).
93. De Vincenzo, R., Conte, C., Ricci, C., Scambia, G. & Capelli, G. Long-term efficacy and safety of human papillomavirus vaccination. *International Journal of Womens Health* **6**, 999-1010 (2014).
94. Crowe, E., Pandeya, N., Brotherton, J.M., Dobson, A.J., Kisely, S., Lambert, S.B. & Whiteman, D.C. Effectiveness of quadrivalent human papillomavirus vaccine for the prevention of cervical abnormalities: case-control study nested within a population based screening programme in Australia. *The BMJ* **348**, g1458 (2014).
95. Gonzalez, P., Hildesheim, A., Herrero, R., Katki, H., Wacholder, S., Porras, C., Safaeian, M., Jimenez, S., Darragh, T.M., Cortes, B., Befano, B., Schiffman, M., Carvajal, L., Palefsky, J., Schiller, J., Ocampo, R., Schussler, J., Lowy, D., Guillen, D., Stoler, M.H., Quint, W., Morales, J., Avila, C., Rodriguez, A.C., Kreimer, A.R. & Costa Rica, H.P.V.V.T.G. Rationale and design of a long term follow-up study of women who did and did not receive HPV 16/18 vaccination in Guanacaste, Costa Rica. *Vaccine* **33**, 2141-2151 (2015).
96. Kreimer, A.R., Struyf, F., Del Rosario-Raymundo, M.R., Hildesheim, A., Skinner, S.R., Wacholder, S., Garland, S.M., Herrero, R., David, M.P., Wheeler, C.M., Costa Rica Vaccine, T. & groups, P.s. Efficacy of fewer than three doses of an HPV-16/18 AS04-adjuvanted vaccine: combined analysis of data from the Costa Rica Vaccine and PATRICIA trials. *Lancet Oncology* **16**, 775-786 (2015).
97. Surviladze, Z., Dziduszko, A. & Ozbun, M.A. Essential roles for soluble virion-associated heparan sulfonated proteoglycans and growth factors in human papillomavirus infections. *PLoS Pathogens* **8**, e1002519 (2012).
98. Surviladze, Z., Sterk, R.T., DeHaro, S.A. & Ozbun, M.A. Cellular entry of human papillomavirus type 16 involves activation of the phosphatidylinositol 3-kinase/Akt/mTOR pathway and inhibition of autophagy. *Journal of Virology* **87**, 2508-2517 (2013).

99. Soonthornthum, T., Arias-Pulido, H., Joste, N., Lomo, L., Muller, C., Rutledge, T., Verschraegen, C. Epidermal growth factor receptor as a biomarker for cervical cancer. *Annals of Oncology* **22**, 2166-2178 (2011).
100. Burgess, A.W., Cho, H.S., Eigenbrot, C., Ferguson, K.M., Garrett, T.P., Leahy, D.J., Lemmon, M.A., Sliwkowski, M.X., Ward, C.W. & Yokoyama, S. An open-and-shut case? Recent insights into the activation of EGF/ErbB receptors. *Molecular Cell* **12**, 541-552 (2003).
101. Roskoski, R., Jr. The ErbB/HER family of protein-tyrosine kinases and cancer. *Pharmacological Research* **79**, 34-74 (2014).
102. Ullrich, A., Coussens, L., Hayflick, J.S., Dull, T.J., Gray, A., Tam, A.W., Lee, J., Yarden, Y., Libermann, T.A., Schlessinger, J. & et al. Human epidermal growth factor receptor cDNA sequence and aberrant expression of the amplified gene in A431 epidermoid carcinoma cells. *Nature* **309**, 418-425 (1984).
103. Wells, A. EGF receptor. *International Journal of Biochemistry and Cell Biology* **31**, 637-643 (1999).
104. Schneider, M.R., Werner, S., Paus, R. & Wolf, E. Beyond wavy hairs: the epidermal growth factor receptor and its ligands in skin biology and pathology. *American Journal of Pathology* **173**, 14-24 (2008).
105. Lemmon, M.A. & Schlessinger, J. Cell Signaling by Receptor Tyrosine Kinases. *Cell* **141**, 1117-1134 (2010).
106. Schlessinger, J. Ligand-induced, receptor-mediated dimerization and activation of EGF receptor. *Cell* **110**, 669-672 (2002).
107. Guo, G., Gong, K., Wohlfeld, B., Hatanpaa, K.J., Zhao, D. & Habib, A.A. Ligand-Independent EGFR Signaling. *Cancer Research* **75**, 3436-3441 (2015).
108. Schneider, M.R. & Wolf, E. The Epidermal Growth Factor Receptor Ligands at a Glance. *Journal of Cellular Physiology* **218**, 460-466 (2008).
109. Longva, K.E., Blystad, F., Stang, E., Larsen, A., Johannessen, L.E. & Madshuh, I.H. Ubiquitination and proteasomal activity is required for transport of the EGF receptor to inner membranes of multivesicular bodies. *Journal of Cell Biology* **156**, 1-12 (2002).
110. Tomas, A., Futter, C.E. & Eden, E.R. EGF receptor trafficking: consequences for signaling and cancer. *Trends in Cell Biology* **24**, 26 (2014).

111. Yarden, Y. & Sliwkowski, M.X. Untangling the ErbB signalling network. *Nature Reviews Molecular Cell Biology* **2**, 127-137 (2001).
112. Yarden, Y. & Pines, G. The ERBB network: at last, cancer therapy meets systems biology. *Nature Reviews Cancer* **12**, 553-563 (2012).
113. Henson, E.S. & Gibson, S.B. Surviving cell death through epidermal growth factor (EGF) signal transduction pathways: implications for cancer therapy. *Cell Signal* **18**, 2089-2097 (2006).
114. Scaltriti, M. & Baselga, J. The Epidermal Growth Factor Pathway: A Model for Targeted Therapy. *Clinical Cancer Research* **12**, 5268-5272 (2006).
115. Lurje, G. & Lenz, H.J. EGFR Signaling and Drug Discovery. *Oncology* **77**, 400-410 (2009).
116. Vecchione, L., Jacobs, B., Normanno, N., Ciardiello, F. & Tejpar, S. EGFR-targeted therapy. *Experimental Cell Research* **317**, 2765-2771 (2011).
117. Baselga, J., Pfister, D., Cooper, M.R., Cohen, R., Burtness, B., Boss, M., D'Andrea, G., Seidman, A., Norton, L., Gunnett, K., Falcey, J., Anderson, V., Waksal, H. & Mendelsohn, J. Phase I studies of anti-epidermal growth factor receptor chimeric antibody C225 alone and in combination with cisplatin. *Journal of Clinical Oncology* **18**, 904-914 (2000).
118. Vincenzi, B., Schiavon, G., Silletta, M., Santini, D. & Tonini, G. The biological properties of cetuximab. *Critical Reviews in Oncology/Hematology* **68**, 93-106 (2008).
119. Kim, E.S., Khuri, F.R. & Herbst, R.S. Epidermal growth factor receptor biology (IMC-C225). *Current Opinions in Oncology* **13**, 506-513 (2001).
120. Yang, X., Zhang, X., Mortenson, E.D., Radkevich-Brown, O., Wang, Y. & Fu, Y.X. Cetuximab-mediated tumor regression depends on innate and adaptive immune responses. *Molecular Therapeutics* **21**, 91-100 (2013).
121. Zyzak, L., MacDonald, L.M., Batova, A., Forand, R., Creek, K.E. & Pirisi, L. Increased Levels and Constitutive Tyrosine Phosphorylation of the Epidermal Growth Factor Receptor Contribute to Autonomous Growth of Human Papillomavirus Type 16 Immortalized Human Keratinocytes. *Cell Growth and Differentiation* **5**, 537-547 (1994).

122. Akerman, G.S., Tolleson, W.H., Brown, K.L., Zyzak, L.L., Mourateva, E., Engin, T.S.W., Basaraba, A., Coker, A.L., Creek, K.E. & Pirisi, L. Human Papillomavirus Type 16 E6 and E7 Cooperate to Increase Epidermal Growth Factor Receptor (EGFR) mRNA Levels, Overcoming Mechanisms by which Excessive EGFR Signaling Shortens the Life Span of Normal Human Keratinocytes. *Cancer Research* **61**, 3837-3843 (2001).
123. Hu, G., Liu, W., Mendelsohn, J., Ellis, L.M., Radinsky, R., Andreeff, M. & Deisseroth, A.B. Expression of epidermal growth factor receptor and human papillomavirus E6/E7 proteins in cervical carcinoma cells. *Journal of the National Cancer Institute* **89**, 1243-1246 (1997).
124. Spangle, J.M. & Munger, K. The HPV16 E6 Oncoprotein Causes Prolonged Receptor Protein Tyrosine Kinase Signaling and Enhances Internalization of Phosphorylated Receptor Species. *PLoS Pathogens* **9**, e1003237 (2013).
125. Hess, J., Angel, P. & Schorpp-Kistner, M. AP-1 subunits: quarrel and harmony among siblings. *Journal of Cell Science* **117**, 5965-5973 (2004).
126. de Wilde, J., De-Castro Arce, J., Snijders, P.J.F, Meijer, C.J.L.M., Rosl, F., Steenbergen, R.D.M. Alterations in AP-1 and AP-1 regulatory genes during HPV-induced carcinogenesis. *Cellular Oncology* **30**, 77-87 (2008).
127. Chong, T., Apt, D., Gloss, B., Isa, M. & Bernard, H.-U. The enhancer of human papillomavirus type 16: binding sites for the ubiquitous transcription factors oct-1, NFA, TEF-2, NF1, and AP-1 participate in epithelial cell-specific transcription. *Journal of Virology* **65**, 5933-5943 (1991).
128. Cripe, T.P., Alderborn, A., Anderson, R.D., Parkkinen, S., Bergman, P., Haugen, T.H., Pettersson, U. & Turek, L.P. Transcriptional activation of the human papillomavirus-16 P97 promoter by an 88-nucleotide enhancer containing distinct cell-dependent and AP-1-responsive modules. *Nature: New Biology* **2**, 450-463. (1990).
129. Kyo, S., Tam, A. & Laimins, L. Transcriptional activity of human papillomavirus type 31b enhancer is regulated through synergistic interaction of AP1 with two novel cellular factors. *Virology* **211**, 184-197 (1995).
130. Peto, M., Tolle-Ersu, I., Kreysch, H.G. & Klock, G. Epidermal growth factor induction of human papillomavirus type 16 E6/E7 mRNA in tumour cells involves two AP-1 binding sites in the viral enhancer. *Journal of General Virology* **76**, 1945-1958 (1995).

131. Prusty, B.K. & Das, B.C. Constitutive activation of transcription factor AP-1 in cervical cancer and suppression of human papillomavirus (HPV) transcription and AP-1 activity in HeLa cells by curcumin. *International Journal of Cancer* **113**, 951-960 (2005).
132. Bouvard, V., Matlashewski, G., Gu, Z.-M., Storey, A. & Banks, L. The human papillomavirus type 16 E5 gene cooperates with E7 gene to stimulate proliferation of primary cells and increases viral gene expression. *Virology* **203**, 73-80 (1994).
133. Hong, A., Dobbins, T., Lee, C.S., Jones, D., Jackson, E., Clark, J., Armstrong, B., Harnett, G., Milross, C., O'Brien, C. & Rose, B. Relationships between epidermal growth factor receptor expression and human papillomavirus status as markers of prognosis in oropharyngeal cancer. *European Journal of Cancer* **46**, 2088-2096 (2010).
134. Yasumoto, S., Taniguchi, A. & Sohma, K. Epidermal growth factor (EGF) elicits down-regulation of human papillomavirus type 16 (HPV-16) E6/E7 mRNA at the transcriptional level in an EGF-stimulated human keratinocyte cell line: functional role of EGF-responsive silencer in the HPV-16 long control region. *Journal of Virology* **65**, 2000-2009 (1991).
135. Genter, S.M., Sterling, S., Duensing, S., Münger, K., Sattler, C. & Lambert, P.F. Quantitative role of the human papillomavirus type 16 E5 gene during the productive stage of the viral life cycle. *Journal of Virology* **77**, 2832-2842 (2003).
136. Allen-Hoffmann, B.L., Schlosser, S.J., Ivarie, C.A.R., Sattler, C.A., Meisner, L.F. & O'Connor, S.L. Normal growth and differentiation in a spontaneously immortalized near-diploid human keratinocyte cell line, NIKS. *Journal of Investigative Dermatology* **114**, 444-455 (2000).
137. Wei, L., Gravitt, P.E., Song, H., Maldonado, A. & Ozbun, M.A. Nitric oxide induces early viral transcription coincident with increased DNA damage and mutation rates in human papillomavirus infected cells. *Cancer Research* **69**, 4878-4884 (2009).
138. Aranda, P.S., LaJoie, D.M. & Jorcyk, C.L. Bleach gel: a simple agarose gel for analyzing RNA quality. *Electrophoresis* **33**, 366-369 (2012).
139. zur Hausen, H. Papillomaviruses and cancer: from basic studies to clinical application. *Nature Reviews Cancer* **2**, 342-350 (2002).
140. Middleton, K., Peh, W., Southern, S., Griffin, H., Sotlar, K., Nakahara, T., El-Sherif, A., Morris, L., Seth, R., Hibma, M., Jenkins, D., Lambert, P., Coleman, N. & Doorbar, J. Organization of human papillomavirus productive cycle during

neoplastic progression provides a basis for the selection of diagnostic markers. *Journal of Virology* **77**, 10186-10201 (2003).

141. Demers, G.W., Foster, S.A., Halbert, C.L. & Galloway, D.A. Growth arrest by induction of p53 in DNA damaged keratinocytes is bypassed by human papillomavirus 16 E7. *Proceedings of the National Academy of Sciences* **91**, 4382-4386 (1994).
142. Jones, D.L., Thompson, D.A. & Munger, K. Destabilization of the RB tumor suppressor protein and stabilization of p53 contribute to HPV type 16 E7-induced apoptosis. *Virology* **239**, 97-107 (1997).
143. DiMaio, D. & Petti, L.M. The E5 proteins. *Virology* **445**, 99-114 (2013).
144. Thierry, F. Transcriptional regulation of the papillomavirus oncogenes by cellular and viral transcription factors in cervical carcinoma. *Virology* **384**, 375-379 (2009).
145. Surviladze, Z., Dziduszko, A. & Ozbun, M.A. Essential roles for soluble virion-associated heparan sulfonated proteoglycans and growth factors in human papillomavirus infections. *PLoS Pathog* **8**, e1002519 (2012).
146. Dziduszko, A. & Ozbun, M.A. Annexin A2 and S100A10 regulate human papillomavirus type 16 entry and intracellular trafficking in human keratinocytes. *Journal of Virology* **87**, 7502-7515 (2013).
147. Shaulian, E. & Karin, M. AP-1 as a regulator of cell life and death. *Nature Cell Biology* **4**, E131-E136 (2002).
148. Thierry, F., Spyrou, G., Yaniv, M. & Howley, P. Two AP1 sites binding JunB are essential for human papillomavirus type 18 transcription in keratinocytes. *Journal of Virology* **66**, 3740-3748 (1992).
149. Zenz, R. & Wagner, E.F. Jun signalling in the epidermis: From developmental defects to psoriasis and skin tumors. *IJBCB* **38**, 1043-1049 (2005).
150. Pim, D., Collins, M. & Banks, L. Human papillomavirus type 16 E5 gene stimulates the transforming activity of the epidermal growth factor receptor. *Oncogene* **7**, 27-32 (1992).
151. Nyati, M.K., Morgan, M.A., Feng, F.Y. & Lawrence, T.S. Integration of EGFR inhibitors with radiochemotherapy. *Nature Reviews Cancer* **6**, 876-885 (2006).

152. Oda, K., Matsuoka, Y., Funahashi, A. & Kitano, H. A comprehensive pathway map of epidermal growth factor receptor signaling. *Molecular Systems Biology*, 1-17 (2005).
153. Goldstein, N., Prewett, M., Zuklys, K., Rockwell, P. & Mendelsohn, J. Biological Efficacy of a Chimeric Antibody to the Epidermal Growth Factor Receptor in a Human Tumor Xenograft Model. *Clinical Cancer Research* **1**, 1311-1318 (1995).
154. Suh, Y., Amelio, I., Guerrero Urbano, T. & Tavassoli, M. Clinical update on cancer: molecular oncology of head and neck cancer. *Cell Death and Disease* **5**, e1018 (2014).
155. Siddik, Z.H. Cisplatin: mode of cytotoxic action and molecular basis of resistance. *Oncogene* **22**, 7265-7279 (2003).
156. Akagi, K., Li, J., Broutian, T.R., Padilla-Nash, H., Xiao, W., Jiang, B., Rocco, J.W., Teknos, T.N., Kumar, B., Wangsa, D., He, D., Ried, T., Symer, D.E. & Gillison, M.L. Genome-wide analysis of HPV integration in human cancers reveals recurrent, focal genomic instability. *Genome Research* **24**, 185-199 (2014).
157. Pett, M. & Coleman, N. Integration of high-risk human papillomavirus: a key event in cervical carcinogenesis? *The Journal of Pathology* **212**, 356-367 (2007).
158. Raybould, R., Fiander, A. & Hibbitts, S. Human Papillomavirus Integration and its Role in Cervical Malignant Progression. *The Open Clinical Cancer Journal* **5**, 1-7 (2011).
159. Wentzensen, N., Vinokurova, S. & von Knebel Doeberitz, M. Systematic Review of Genomic Integration Sites of Human Papillomavirus Genomes in Epithelial Dysplasia and Invasive Cancer of the Female Lower Genital Tract. *Cancer Research* **64**, 3878-3884 (2004).
160. Ferber, M.J., Thorland, E.C., Brink, A.A., Rapp, A.K., Phillips, L.A., McGovern, R., Gostout, B.S., Cheung, T.H., Chung, T.K., Fu, W.Y. & Smith, D.I. Preferential integration of human papillomavirus type 18 near the c-myc locus in cervical carcinoma. *Oncogene* **22**, 7233-7242 (2003).
161. Woodworth, C.D., Diefendorf, L.P., Jette, D.F., Mohammed, A., Moses, M.A., Searleman, S.A., Stevens, D.A., Wilton, K.M. & Mondal, S. Inhibition of the epidermal growth factor receptor by erlotinib prevents immortalization of human cervical cells by Human Papillomavirus type 16. *Virology* **421**, 19-27 (2011).

162. Benhar, M., Engelberg, D. & Levitzki, A. Cisplatin-induced activation of the EGF receptor. *Oncogene* **21**, 8723-8731 (2002).
163. Yoshida, T., Okamoto, I., Iwasa, T., Fukuoka, M. & Nakagawa, K. The anti-EGFR monoclonal antibody blocks cisplatin-induced activation of EGFR signaling mediated by HB-EGF. *FEBS Letters* **582**, 4125-4130 (2008).
164. Kwon, J., Yoon, H.J., Kim, J.H., Lee, T.S., Song, I.H., Lee, H.W., Kang, M.C. & Park, J.H. Cetuximab inhibits cisplatin-induced activation of EGFR signaling in esophageal squamous cell carcinoma. *Oncology Reports* **32**, 1188-1192 (2014).
165. Meira, D.D., de Almeida, V.H., Mororo, J.S., Nobrega, I., Bardella, L., Silva, R.L.A., Albano, R.M. & Ferreira, C.G. Combination of cetuximab with chemoradiation, trastuzumab or MAPK inhibitors: mechanisms of sensitisation of cervical cancer cells. *British Journal of Cancer* **101**, 782-791 (2009).
166. Kimple, R.J., Harari, P.M., Torres, A.D., Yang, R.Z., Soriano, B.J., Yu, M., Armstrong, E.A., Blitzer, G.C., Smith, M.A., Lorenz, L.D., Lee, D., Yang, D.T., McCulloch, T.M., Hartig, G.K. & Lambert, P.F. Development and characterization of HPV-positive and HPV-negative head and neck squamous cell carcinoma tumorgrafts. *Clinical Cancer Research* **19**, 855-864 (2013).
167. Wang, S.S., Zuna, R.E., Wentzensen, N., Dunn, S.T., Sherman, M.E., Gold, M.A., Schiffman, M., Wacholder, S., Allen, R.A., Block, I., Downing, K., Jeronimo, J., Carreon, J.D., Safaeian, M., Brown, D. & Walker, J.L. Human Papillomavirus Cofactors by Disease Progression and Human Papillomavirus Types in the Study to Understand Cervical Cancer Early Endpoints and Determinants. *Cancer Epidemiology Biomarkers Prevention* **18**, 113-120 (2009).
168. Yetimalar, H., Kasap, B., Cukurova, K., Yildiz, A., Keklik, A. & Soylu, F. Cofactors in human papillomavirus infection and cervical carcinogenesis. *Archives of Gynecology and Obstetrics* **285**, 805-810 (2012).
169. Limsukon, A., Susanto, I., Hoo, G.W., Dubinett, S.M. & Batra, R.K. Regression of recurrent respiratory papillomatosis with celecoxib and erlotinib combination therapy. *Chest* **136**, 924-926 (2009).
170. Hao, Z., Dillard, T., Biddinger, P. & Patel, V. Suppression of respiratory papillomatosis with malignant transformation by erlotinib in a kidney transplant recipient. *BMJ Case Reports* **2013** (2013).
171. Carifi, M., Napolitano, D., Morandi, M. & Dall'Olio, D. Recurrent respiratory papillomatosis: current and future perspectives. *Journal of Therapeutics and Clinical Risk Management* **11**, 731-738 (2015).

172. Egloff, A.M., Lee, J.W., Langer, C.J., Quon, H., Vaezi, A., Grandis, J.R., Seethala, R.R., Wang, L., Shin, D.M., Argiris, A., Yang, D., Mehra, R., Ridge, J.A., Patel, U.A., Burtneess, B.A. & Forastiere, A.A. Phase II study of cetuximab in combination with cisplatin and radiation in unresectable, locally advanced head and neck squamous cell carcinoma: Eastern cooperative oncology group trial E3303. *Clinical Cancer Research* **20**, 5041-5051 (2014).
173. Kies, M.S., Holsinger, F.C., Lee, J.J., William, W.N., Jr., Glisson, B.S., Lin, H.Y., Lewin, J.S., Ginsberg, L.E., Gillaspay, K.A., Massarelli, E., Byers, L., Lippman, S.M., Hong, W.K., El-Naggar, A.K., Garden, A.S. & Papadimitrakopoulou, V. Induction chemotherapy and cetuximab for locally advanced squamous cell carcinoma of the head and neck: results from a phase II prospective trial. *Journal of Clinical Oncology* **28**, 8-14 (2010).
174. Farley, J., Sill, M.W., Birrer, M., Walker, J., Schilder, R.J., Thigpen, J.T., Coleman, R.L., Miller, B.E., Rose, P.G. & Lankes, H.A. Phase II study of cisplatin plus cetuximab in advanced, recurrent, and previously treated cancers of the cervix and evaluation of epidermal growth factor receptor immunohistochemical expression: a Gynecologic Oncology Group study. *Gynecologic Oncology* **121**, 303-308 (2011).
175. Santin, A.D., Sill, M.W., McMeekin, D.S., Leitao, M.M., Jr., Brown, J., Sutton, G.P., Van Le, L., Griffin, P. & Boardman, C.H. Phase II trial of cetuximab in the treatment of persistent or recurrent squamous or non-squamous cell carcinoma of the cervix: a Gynecologic Oncology Group study. *Gynecologic Oncology* **122**, 495-500 (2011).
176. Isaacson Wechsler, E., Wang, Q., Roberts, I., Pagliarulo, E., Jackson, D., Untersperger, C., Coleman, N., Griffin, H. & Doorbar, J. Reconstruction of human papillomavirus type 16-mediated early-stage neoplasia implicates E6/E7 deregulation and the loss of contact inhibition in neoplastic progression. *Journal of Virology* **86**, 6358-6364 (2012).
177. Ferlay, J., Shin, H.-R., Bray, F., Forman, D., Mathers, C. & Parkin, D.M. Estimates of worldwide burden of cancer in 2008: GLOBOCAN 2008. *International Journal of Cancer* **127**, 2893-2917 (2010).
178. Leemans, C.R., Braakhuis, B.J.M. & Brakenhoff, R.H. The molecular biology of head and neck cancer. *Nature Reviews Cancer* **11**, 9-22 (2011).
179. Chaturvedi, A.K., Engels, E.A., Anderson, W.F. & Gillison, M.L. Incidence Trends for Human Papillomavirus–Related and –Unrelated Oral Squamous Cell Carcinomas in the United States. *Journal of Clinical Oncology* **26**, 612-619 (2008).

180. Klussmann, J.P., Mooren, J.J., Lehnen, M., Claessen, S.M., Stenner, M., Huebbers, C.U., Weissenborn, S.J., Wedemeyer, I., Preuss, S.F., Staetmans, J.M., Manni, J.J., Hopman, A.H. & Speel, E.J. Genetic signatures of HPV-related and unrelated oropharyngeal carcinoma and their prognostic implications. *Clinical Cancer Research* **15**, 1779-1786 (2009).
181. Seiwert, T.Y., Zuo, Z., Keck, M.K., Khattri, A., Pedamallu, C.S., Stricker, T., Brown, C., Pugh, T.J., Stojanov, P., Ho, J., Lawrence, M.S., Getz, G., Bragelmann, J., DeBoer, R., Weichselbaum, R.R., Langerman, A., Porugal, L., Blair, E., Stenson, K., Lingen, M.W., Cohen, E.E., Vokes, E.E., White, K.P. & Hammerman, P.S. Integrative and comparative genomic analysis of HPV-positive and HPV-negative head and neck squamous cell carcinomas. *Clinical Cancer Research* **21**, 632-641 (2015).
182. Stransky, N., Egloff, A., Tward, A., Kostic, A., Cibulskis, K. & Sivachenko, A. The mutational landscape of head and neck squamous cell carcinoma. *Science* **333**, 1157-1160 (2011).
183. Rusan, M., Li, Y. & Hammerman, P.S. Genomic landscape of human papillomavirus-associated cancers. *Clinical Cancer Research* **21**, 2009-2019 (2015).
184. Agrawal, N., Frederick, M., Pickering, C., Bettegowda, C., Chang, K., Li, R. & Fakhry, C. Exosome sequencing of head and neck squamous cell carcinoma reveals inactivating mutations in NOTCH1. *Science* **333**, 1154-1157 (2011).
185. Ankola, A.A., Smith, R.V., Burk, R.D., Prystowsky, M.B., Sarta, C. & Schlecht, N.F. Comorbidity, human papillomavirus infection and head and neck cancer survival in an ethnically diverse population. *Oral Oncology* **49**, 911-917 (2013).
186. Lohaus, F., Linge, A., Tinhofer, I., Budach, V., Gkika, E., Stuschke, M., Balermas, P., Rodel, C., Avlar, M., Grosu, A.L., Abdollahi, A., Debus, J., Bayer, C., Belka, C., Pigorsch, S., Combs, S.E., Monnich, D., Zips, D., von Neubeck, C., Baretton, G.B., Lock, S., Thames, H.D., Krause, M., Baumann, M. & DKTK, R.O.G. HPV16 DNA status is a strong prognosticator of loco-regional control after postoperative radiochemotherapy of locally advanced oropharyngeal carcinoma: results from a multicentre explorative study of the German Cancer Consortium Radiation Oncology Group (DKTK-ROG). *Radiotherapy and Oncology* **113**, 317-323 (2014).
187. Ang, K.K., Harris, J., Wheeler, R., Weber, R., Rosenthal, D.I., Nguyen-Tân, P.F., Westra, W.H., Chung, C.H., Jordan, R.C., Lu, C., Kim, H., Axelrod, R., Silverman, C.C., Redmond, K.P. & Gillison, M.L. Human Papillomavirus and

Survival of Patients with Oropharyngeal Cancer. *New England Journal of Medicine* **363**, 24-35 (2010).

188. Adelstein, D.J., Li, Y., Adams, G.L., Wagner, H., Kish, J.A., Ensley, J.F., Schuller, D.E. & Forastiere, A.A. An Intergroup Phase III Comparison of Standard Radiation Therapy and Two Schedules of Concurrent Chemoradiotherapy in Patients With Unresectable Squamous Cell Head and Neck Cancer. *Journal of Clinical Oncology* **21**, 92-98 (2003).
189. Bonner, J.A., Harari, P.M., Giralt, J., Azarnia, N., Shin, D.M., Cohen, R.B., Jones, C.U., Sur, R., Raben, D., Jassem, J., Ove, R., Kies, M.S., Baselga, J., Youssoufian, H., Amellal, N., Rowinsky, E.K. & Ang, K.K. Radiotherapy plus cetuximab for squamous-cell carcinoma of the head and neck. *New England Journal of Medicine* **354**, 567-578 (2006).
190. Kyo, S., Klumpp, D., Inoue, M., Kanaya, T. & Laimins, L. Expression of AP1 during cellular differentiation determines human papillomavirus E6/E7 expression in stratified epithelial cells. *Journal of General Virology* **78**, 401-411 (1997).
191. Talora, C., Sgroi, D.C., Crum, C.P. & Dotto, G.P. Specific down-modulation of Notch1 signaling in cervical cancer cells is required for sustained HPV-E6/E7 expression and late steps of malignant transformation. *Genes and Development* **16**, 2252-2263 (2002).
192. Rösl, F., Das, B.C., Lengert, M., Geletneky, K. & zur Hausen, H. Antioxidant-induced changes of the AP-1 transcription complex are paralleled by a selective suppression of human papillomavirus transcription. *Journal of Virology* **71**, 362-370 (1997).
193. Stein, A.P., Swick, A.D., Smith, M.A., Blitzer, G.C., Yang, R.Z., Saha, S., Harari, P.M., Lambert, P.F., Liu, C.Z. & Kimple, R.J. Xenograft assessment of predictive biomarkers for standard head and neck cancer therapies. *Cancer Medicine* **4**, 699-712 (2015).
194. De Cesare, M., Lauricella, C., Veronese, S.M., Cominetti, D., Pisano, C., Zunino, F., Zaffaroni, N. & Zuco, V. Synergistic antitumor activity of cetuximab and namitecan in human squamous cell carcinoma models relies on cooperative inhibition of EGFR expression and depends on high EGFR gene copy number. *Clinical Cancer Research* **20**, 995-1006 (2014).
195. Friedl, F., Kimura, I., Osato, T. & Ito, Y. Studies on a new human cell line (SiHa) derived from carcinoma of uterus. I. Its establishment and morphology. *Proceedings of the Society for Experimental Biology and Medicine* **135**, 543-545 (1970).

196. Pattillo, R.A., Husa, R.O., Story, M.T., Ruckert, A.C., Shalaby, M.R. & Mattingly, R.F. Tumor antigen and human chorionic gonadotropin in CaSki cells: a new epidermoid cervical cancer cell line. *Science* **196**, 1456-1458 (1977).
197. Sano, D., Xie, T.X., Ow, T.J., Zhao, M., Pickering, C.R., Zhou, G., Sandulache, V.C., Wheeler, D.A., Gibbs, R.A., Caulin, C. & Myers, J.N. Disruptive TP53 mutation is associated with aggressive disease characteristics in an orthotopic murine model of oral tongue cancer. *Clinical Cancer Research* **17**, 6658-6670 (2011).
198. Tang, A.L., Hauff, S.J., Owen, J.H., Graham, M.P., Czerwinski, M.J., Park, J.J., Walline, H., Papagerakis, S., Stoerker, J., McHugh, J.B., Chepeha, D.B., Bradford, C.R., Carey, T.E. & Prince, M.E. UM-SCC-104: a new human papillomavirus-16-positive cancer stem cell-containing head and neck squamous cell carcinoma cell line. *Head and Neck* **34**, 1480-1491 (2012).
199. Olthof, N.C., Huebbers, C.U., Kolligs, J., Henfling, M., Ramaekers, F.C., Cornet, I., van Lent-Albrechts, J.A., Stegmann, A.P., Silling, S., Wieland, U., Carey, T.E., Walline, H.M., Gollin, S.M., Hoffmann, T.K., de Winter, J., Kremer, B., Klussmann, J.P. & Speel, E.J. Viral load, gene expression and mapping of viral integration sites in HPV16-associated HNSCC cell lines. *International Journal of Cancer* **136**, E207-218 (2015).
200. Nagel, R., Martens-de Kemp, S.R., Buijze, M., Jacobs, G., Braakhuis, B.J. & Brakenhoff, R.H. Treatment response of HPV-positive and HPV-negative head and neck squamous cell carcinoma cell lines. *Oral Oncology* **49**, 560-566 (2013).
201. Vermeer, P.D., Colbert, P.L., Wieking, B.G., Vermeer, D.W. & Lee, J.H. Targeting ERBB receptors shifts their partners and triggers persistent ERK signaling through a novel ERBB/EFNB1 complex. *Cancer Research* **73**, 5787-5797 (2013).
202. Sun, Q., Tang, S.C., Pater, M.M. & Pater, A. Different HPV16 E6/E7 oncogene expression patterns in epithelia reconstructed from HPV16-immortalized human endocervical cells and genital keratinocytes. *Oncogene* **15**, 2399-2408 (1997).
203. Flores, E.R., Allen, H.B.L., Lee, D. & Lambert, P.F. The human papillomavirus type 16 E7 oncogene is required for the productive stage of the viral life cycle. *Journal of Virology* **74**, 6622-6631 (2000).
204. Cancer Genome Atlas, N. Comprehensive genomic characterization of head and neck squamous cell carcinomas. *Nature* **517**, 576-582 (2015).

205. Daniel, B., Rangarajan, A., Mukherjee, G., Vallikad, E. & Krishna, S. The link between integration and expression of human papillomavirus type 16 genomes and cellular changes in the evolution of cervical intraepithelial neoplastic lesions. *Journal of General Virology* **78 (Pt 5)**, 1095-1101 (1997).
206. Zagouras, P., Stifani, S., Blaumueller, C.M., Carcangiu, M.L. & Artavanis-Tsakonas, S. Alterations in Notch signaling in neoplastic lesions of the human cervix. *Proceedings of the National Academy of Sciences United States of America* **92**, 6414-6418 (1995).
207. Keck, M.K., Zuo, Z., Khattri, A., Stricker, T.P., Brown, C.D., Imanguli, M., Rieke, D., Endhardt, K., Fang, P., Bragelmann, J., DeBoer, R., El-Dinali, M., Aktolga, S., Lei, Z., Tan, P., Rozen, S.G., Salgia, R., Weichselbaum, R.R., Lingen, M.W., Story, M.D., Ang, K.K., Cohen, E.E., White, K.P., Vokes, E.E. & Seiwert, T.Y. Integrative analysis of head and neck cancer identifies two biologically distinct HPV and three non-HPV subtypes. *Clinical Cancer Research* **21**, 870-881 (2015).
208. Maliekal, T.T., Bajaj, J., Giri, V., Subramanyam, D. & Krishna, S. The role of Notch signaling in human cervical cancer: implications for solid tumors. *Oncogene* **27**, 5110-5114 (2008).
209. Deberne, M., Levy, A., Mondini, M., Dessen, P., Vivet, S., Supiramaniam, A., Vozenin, M.C. & Deutsch, E. The combination of the antiviral agent cidofovir and anti-EGFR antibody cetuximab exerts an antiproliferative effect on HPV-positive cervical cancer cell lines' in-vitro and in-vivo xenografts. *Anticancer Drugs* **24**, 599-608 (2013).
210. Pogorzelski, M., Ting, S., Gauler, T.C., Breitenbuecher, F., Vossebein, I., Hoffarth, S., Markowitz, J., Lang, S., Bergmann, C., Brandau, S., Jawad, J.A., Schmid, K.W., Schuler, M. & Kasper, S. Impact of human papilloma virus infection on the response of head and neck cancers to anti-epidermal growth factor receptor antibody therapy. *Cell Death and Disease* **5**, e1091 (2014).
211. Pollock, N.I., Wang, L., Wallweber, G., Gooding, W.E., Huang, W., Chenna, A., Winslow, J., Sen, M., DeGrave, K.A., Li, H., Zeng, Y. & Grandis, J.R. Increased Expression of HER2, HER3, and HER2:HER3 Heterodimers in HPV-Positive HNSCC Using a Novel Proximity-Based Assay: Implications for Targeted Therapies. *Clinical Cancer Research* **21**, 4597-4606 (2015).
212. Muller, P.A. & Vousden, K.H. p53 mutations in cancer. *Nature Cell Biology* **15**, 2-8 (2013).

213. Pietras, K. & Ostman, A. Hallmarks of cancer: interactions with the tumor stroma. *Experimental Cell Research* **316**, 1324-1331 (2010).
214. Castellsagué, X., Bosch, F.X. & Muñoz, N.M. Environmental co-factors in HPV carcinogenesis. *Virus Research* **89**, 191-199 (2002).
215. Castellsagué, X. & Muñoz, N. Chapter 3: Cofactors in Human Papillomavirus Carcinogenesis--Role of Parity, Oral Contraceptives, and Tobacco Smoking. *JNCI Monographs* **2003**, 20-28 (2003).
216. Herrero, R., Castellsague, X., Pawlita, M., Lissowska, J., Kee, F., Balam, P., Rajkumar, T., Sridhar, H., Rose, B., Pintos, J., Fernandez, L., Idris, A., Sanchez, M.J., Nieto, A., Talamini, R., Tavani, A., Bosch, F.X., Reidel, U., Snijders, P.J.F., Meijer, C.J.L.M., Viscidi, R., Munoz, N. & Franceschi, S. Human Papillomavirus and Oral Cancer: The International Agency for Research on Cancer Multicenter Study. *Journal of the National Cancer Institute* **95**, 1772-1783 (2003).
217. Plummer, M., Schiffman, M., Castle, P.E., Maucort-Boulch, D. & Wheeler, C.M. A 2-Year Prospective Study of Human Papillomavirus Persistence among Women with a Cytological Diagnosis of Atypical Squamous Cells of Undetermined Significance or Low-Grade Squamous Intraepithelial Lesion. *The Journal of Infectious Diseases* **195**, 1582-1589 (2007).
218. Trottier, H. & Burchell, A.N. Epidemiology of mucosal human papillomavirus infection and associated diseases. *Public Health Genomics* **12**, 291-307 (2009).
219. Schiffman, M., Castle, P.E., Jeronimo, J., Rodriguez, A.C. & Wacholder, S. Human papillomavirus and cervical cancer. *The Lancet* **370**, 890-907 (2007).
220. Timmons, B., Akins, M. & Mahendroo, M. Cervical remodeling during pregnancy and parturition. *Trends in Endocrinology and Metabolism* **21**, 353-361 (2010).
221. Hanahan, D. & Weinberg, R.A. Hallmarks of cancer: the next generation. *Cell* **144**, 646-674 (2011).
222. Sharkey, D.J., Macpherson, A.M., Tremellen, K.P. & Robertson, S.A. Seminal plasma differentially regulates inflammatory cytokine gene expression in human cervical and vaginal epithelial cells. *Molecular Human Reproduction* **13**, 491-501 (2007).
223. Gaiotti, D., Chung, J., Iglesias, M., Nees, M., Baker, P.D., Evans, C.H. & Woodworth, C.D. Tumor necrosis factor-alpha promotes human papillomavirus

- (HPV) E6/E7 RNA expression and cyclin-dependent kinase activity in HPV-immortalized keratinocytes by a ras-dependent pathway. *Molecular Carcinogenesis* **27**, 97-109 (2000).
224. Boccardo, E., Lepique, A.P. & Villa, L.L. The role of inflammation in HPV carcinogenesis. *Carcinogenesis* **31**, 1905-1912 (2010).
225. Wei, L., Griego, A.M., Chu, M. & Ozbun, M.A. Tobacco exposure results in increased E6 and E7 oncogene expression, DNA damage and mutation rates in cells maintaining episomal human papillomavirus 16 genomes. *Carcinogenesis* **35**, 2373-2381 (2014).
226. Alam, S., Conway, M.J., Chen, H.-S. & Meyers, C. The Cigarette Smoke Carcinogen Benzo[a]pyrene Enhances Human Papillomavirus Synthesis. *The Journal of Virology* **82**, 1053-1058 (2008).
227. Zhong, R., Bao, R., Faber, P.W., Bindokas, V.P., Bechill, J., Lingen, M.W. & Spiotto, M.T. Notch1 Activation or Loss Promotes HPV-Induced Oral Tumorigenesis. *Cancer Research* **75**, 3958-3969 (2015).
228. Bol, V. & Gregoire, V. Biological basis for increased sensitivity to radiation therapy in HPV-positive head and neck cancers. *BioMed Research International* **2014**, 696028 (2014).
229. Song, S., Gulliver, G.A. & Lambert, P.F. Human papillomavirus type 16 E6 and E7 oncogenes abrogate radiation-induced DNA damage responses in vivo through p53-dependent and p53-independent pathways. *Proceedings of the National Academy of Sciences United States of America* **95**, 2290-2295 (1998).